CONTINUOUS MICROCELLULAR FOAMING OF POLYLACTIC ACID/NATURAL FIBER COMPOSITES

By

Carlos A. Diaz-Acosta

A DISSERTATION

Submitted to
Michigan State University
in partial fulfillment of the requirements
for the degree of

DOCTOR OF PHILOSOPHY

Packaging

2011

ABSTRACT

CONTINUOUS MICROCELLULAR FOAMING OF POLYLACTIC ACID/NATURAL FIBER COMPOSITES

By

Carlos A. Diaz-Acosta

Poly(lactic acid) (PLA), a biodegradable thermoplastic derived from renewable resources, stands out as a substitute to petroleum-based plastics. In spite of its excellent properties, commercial applications are limited because PLA is more expensive and more brittle than traditional petroleum-based resins. PLA can be blended with cellulosic fibers to reduce material cost. However, the lowered cost comes at the expense of flexibility and impact strength, which can be enhanced through the production of microcellular structures in the composite.

Microcellular foaming uses inert gases (e.g., carbon dioxide) as physical blowing agents to make cellular structures with bubble sizes of less than 10 µm and cell-population densities (number of bubbles per unit volume) greater than 10^9 cells/cm^3. These unique characteristics result in a significant increase in toughness and elongation at break (ductility) compared with unfoamed parts because the presence of small bubbles can blunt the crack-tips increasing the energy needed to propagate the crack. Microcellular foams have been produced through a two step batch process. First, large amounts of gas are dissolved in the solid plastic under high pressure (sorption process) to form a single-phase solution. Second, a thermodynamic instability (sudden drop in solubility) triggers cell nucleation and growth as the gas diffuses out of the plastic. Batch production of microcellular PLA has addressed some of the drawbacks of PLA. Unfortunately, the batch foaming

process is not likely to be implemented in the industrial production of foams because it is not cost-effective.

This study investigated the continuous microcellular foaming process of PLA and PLA/wood-fiber composites. The effects of the processing temperature and material compositions on the melt viscosity, pressure drop rate, and cell-population density were examined in order to understand the nucleation mechanisms in neat and filled PLA foams. The results indicated that the processing temperature had a strong effect of the rheology of the melt and cell morphology. Processing at a lower temperature significantly increased the cell nucleation rate of neat PLA (amorphous and semi-crystalline) because of the fact that a high melt viscosity induced a high pressure drop rate in the polymer/gas solution. The presence of nanoclay did not affect the homogeneous nucleation but increased the heterogeneous nucleation, allowing both nucleation mechanisms to occur during the foaming process.

The effect of wood-flour (0-30 wt.%) and rheology modifier contents on the melt viscosity and cell morphology of microcellular foamed composites was investigated. The viscosity of the melt increased with wood-flour content and decreased with rheology modifier content, affecting the processing conditions (i.e., pressure drop and pressure drop rate) and foamability of the composites. Matching the viscosity of the composites with that of neat PLA resulted in the best cell morphologies.

Physico-mechanical characterization of microcellular foamed PLA as a function of cell morphology was performed to establish process-morphology-property relationships. The processing variables, i.e., amount of gas injected, flow rate, and processing temperature affected the development of the cellular structure and mechanical properties of the foams.

Dedicated to my parents

Aurelio Diaz and Carmen J. Acosta

ACKNOWLEDGEMENTS

First, I would like to thank my advisor, Dr. Laurent Matuana, for his mentoring, guidance, and support throughout the program. He gave me the opportunity to think about the idea of a doctorate and push me to always higher standards. I acknowledge my guidance committee, Dr. Maria Rubino, Dr. Pascal Nzokou, and Dr. Rafael Auras, for their interest and valuable input in my dissertation. They were always there for advice or a word of encouragement. I extent my gratitute to the people at the Center for Advanced Microscopy, Dr. Stanley Flegler, Carol Flegler, Dr. Alicia Pastor, Ewa Danielewicz, Abigail Tirrell, for their help, counsel and assistance. I want to acknowledge the involvement of the Physical Plant Division, especially Mr. Dennis Lehman, in the setting up and maintaining of equipment. I am thankful to the Department of Forestry, their faculty and staff, specially: Juli Kerr, Carol Graysmith, Barb Anderson, Sue Plesko, and Karen Ellerhorst. I extend my heartfelt gratitude to the School of Packaging, their faculty and staff, specially the director Dr. Joseph Hotchkiss, Dr. Susan Selke, Kelby Thayer, Colleen Wager, April Meersdom, and Sherrie Lenneman. I am also grateful to my fellow grad students and colleagues, Dr. Omar Faruk, Dr. Shan Jin, Kojo Afrifah, the under graduates who worked with us Deja Torrence, Thomas McKay, Anthony Weatherspoon. I would like to acknowledge the financial support from the National Research Initiative of the USDA Cooperative State Research, Education and Extension Service (Grant 2006-35504-17414). Finally, I would like to recognize my family and friends for their unconditional love and support.

TABLE OF CONTENTS

CHAPTER 3

Study of Cell Nucleation in Microcellular Poly(lactic acid) Foamed with Supercritical CO_2 through a Continuous-Extrusion Process 82

CHAPTER 4

Rheology Modification Approach to Continuous Microcellular Foaming of Polylactic Acid/Wood-Flour Composites...128

CHAPTER 5

CHAPTER 6

LIST OF TABLES

LIST OF FIGURES

CHAPTER 1

Introduction

1.1 Introduction

The consumption of plastics per capita in the US has been estimated to reach more than 300 pounds a year by 2010 [1]. Most polymeric materials are currently based on non-renewable fossil resources [2]. As the petrochemical sources are depleting and the demand is forecasted to continue to grow in the foreseeable future, prices are expected to increase [3, 4]. Also, main petroleum suppliers are countries with unstable political situations, which affects the price of crude oil. At the same time, environmental concerns such as contribution to global warming and disposal of traditional plastics call for sustainable alternatives. Recognizing these issues, research and industrial efforts have developed plant-based bioplastics such as polylactic acid (PLA). In general, bioplastics refers to biodegradable plastics whose components are derived entirely from renewable raw materials [1]. Potential exist for bioplastics to replace traditional plastics, thus reducing our dependence on petroleum resources.

Polylactic acid (PLA) is a thermoplastic made from the polymerization of lactic acid derived by fermentation of sugars from corn, sugarcane, tapioca, etc. This bioplastic exhibits physical properties close to those of many synthetic plastics in addition to being completely biodegradable to carbon dioxide, water, and humus-like matter [5]. In addition, PLA has excellent mechanical properties and can be processed using existing machinery with only minor adjustments [5].

Currently, there is no commercial production of PLA that is price competitive with petroleum-based counterparts [5]. Moreover, most biodegradable plastics currently on the market are between two and ten times more expensive than traditional plastics [5]. Despite PLA's many properties that are equivalent to or better than many petroleum-based plastics, there have been few commercial applications mainly in the textile industry and in biomedical field for orthopedic surgery [5]. High brittleness and low impact resistance of PLA are major issues for its commercialization in applications such as packaging.

The packaging industry is one of the potential markets for PLA. However, brittle polymers break in a thermoforming production line, which is not tolerable. To broaden its applications, PLA is often blended with various additives such as lubricants, plasticizers, or a second polymer [6-8]. Plasticizers such as low molecular weight esters, oligomeric lactic acid, poly(ethylene glycol), etc., have been investigated to obtain PLA with higher flexibility and higher impact resistance [7, 8]. Significant improvement in flexibility (up to 180% elongation at break compared to 4% for neat PLA) and impact resistance (over 200% increase) was obtained with the use of up to 10 wt.% low molecular weight poly(ethy1ene-glycol) [7]. However, Increase in flexibility, accomplished by decreasing the glass transition temperature ($T_{g)}$ with the use of plasticizers, is linked to the decrease in tensile strength and modulus. Therefore, performance in terms of impact resistance and toughness is achieved at the expense of other important properties. Additionally, the cost of the final products increases due to the cost of additives. It is important to improve the flexibility and impact resistance of PLA while reducing the cost of manufactured parts.

To reduce the cost, compounding PLA with less expensive fillers such as wood fibers has been reported [9-11]. Wood-flour, kenaf fibers, recycled newspaper fibers, flax fibers, etc, have been blended with PLA in concentrations varying from 20 to 50 wt. % [9-12]. Because of the high specific modulus of cellulosic fibers, increased flexural and tensile modulus with increased fiber contents is achieved. However, tensile and flexural strength, and impact resistance generally decrease with increasing fiber content [10, 12]. Additionally, the incorporation of brittle cellulose fibers alters the ductile mode of failure of the matrix making the composites more brittle than the neat polymer [13].

Foaming technology, such as microcellular foaming, enhances the ductility and impact resistance of polymer matrices while achieving a significant volume expansion ratio and weight reduction [14]. Microcellular foaming uses inert gases (e.g., carbon dioxide) as physical blowing agents to make cellular structures with bubble sizes of less than 10 μm and cell-population densities (number of bubbles per unit volume) greater than 10^9 cells/cm^3. These unique characteristics results in a significant increase in toughness and elongation at break (ductility) compared with unfoamed parts. Additionally, compared to conventional foaming, strength and stiffness are not compromised [15]. By creating a microcellular structure, a considerable expansion ratio is obtained. For example, a twofold expansion means that only half of the resin is needed to produce the same volume, thus less material is needed, reducing the overall cost. If microcellular structures can be created in PLA and PLA/wood-flour composites, an expanded range of properties in terms of ductility and impact resistance would be attained. Consequently, the market for PLA will be expanded, especially in applications in the packaging sector.

Microcellular plastics were first produced in a two-step batch process [15, 16]. In the first step, a sample is placed in a pressurized chamber with an inert gas atmosphere. Under these conditions, the gas diffuses into the sample and, after enough time (from hours to days), the sample become saturated (Figure 1.1a, sorption), forming a single-phase solution. The second step consists on creating a thermodynamic instability by suddenly releasing the pressure and increasing the temperature (Figure 1.1b, temperature bath), which triggers cell nucleation and growth as the gas diffuses out of the plastic.

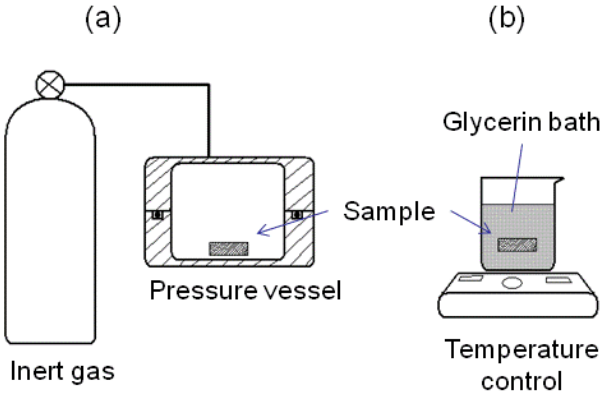

Figure 1.1. Schematic of a batch microcellular foaming process. (a) Sample saturation with CO_2 (sorption). (b) Sample foaming (diffusion).

Batch production of microcellular PLA has been shown to overcome some of the drawbacks of PLA [5, 17, 18]. Results of microcellular foamed neat PLA in the batch process showed significant improvements in the volume expansion ratio (a twofold expansion over unfoamed PLA), impact resistance (up to fourfold increase over unfoamed PLA), strain at break (up to twofold increase over unfoamed PLA), and toughness (up to fourfold increase over unfoamed PLA) [5]. Unfortunately, the batch foaming process used to generate microcellular foamed structures is not likely to be implemented in the industrial production of foams because it is not cost-effective. Multiple steps involved in the microcellular batch foaming process and the long saturation times required (from hours to days) limit this technique to be scaled up to industrial level. It is important to develop the technology to manufacture microcellular PLA foams in a continuous process, such as extrusion, to facilitate its mass production.

Compared to the batch foaming process, relatively few publications feature continuous microcellular foaming of PLA in extrusion. Reignier and co-workers reported a thorough investigation of the continuous extrusion foaming of amorphous PLA, using CO_2 as a blowing agent [19]. They produced low density foams under various injection pressures (2.5-9.0 MPa), CO_2 contents (1.8-9.3 wt.%), processing temperatures (90-100 °C), and by adding 0.5 wt.% talc in the resin as a nucleating agent. Neat PLA foamed samples achieved densities down to 21 kg/m^3 with cell sizes of 60 to 420 μm and the number of nucleated cells (or cell-population densities) in the range of 10^4 to 10^8 $cells/cm^3$. Other investigators reported microcellular extrusion of semi-crystalline

PLA and starch (75% amylopectin and 25% amylose) blends using a CO_2 concentration of 8 wt.%. They created low density neat PLA foams (25 kg/m^3) [20] but the cell morphology was not discussed in detail. The micrographs suggest the cells have sizes of 80 μm and up. Lee and coworkers produced microcellular foams from amorphous PLA resin (6300D from NatureWorks) intended for fiber melt spinning with CO_2 to study the expansion and cell-population density dependence on the amount of blowing agent (2-9 wt.%) [21]. Densities in the 20 to 700 kg/m^3 range were produced with cell sizes of around 100 μm and cell-population density of 10^5 cells/cm^3. Pilla and coworkers used epoxy-functionalized chain extender to improve rheological properties of the melt of semi-crystalline PLA (3001D, NatureWorks) and investigated its effects on the foamability of the PLA. The addition of 1.0% chain extender doubled the volume expansion ratio of the foams compared to the foamed neat PLA. Densities down to 300 kg/m^3 and cell densities in the 10^7 cells/cm^3 range were produced, averaging 30 μm and up in cell size.

These previous studies clearly demonstrate the continuous extrusion process of PLA foamed with supercritical CO_2. However, distinction between the cell morphology achieved and microcellular foams persist due to lower cell-population density (less than 10^9 cells/cm^3) with cells being larger than 60 μm on average [22]. Continuous extrusion of microcellular foamed PLA with fine cell size (< 10 μm) and high cell-population density (>10^9 cells/cm^3) will make possible not only the production of foamed materials with superior mechanical properties compared to their solid counterparts, but also the production of foamed structures in thin film [22].

The basis for the continuous microcellular process lies in the concept of thermodynamic instability to promote high cell nucleation rates in a flowing polymer matrix [22]. The nucleation phenomena has been clearly described by Matuana and Diaz [22]. In this paper the authors claim that achieving these high nucleation rates involves first forming a polymer/gas solution under high pressure, followed by rapidly decreasing the solubility of gas in the polymer by a rapid pressure drop and/or a rapid temperature increase, which induces a greater thermodynamic instability in the system. The classical nucleation theory (Equation 1.1) predicts this phenomenon [22, 23]:

$$N_{nucl} = C_o \cdot f_o \exp\left(\frac{-\Delta G}{kT}\right) \qquad \text{(Equation 1.1)}$$

with N_{nucl} as the cell nucleation rate, C_o the concentration of gas molecules, f_o the frequency factor for gas molecules joining the nucleus, k Boltzmann's constant, T the system temperature, and ΔG the free energy barrier to initiate homogeneous (ΔG_{hom}) or heterogeneous (ΔG_{het}) cell nucleation, given by the equations

$$\Delta G_{\text{hom}} = \frac{16 \cdot \pi \cdot \gamma_{bp}^{3}}{3\Delta p^{2}} \qquad \text{(Equation 1.2)}$$

$$\Delta G_{het} = \frac{16 \cdot \pi \cdot \gamma_{bp}^{3}}{3\Delta p^{2}} f(\theta) \qquad \text{(Equation 1.3)}$$

with γ_{bp} as the surface energy of the polymer-bubble interface, Δp the pressure drop of the gas/polymer solution [22, 24], and $f(\theta)$ depending on the contact angle at the polymer-nucleating agent interface. Heterogeneous nucleation occurs at the interface between the polymer and another phase.

The classical nucleation theory (Equation1.1) predicts that minimization of the free energy barrier for nucleation (ΔG) will promote high cell nucleation rates [22]. Although many relevant factors can affect the cell nucleation rate (Equation1.1), a higher pressure drop of the gas/polymer solution lowers the free energy barrier to initiate nucleation (equations 1.2 and 1.3), resulting in a higher nucleation rate. Park and co-workers demonstrated that the pressure drop rate in the die ($-dp/dt$) given by Equation1.4 correlates with the thermodynamic instability necessary to nucleate high numbers of cells; i.e., the higher the pressure drop rates, the higher the cell-population densities [22, 25-28]:

$$\frac{-dp}{dt} \approx \frac{-\Delta p}{\Delta t} \approx \frac{-\Delta p \cdot q}{\pi \cdot r_{o}^{2} \cdot L} \qquad \text{(Equation 1.4)}$$

with Δt as the average residence time of the flowing polymer/gas solution in the nozzle, L the length of the nozzle, q the volumetric flow rate of the polymer through the nozzle, and r_o the radius of the nozzle.

Matuana and Diaz explained that because the pressure drop rate depends on the nozzle geometry (r_o and L) and polymer flow properties (Δp and q), the potential in using these parameters as effective process and material variables for controlling the cell nucleation in continuous microcellular processing exists [22].

The processing temperature influences the density and cell morphology of foams because of its effect on the melt viscosity [22], as described by the Arrhenius relation

$$\eta = A_o \exp\left(\frac{E_a}{RT}\right) \qquad \text{(Equation 1.5)}$$

with η as the melt viscosity, A_o a constant, R the universal gas constant, T the absolute temperature, and E_a the activation energy for melt flow [29].

Generally, as the processing temperature is varied, the melt viscosity changes inversely; i.e., the lower the processing temperature, the higher the melt viscosity, and vice versa, subsequently leading to a change in the pressure generated during the extrusion process. The melt viscosity affects the pressure built into the system, thus affecting the cell nucleation rate. Additionally, the melt viscosity plays an important role during the growth and stabilization of nucleated cells [30].

Melt viscosity can also be tailored by varying the material formulation, e.g. additives and fillers contents [30, 31]. Incorporation of wood-flour in the polymer matrix is known to increase the viscosity of the resin [31-33]. Also, additives such as plasticizers, acrylic modifiers, compatibilizers, lubricants, and elastomers, significantly affect the melt viscosity of filled and unfilled matrices [31, 34, 35]. Li and co-workers studied the effects of wood-flour and internal lubricant contents on the rheological properties of wood-flour filled polypropylene. The results showed that increasing the wood-flour content increased the apparent viscosity of the melt because the solid wood particles in the molten polymer increased the resistance against the flow. By contrast, the addition of internal lubricant significantly decreased the melt viscosity of the composites by reducing the friction between polymer chains and wood particles [36]. Nearly a 50% reduction in apparent viscosity was observed by adding 5 wt.% of an ester based internal lubricant. Consequently, the effects of the processing temperature and material compositions on the melt viscosity, pressure drop rate, and cell-population density must be examined to understand the nucleation mechanisms in neat and filled PLA foams.

1.2 Objectives

The goal of the project is to develop the fundamental and engineering basis needed to manufacture microcellular foamed PLA/wood-flour composites through a continuous extrusion process using supercritical CO_2. To achieve this goal, the following specific objectives were proposed:

1. Examine the effect of processing temperature on melt viscosity, pressure drop rate and cell-population density to gain in-depth understanding of the nucleation mechanisms in neat PLA to generate microcellular foams.
2. Investigate the effect of the addition of nanoclay as nucleating agent in the formulation on the cell morphology to understand the heterogeneous nucleation mechanism in the continuous extrusion process.
3. Study the effects of wood-flour and rheology modifier contents on the melt viscosity and cell morphology of foamed samples to assess the influence of incorporation of wood-flour on the foamability of PLA.
4. Characterize the physico-mechanical properties of foamed samples as a function of cell morphology to establish process-morphology-property relationships and develop predictive models for the foamed materials.

1.3 Hypotheses

This research is intended to test the hypotheses that: (i) the control of the melt rheology through processing temperature and material composition can lead to the production of microcellular foams in PLA and PLA/natural fiber composites in a continuous extrusion process using physical blowing agents; and (ii) creating cellular structures in PLA products is an efficient way to improve flexibility and impact strength.

1.4 Structure of Dissertation

The first chapter introduced the rationale of this research. A background on foam technology and polylactic acid is reviewed in the second chapter. The influence of processing temperature on melt rheology and cell morphology of PLA (amorphous vs. semicrystalline), and the effect of addition of nanoclay as nucleating agent are discussed in Chapter 3. The effect of material composition, i.e. wood-flour content and rheology modifier contents, on melt rheology, and the effect of wood-flour content on cell morphology are discussed in Chapter 4. The mechanical characterization of foamed PLA and as well as process-morphology and morphology property relations are discussed in chapter 5.

REFERENCES

REFERENCES

1 Fuji-Keizai, USA Inc. (2007) Bioplastics market trends and U.S. & E.U. outlook. Research and Markets. pp. 132

2 Dorgan, J. R., Lehermeier, H. J., Palade, L. I. and Cicero, J. (2001) Polylactides: Properties and prospects of an environmentally benign plastic from renewable resources. Macromolecular Symposia. **175**, 55-66

3 Snow, N. (2006) EIA: World energy forecast reflects higher oil prices. Oil & Gas Journal. **104**(25), 34

4 Houlton, G. (2010) Crude demand to increase, feed-quality changes in store. Oil & Gas Journal. **108**(46), 118

5 Matuana, L. M. (2008) Solid state microcellular foamed poly(lactic acid): Morphology and property characterization. Bioresource Technology. **99**, 3643-3650

6 Semba, T., Kitagawa, K., Ishiaku, U. S. and Hamada, H. (2006) The effect of crosslinking on the mechanical properties of polylactic acid/polycaprolactone blends. Journal of Applied Polymer Science. **101**, 1816-1825

7 Jacobsen, S. and Fritz, H. G. (1999) Plasticizing polylactide - The effect of different plasticizers on the mechanical properties. Polymer Engineering and Science. **39**, 1303-1310

8 Baiardo, M., Frisoni, G., Scandola, M., Rimelen, M., Lips, D., Ruffieux, K. and Wintermantel, E. (2003) Thermal and mechanical properties of plasticized poly(L-lactic acid). Journal of Applied Polymer Science. **90**, 1731-1738

9 Avella, M., Bogoeva-Gaceva, G., Bularovska, A., Errico, M. E., Gentile, G. and Grozdanov, A. (2008) Poly(lactic acid)-based biocomposites reinforced with kenaf fibers. Journal of Applied Polymer Science. **108**, 3542-3551

10 Huda, M. S., Drzal, L. T., Misra, M., Mohanty, A. K., Williams, K. and Mielewski, D. F. (2005) A study on biocomposites from recycled newspaper fiber and poly(lactic acid). Industrial & Engineering Chemistry Research. **44**, 5593-5601

11 Pilla, S., Gong, S., O'Neill, E., Rowell, R. M. and Krzysik, A. M. (2008) Polylactide-pine wood flour composites. Polymer Engineering and Science. **48**, 578-587

12 Oksman, K., Skrifvars, M. and Selin, J. F. (2003) Natural fibres as reinforcement in polylactic acid (PLA) composites. Composites Science and Technology. **63**, 1317-1324

13 Matuana, L. M., Woodhams, R. T., Balatinecz, J. J. and Park, C. B. (1998) Influence of interfacial interactions on the properties of PVC cellulosic fiber composites. Polymer Composites. **19**, 446-455

14 Matuana, L. M., Faruk, O. and Diaz, C. A. (2009) Cell morphology of extrusion foamed poly(lactic acid) using endothermic chemical foaming agent. Bioresource Technology. **100**, 5947-5954

15 Martini, J., Waldman, F. and Suh, N. P. (1982) Production and analysis of microcellular thermoplastic foams. SEP ANTEC Technical Papers. pp. 674-676, San Francisco, CA

16 Matuana, L. M., Park, C. B. and Balatinecz, J. J. (1997) Processing and cell morphology relationships for microcellular foamed PVC/wood-fiber composites. Polymer Engineering and Science. **37**, 1137-1147

17 Ema, Y., Ikeya, M. and Okamoto, M. (2006) Foam processing and cellular structure of polylactide-based nanocomposites. Polymer. **47**, 5350-5359

18 Wang, X. X., Kumar, V. and Li, W. (2007) Low density sub-critical CO_2-blown solid-state PLA foams. Cellular Polymers. **26**, 11-35

19 Reignier, J., Gendron, R. and Champagne, M. F. (2007) Extrusion foaming of poly(lactic acid) blown with Co-2: Toward 100% green material. Cellular Polymers. **26**, 83-115

20 Mihai, M., Huneault, M. A., Favis, B. D. and Li, H. B. (2007) Extrusion foaming of semi-crystalline PLA and PLA/thermoplastic starch blends. Macromolecular Bioscience. **7**, 907-920

21 Lee, S. T., Kareko, L. and Jun, J. (2008) Study of thermoplastic PLA foam extrusion. Journal of Cellular Plastics. **44**, 293-305

22 Matuana, L. M. and Diaz, C. A. (2010) Study of cell nucleation in microcellular poly(lactic acid) foamed with supercritical CO_2 through a continuous-extrusion process. Industrial & Engineering Chemistry Research. **49**, 2186-2193

23 Colton, J. S. and Suh, N. P. (1987) The nucleation of microcellular thermoplastic foam with additives .1. Theoretical considerations. Polymer Engineering and Science. **27**, 485-492

24 Park, C. B., Baldwin, D. F. and Suh, N. P. (1995) Effect of the pressure drop rate on cell nucleation in continuous processing of microcellular polymers. Polymer Engineering and Science. **35**, 432-440

25 Park, C. B. and Suh, N. P. (1996) Filamentary extrusion of microcellular polymers using a rapid decompressive element. Polymer Engineering and Science. **36**, 34-48

26 Xu, X., Park, C. B., Xu, D. L. and Pop-Iliev, R. (2003) Effects of die geometry on cell nucleation of PS foams blown with CO_2. Polymer Engineering and Science. **43**, 1378-1390

27 Lee, J. W. S., Wang, K. Y. and Park, C. B. (2005) Challenge to extrusion of low-density microcellular polycarbonate foams using supercritical carbon dioxide. Industrial & Engineering Chemistry Research. **44**, 92-99

28 Wong, A., Leung, S. N., Li, G. Y. G. and Park, C. B. (2007) Role of processing temperature in polystyrene and polycarbonate foaming with carbon dioxide. Industrial & Engineering Chemistry Research. **46**, 7107-7116

29 Muksing, N., Nithitanakul, M., Grady, B. P. and Magaraphan, R. (2008) Melt rheology and extrudate swell of organobentonite-filled polypropylene nanocomposites. Polymer Testing. **27**, 470-479

30 Diaz, C. A. and Matuana, L. M. (2009) Continuous extrusion production of microcellular rigid PVC. Journal of Vinyl & Additive Technology. **15**, 211-218

31 Shah, B. L. and Matuana, L. M. (2004) Online measurement of rheological properties of PVC/wood-flour composites. Journal of Vinyl & Additive Technology. **10**, 121-128

32 Guo, G., Lee, Y. H., Rizvi, G. M. and Park, C. B. (2008) Influence of wood fiber size on extrusion foaming of wood fiber/HDPE composites. Journal of Applied Polymer Science. **107**, 3505-3511

33 Li, T. Q. and Wolcott, M. P. (2005) Rheology of wood plastics melt. Part 1. Capillary rheometry of HDPE filled with maple. Polymer Engineering and Science. **45**, 549-559

34 Huang, H. X. and Zhang, J. J. (2009) Effects of filler-filler and polymer-filler interactions on rheological and mechanical properties of HDPE-wood composites. Journal of Applied Polymer Science. **111**, 2806-2812

35 Münstedt, H. (1981) Rheology of rubber-modified polymer melts. Polymer Engineering & Science. **21**, 259-270

36 Li, H. J., Law, S. and Sain, M. (2004) Process rheology and mechanical property correlationship of wood flour-polypropylene composites. Journal of Reinforced Plastics and Composites. **23**, 1153-1158

CHAPTER 2

Background and Literature Review

2.1 Thermoplastic foams

As a general definition, a foam consists of gas bubbles immersed in a continuous solid matrix [1]. Thermoplastic foams are those made of thermoplastic polymers such as polyethylene, polypropylene, polystyrene, polyvinyl chloride, polylactic acid, etc. Foamed thermoplastics are used in a variety of applications such as insulation, cushioning, flotation devices, packaging, shock and sound attenuation, gaskets, sport goods, etc. Moreover, highly porous biodegradable plastics have been used as tissue engineering scaffolds, facilitating tissue regeneration (i.e., cell growth and attachment) [2, 3].

2.1.1 Cellular structure and foam properties

The properties of plastic foams are dictated by the type of polymer matrix and the cellular structure. In general flexible polymers will produce flexible foams and rigid polymers will produce rigid foams. The cellular structure or cell morphology refers to the parameters that characterize the foam such as density, number of bubbles per unit volume (cell-population density), cell size distribution, open-cell content, etc. The performance of the foam is correlated with the cell structure and strongly depends on the technology and polymer matrix used to produce the foam [4, 5]. For instance, foams with interconnected cells (open-cell structure) provide higher absorptive capacity and cushioning [6] whereas foams with isolated cells and a well defined cell wall (closed-cell structure) result in better thermal and acoustic isolation properties [7].

2.1.2 Foaming agents

The gaseous phase of thermoplastic foams derives from the use of a blowing or foaming agent. There are two types of foaming agents: chemical and physical foaming agents. A chemical foaming agent (CFA) is a solid compound in the form of powder or pellets which undergoes a chemical reaction in the foaming process to produce blowing gas. The reaction occurs because of a heat-induced decomposition. On the other hand, a physical foaming agent (PFA) does not change chemically. Instead, the PFA is dissolved directly into the polymer under pressure. Its blowing effect comes as a result of a change in physical state, e.g., liquid to vapor or supercritical fluid to vapor. The foaming agent is added to the polymer and the quantity is usually expressed as a fraction of the weight of the resin, e.g., 1 to 5 wt.%.

2.1.2.1 Chemical foaming agents

Chemical foaming agents can be divided into two families, i.e., exothermic and endothermic foaming agents, depending on their enthalpy of reaction. Exothermic foaming agents release heat as they decompose, mainly into nitrogen. An example of an exothermic CFA is azodicarbonamide (ADC). In general exothermic CFA have high yield (large volume of gas per unit weight) and have the ability to customize the decomposition temperature through the use of activators [8]. Nitrogen possesses a low diffusion rate, which is beneficial for bubble growth, maximizing the blowing efficiency of the CFA. Endothermic foaming agents, such as sodium bicarbonate, absorb heat during the decomposition reaction and decompose mainly into carbon dioxide (CO_2).

The endothermic reaction produces a cooling effect that has a stabilizing effect on the melt. In bubble formation, the CO_2 exerts lower pressure than nitrogen resulting in smaller cell sizes [8].

2.1.2.2 Physical foaming agents

Physical foaming agents include volatile hydrocarbons such as propane, butane, pentane, etc., low boiling points liquids such as chlorofluorocarbons (CFC's), hydrofluorocarbons (HFC's) and hydrochlorofluorocarbons (HCFC's), as well as inert gases such as carbon dioxide or nitrogen. Hydrocarbons are used in the production of low density polystyrene. However, hydrocarbons are flammable which can lead to handling and shipping hazards [9]. Chlorinated hydrocarbons (e.g., methyl chloride and methylene chloride) have low flammability but are considered toxic and have been used to a limited extent. For a long time, chlorofluorocarbon (R12) was the preferred foaming agent because of its nonflammability, low thermal conductivity and high solubility in the plastic matrix [9]. Unfortunately, the use of CFCs has been discontinued because they react with the ozone in the atmosphere depleting the ozone layer. Hydrofluorocarbons (HFC's) and hydrochlorofluorocarbons (HCFC's) were developed as replacements for CFCs with lower ozone depletion potential, but are still subjected to phaseout. Inert gases such as nitrogen and carbon dioxide have been gaining a lot of attention as blowing agents for they can replace conventional organic blowing agents since they are not associated with environmental issues. Also, inert gases have been used to produce microcellular plastics where uniform cellular structures with cell sizes of less than 10 μm render unique material properties, superior to conventional foams. A detailed explanation is provided in section 2.1.4.

2.1.3 Formation of a cellular structure

Cellular plastics are produced by different methods and equipment in continuous and batch processes. In the continuous process, single and twin screw extruders are extensively used to produce foams with CFA. The heat and shear provided by the extruder melt the plastic, mix the ingredients and supply heat for thermal decomposition of the foaming agent generating nitrogen or carbon dioxide. On the other hand, physical foaming agents are directly injected into the extrusion system. The gas and the polymer mix and dissolve forming a single phase solution, which is forced through a shaping die to produce the desired profile. As the polymer exits the extruder it experiences a high pressure drop as it goes from high pressure inside the extruder to atmospheric pressure outside the extruder. This pressure drop lowers the solubility of the gas in the polymer forcing the gas to come out of the solution forming bubbles [4]. Foams are also produced through injection and blow molding following the same principles [9].

The batch or solid state foaming process is another method which consists in placing a solid sample in a high pressure chamber under an inert gas atmosphere. The gas dissolves in the polymer until saturation is reached. Through pressure drop and temperature increase, the solubility is lowered and the gas comes out of the matrix forming bubbles. Irrespective of the blowing agent or production method, three steps are required in the manufacture of plastic foams:

1. Dissolution of the blowing agent in the polymer;
2. Cell nucleation;
3. Bubble growth and stabilization.

Irrespective of the nature of the foaming agent, chemical or physical, the foaming process follows these steps which correspond to thermodynamic states of the polymer/gas system.

2.1.3.1 Dissolution of the blowing agent in the polymer

Quality foams begin with blowing agent being thoroughly dissolved in the plastic melt. Once the chemical foaming agent has decomposed into CO_2 or N_2, or the physical foaming agent has been in contact with the polymer they should mix and dissolve to form a single phase solution. This process in controlled by the solubility of the blowing gas in the polymer. Solubility is the ability of the polymer to accept and retain small molecules, which reside in the free volume. The solubility limit is the maximum amount of gas or liquid that can be dissolved in a polymer at a given temperature and pressure. For instance in extrusion foaming, undissolved foaming gas reside in the melt as microdroplets or microbubbles which grow nearly explosively when the pressure is release [9]. As a result, large voids and a deteriorated cellular structure are developed, thus affecting the mechanical properties. For this reason, dissolution of the blowing agent into a homogeneous solution is a prerequisite to produce uniform cellular structures.

Another important factor in the formation of the polymer/gas solution is the time require for the dissolution process which is controlled by the diffusivity. The driving forces are chemical potential, gas concentration gradient, differential partial pressure, or temperature gradient [9]. The diffusivity parameter is affected by temperature, pressure, and shear mixing. Processing at higher temperatures and the use of mixing screws accelerates the sorption process.

2.1.3.2 Cell nucleation

Nucleation is the physical process by which a new stable phase is created. In the context of foaming gas bubbles nucleate from the polymer/gas solution. The nucleation is driven by a drop in solubility which can be attained by a sudden pressure drop or temperature increase. A sudden drop in solubility will make the polymer/gas solution supersaturated forcing the gas to form bubbles or escape to the atmosphere through the surface. Gas concentration, degree of supersaturation and pressure drop rate are important factors controlling the nucleation process.

The nucleation in the polymer can be homogeneous, heterogeneous, or a mixed-mode nucleation (both). In homogeneous nucleation, nucleation occurs right through the mass of the polymer when a critical amount of gas precipitates to form a stable second phase. In contrast, heterogeneous nucleation occurs at the interface between the polymer and another phase, such as a particle. Generally, the addition of external nucleating agents (e.g., nanoparticles, talc, stearates, TiO_2, etc.) reduces the polymer-bubble interfacial energy and provides sites for the heterogeneous nucleation of cells [10-13].

2.1.3.3 Bubble growth and stabilization

Once cells are nucleated they will continue to grow given the little resistance encountered. Cell growth rate is controlled by the gas pressure inside the bubble, the diffusion rate of gas from the polymer/gas solution to the growing bubble, and the viscoelastic properties of the melt. The viscoelastic properties of the melt and the processing temperature are of vital importance during cell growth and stabilization [14-16]. While melts with relatively low viscosity are needed to facilitate bubble growth, viscosity must increase, by cooling or strain hardening, to a level adequate for bubble stabilization [17, 18]. Consequently, melt viscosity, melt strength, and melt elasticity, which control the cell growth and stabilization, should be tailored to provide the conditions for a proper expansion and stabilization of the cellular structure.

Melt strength/elasticity is the capability of the melt to undergo stretching without rupture [18] and should be high to resist the membrane tearing. At the same time moderately high elongational viscosity allows biaxial stretching. These characteristics are especially important for the production of closed-cell foam morphologies. Also, if the polymer can crystallize, high crystallization rates will improve the stabilization process.

Polymers with poor melt strength/elasticity hinder controlled cell expansion and the stabilization of growing bubbles. In this case, changes in molecular weight by grafting, chain extension, branching or crosslinking enhance the viscoelastic properties of the polymers [18, 19].

2.1.4 Microcellular plastics

Industrially, most thermoplastic foams are manufactured through an extrusion process using either CFA or low boiling point PFA [1]. Conventional foams are characterized by average cell sizes ranging from 100 μm to 10 mm with cell-population densities of around 10^4 to 10^6 cells/cm^3. Large and nonuniform cells, typical of conventional foaming, decrease mechanical properties and necessitate relatively thick cross sections to ensure that the cells are contained within the part. In addition to this, foam manufactures are looking for alternatives to CFA and volatile organic compounds due to environmental the environmental issues associated with them.

Supercritial fluids such as N_2 and CO_2 are environmentally friendly and offer many advantageous properties including inertness, nonflamablity and low cost. Supercritical fluids are compressed gases that show properties of both liquids and gases [20]. They combine gas-like viscosity and diffusivity, and liquid-like density, making them excellent candidates for continuous extrusion foaming. Foaming technology makes use of supercritical fluids in order to accelerate diffusion processes and completely dissolve the gas into the polymer in a short timeframe [21]. Above the critical temperature and pressure (critical point) a gas is considered to be in its supercritical state. Carbon dioxide is ideal for extrusion foaming because of is high solubility in most polymer matrices and because its supercritical conditions ($T_c = 304.1$ K, $P_c = 7.38$ MPa) can be easily attained by the use of a syringe pump of a high pressure gas delivery system [22].

Supercritical fluids can overcome the drawbacks of conventional foaming and produce more uniform cell morphologies with higher cell-population densities and smaller cell sizes. High amounts of small cells uniformly distributed in the matrix would improve the mechanical properties of the foam. Classified by size, foams can be conventional or microcellular. Microcellular foams are characterized by cell sizes smaller than 10 μm with a narrow cell size distribution and a large cell-population density (greater than 10^9 cells/cm^3). The production of foamed structures in thinner parts and foamed films is conceivable in microcellular foams.

The concept of microcellular plastics was developed in the 80s by researchers at Massachusetts Institute of Technology with the dual goal of reducing material usage and increase toughness. The rationale was that by creating microscopic cells smaller than preexisting flaws in the material in large amounts, density reduction can be attained while maintaining mechanical properties [23, 24]. Studies have reported improvements in impact strength and toughness [23, 25], fatigue life [26], and thermal stability [27] in microcellular plastics compared to unfoamed specimens. Small bubbles inhibit crack propagation by blunting the crack tip and increasing the amount of energy to propagate the crack [23]. Density reductions of 75% or more can be attained in microcellular plastics due to the presence of microcells [25]. The unique properties of microcellular foams can be used in a large number of innovative applications such as packaging, automotive, sports equipment, etc. [28]

Microcellular plastics can be manufactured through noncontinuous [12, 25, 29, 30], semi-continuous [31], and continuous processes [17, 28, 32, 33]. Microcellular structures have been produced in amorphous and semi-crystalline polymers. Recently, microcellular structures have also been produced in composite materials with cellulosic fibers [30] and plastics filled with inorganic particles [34]. The next section discusses the two main processing methods used to produce microcellular foams, the batch process and the continuous extrusion process.

2.1.5 Solid state microcellular foaming (the batch process)

The microcellular foaming process dissolves an inert gas into a plastic to create a swarm of bubbles. Microcellular plastics, produced first in a batch process, involve a solid sample placed into a chamber under high pressure in an inert gas atmosphere (e.g., CO_2, N_2, etc.) where gas molecules diffuse into the plastic, forming a single-phase solution (Figure 2.1a, sorption). Subsequently, nucleated and grown cells form by creating a thermodynamic instability (i.e., sudden pressure drop and/or temperature increase, Figure 2.1b, temperature bath).

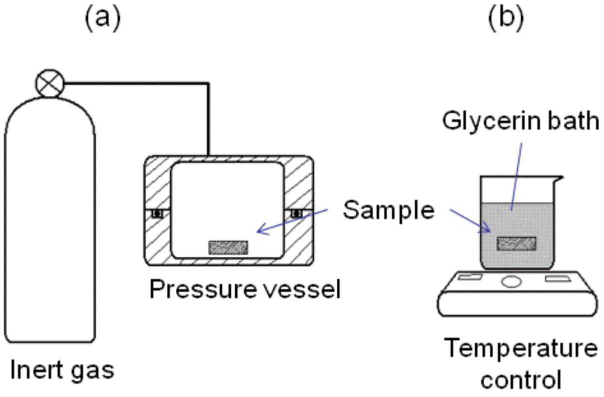

Figure 2.1. Schematic of a batch microcellular foaming process. (a) Sample saturation with CO_2 (sorption). (b) Sample foaming (diffusion).

Cell morphology in the batch process is controlled by the amount of gas absorbed, which is influenced by the pressure in the vessel and time allowed to saturate (Figure 2.1a); and by the viscosity of the melt in the foaming stage, which is dictated by the temperature of the bath (Figure 2.1b). Cell stabilization is accomplished by freezing the matrix by dipping the sample in cold water. This additional step is required to stop the bubble growth and stabilize the cell structure. Longer times in the temperature bath may result in cell coalescence and bubble collapse; whereas very short temperature bath may result in insufficient time to develop the cellular structure. Optimum processing windows are usually determined experimentally and with the help of statistical packages for experiment design.

2.1.5.1 Formation of a single-phase solution

In solid state microcellular foaming the amount of gas to be dissolved in the polymer is determined by temperature, pressure, and time the samples stay in the chamber. These conditions are usually room temperature and high pressure or high temperature and pressure (autoclave). In the former case a sample may take days to reach equilibrium while in the latter case a few hours may be enough. The dependence of solubility on temperature and pressure is illustrated in Figure 2. In general higher pressures induce higher solubilities whereas temperature has the opposite effect.

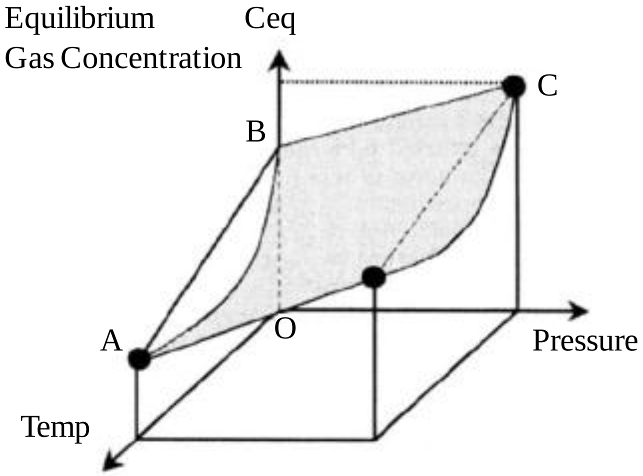

Figure 2.2. Typical equilibrium gas concentrations in polymers in function of temperature and pressure [35].

Sorption isotherms show the dependence of solubility on pressure. If the relation is linear, the polymer gas system is said to follow Henry's law expressed by Eq. 2.1:

$$C = k_D \cdot P \qquad \text{(Equation 2.1)}$$

where C is the volumetric concentration of gas (standard temperature and pressure, STP) per volume of polymer, K_D is the Henry's law constant and P is the pressure [36]. Henry's law is a good fit at low pressures. At higher pressure ranges an isotherm may differ from a linear form having some curvature due to interactions between the gas and the polymer. In this case other models such as the dual sorption model, the Flory–Huggings based models and the equation-of-state-based models should be considered [37].

2.1.5.2 Nucleation dynamics

Colton and Suh modeled the nucleation of batch microcellular foams in polystyrene. Classical nucleation theory was used as the basis to describe the nucleation phenomena. Equation 2.2 predicts that the rate of nucleation is proportional to the gas concentration and exponential with respect to the activation energy barrier (ΔG) [10-12, 29]:

$$N_{nucl} = C_o \cdot f_o \exp\left(\frac{-\Delta G}{kT}\right) \qquad \text{(Equation 2.2)}$$

with N_{nucl} as the cell nucleation rate, C_o the concentration of gas molecules, f_o the frequency factor for gas molecules joining the nucleus, k Boltzmann's constant, T the system temperature, and ΔG the free energy barrier. The activation energy barrier is derived from the Gibbs free energy balance between interfacial free energy and volume free energy [10]. Clusters of gas need to be greater than a critical size to overcome the activation energy and create a stable bubble. Activation energy for homogeneous nucleation is given by Equation 2.3:

$$\Delta G_{\mathrm{hom}} = \frac{16 \cdot \pi \cdot \gamma_{bp}^{3}}{3\Delta p^{2}} \qquad \text{(Equation 2.3)}$$

with γ_{bp} as the surface energy of the polymer-bubble interface, and Δp the pressure drop of the gas/polymer solution. Based on equation 2.3, minimizing the free energy calls for reducing the surface energy or increasing the pressure drop in the system. In a polystyrene/nitrogen system Colton and Suh [11] showed an increase in the number of cells nucleated of three orders of magnitude by increasing the saturation pressure from 2 to 10 MPa. Furthermore, adding zinc stearate below the solubility limit increased the bubbles nucleated for the same saturation pressure because of the reduced surface energy. Above the solubility limit, additives precipitate providing sites for heterogeneous nucleation almost eliminating the dependence of nucleation on saturation pressure [11]. Goel and Beckman [29] used classical nucleation theory to predict homogeneous nucleation in a poly(methyl methacrylate) (PMMA)/CO_2 system with a good agreement between experimental and calculated nucleation rates [29].

Heterogeneous nucleation occurs at the interface between the polymer and a particle and effectively reduces the activation energy. Equation 2.4 describe the heterogeneous nucleation activation energy:

$$\Delta G_{het} = \frac{16 \cdot \pi}{3 \Delta p^2} \cdot \gamma_{bp}^3 \cdot f(\theta) \qquad \text{(Equation 2.4)}$$

with $f(\theta)$ depending on the wetting angle (θ) at the polymer-nucleating agent interface. A typical wetting angle of 20° will result in a $f(\theta)$ in the order of 10^{-3} [10].

2.1.6 Continuous microcellular extrusion process

Continuous microcellular foaming follows the same principles as the batch process. A single-phase solution of plastic and gas needs to be created, and a thermodynamic instability is required to nucleate and grow bubbles. Inert gases in their supercritical state are injected into the extrusion barrel. The gas will mix with and diffuse into the molten polymer and form a single-phase solution. Thermodynamic instability will occur as the polymer/gas solution leaves the extruder through the use of a nozzle die

(Figure 2.3). As the melt passes through the nozzle, the solution is taken from high pressure in the extrusion system to atmospheric pressure [28, 38]. Nucleation, cell growth and stabilization occur while the polymer leaves the extruder. In contrast to the batch process, all stages of foaming in the continuous process have to take place in a matter of seconds.

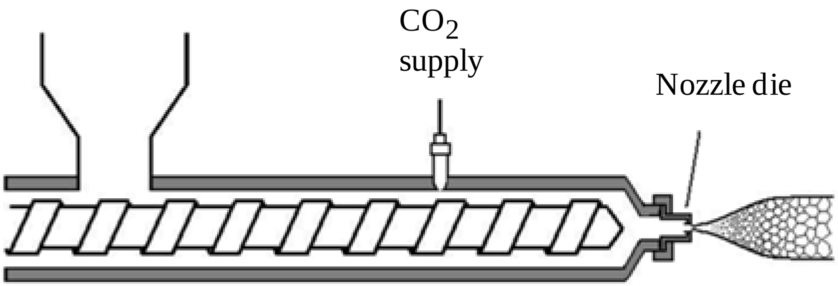

Figure 2.3. Schematics of a continuous microcellular extrusion process.

The continuous microcellular foaming implies that the polymer/gas mixing requires a shorter time frame, from hours/days in the batch process to seconds in the continuous process. Using gas in supercritical conditions and the polymer in the molten state enhances the diffusion. The independent variables in the continuous extrusion process are the amount of gas injected, and the processing conditions, i.e., rotational screw speed and temperature profile.

2.1.6.1 Formation of a single-phase solution

In continuous microcellular foaming the amount of gas to be dissolved in the polymer is set by injecting a metered amount of gas in the extrusion barrel. The gas will mix and diffuse in the polymer given that the high pressure in the system is sufficient to solubilize the gas. In other words, the metered amount of gas injected in the barrel should be lower than the solubility of the gas in the polymer at the pressure and temperature in the system; otherwise a single phase solution cannot be attained. By using gas in supercritical conditions and the polymer in the molten state, the diffusion is enhanced [17]. By comparing reported values of diffusivity from the literature [22, 39] going from room temperature to 180°C will increase the diffusivity by two orders of magnitude. The dependence on temperature of the diffusion coefficient obeys an Arrhenius relationship as follows:

$$D = D_o \exp\left(-\frac{E_a}{RT} \right) \qquad \text{(Equation 2.5)}$$

where D_o is the pre-exponential factor; E_a is the activation energy for the gas diffusion; R is the universal gas constant, and T is the temperature in the absolute scale [40]. Although a high diffusion is preferred in the continuous microcellular foaming process to ensure the creation of a single-phase solution, it can also be detrimental during nucleation and cell growth because gas molecules can quickly move to the surface and escape to the atmosphere reducing the efficiency of the foaming agent [41].

2.1.6.2 Nucleation dynamics

Nucleation in the continuous system is also explained using classical nucleation theory [41]. However, the time period over which the thermodynamic instability occurs plays an important role in the number of bubbles nucleated. Park and coworkers identified a link between pressure drop rate and nucleation [42]. Higher pressure drop rates result in nucleation rates (higher number of bubbles nucleated). Basically, depending on the time allowed for the pressure drop, cells can prematurely nucleate in the nozzle creating a region around them with low gas concentration where nucleation does not occur and the dissolved gas is used to grow the bubble. This competition between nucleation and cell growth mechanisms limits the nucleation ability. Therefore, higher pressure drop rates translate into more gas used to nucleate rather than grow bubbles, resulting in higher nucleation rates [41, 43]. Equation 2.6 shows the relationship of the pressure drop rate with the flow characteristics and nozzle geometry.

$$\frac{-dp}{dt} \approx \frac{-\Delta p}{\Delta t} \approx \frac{-\Delta p \cdot q}{\pi \cdot r_o^2 \cdot L} \qquad \text{(Equation 2.6)}$$

with Δt as the average residence time of the flowing polymer/gas solution in the nozzle, L the length of the nozzle, q the volumetric flow rate of the polymer through the nozzle, and r_o the radius of the nozzle. Based on Equation 2.6, the pressure drop rate depends on the nozzle geometry (r_o and L) and the polymer flow properties (Δp and q). Therefore, the geometry of the nozzle or the flow properties of the material are variables for controlling the cell nucleation in continuous microcellular processing [44].

2.2 Polylactic acid (PLA)

Poly(lactic acid) (PLA) is a biodegradable thermoplastic obtained from annually renewable resources such as corn, beets, sugar cane, etc. The monomer lactic acid can be obtained from starch fermentation (biological process), or by chemical processes. PLA has excellent mechanical properties, good biocompatibility and low toxicity. It has been used in biomedical and packaging applications and has the potential to replace petroleum-based plastics.

2.2.1 Structure and synthesis

Lactic acid is the chemical repeat unit (constitutional unit) of PLA. Because of its chiral nature, lactic acid exists as two enantiomers, L- and D-lactic acid, giving place to three types of the cyclic dimmers of lactic acid (lactide monomer), i.e., L-lactide, D-lactide, and meso-lactide (see Figure 2.4). Because of this, PLA can be systhetize into a variety of primary structures. Examples of this can be the isotactic homopolymers poly(L-lactide) (PLLA) or poly(D-lactide) (PDLA) where all of the monomers in the chain are of the same optical composition [45], or random copolymers of L-, D- and meso lactide. Most commercial PLAs are copolymers of L-lactide and lesser amounts of D- and meso-lactide. The effect of stereochemistry on crystallinity and thermal properties is discussed in the next section.

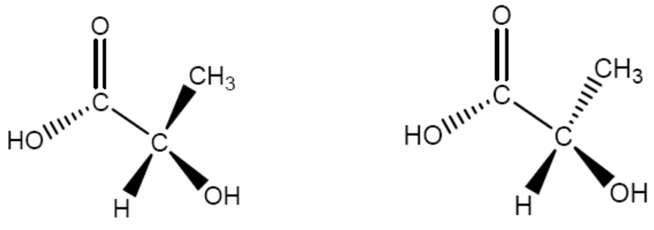

L-lactic acid D-lactic acid

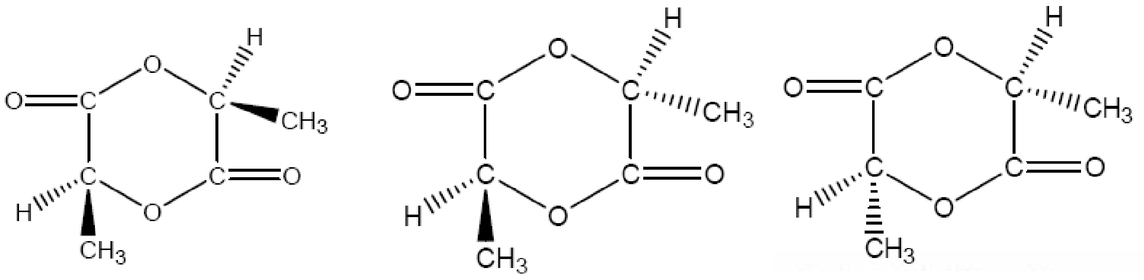

L-lactide meso-lactide D-lactide

Figure 2.4. Stereochemistry of lactic acid and lactide [46].

Figure 2.5 shows a schematic of the PLA production. First, anaerobic bacteria converts plant sugars into lactic acid. Second, condensation reaction of aqueous lactic acid produces PLA with low molecular weight, which is then depolymerized into the cyclic dimer of lactic acid or lactide monomer. Third, ring-open polymerization produces PLA with high molecular weight [47, 48]. PLA possesses physical and mechanical properties similar to those of polystyrene or poly ethylene terephthalate (PET) and can be processed with existing machinery such as extrusion, injection molding, etc., without major adjustments [36].

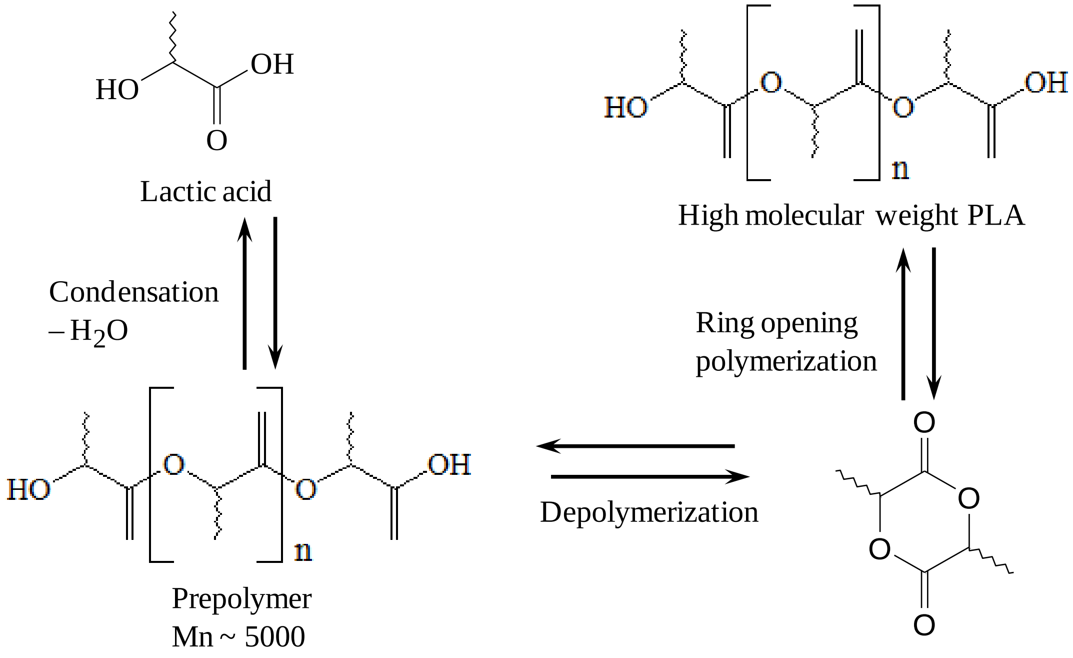

Figure 2.5. Schematic of PLA production via prepolymer and lactide [48].

2.2.2 Properties of PLA

2.2.2.1 Thermal properties and crystallinity

Thermal properties such as glass transition temperature (T_g) and melting temperature (T_m), and degree of crystallinity of PLA depend on molecular weight, relative amounts of L- and D-lactic stereoisomers, and thermal history. Poly(L-lactic acid) (PLLA), made entirely from L-lactide, is a semi-crystalline polymer due to stereoregularity. Similarly, Poly(D-lactic acid) (PDLA), made entirely from D-lactide is also semi-crystalline. Most commercial grades of PLA are made from L-lactide with lesser amount of Meso- and D-lactide. These last two components induce twists in the regular poly(L-lactic acid) molecular architecture resulting in a decreased rate and extent of crystallinity [49].

The extent of crystallinity can be controlled by tuning the relative amounts of L- and D-lactic stereoisomers in the polymer. In general, PLA made from more than 93% L-lactic acid is semicrystalline. Lesser relative amounts of L-lactic acid, between 50 and 93%, will result in an amorphous PLA [49]. One drawback of PLA is its low crystallization rate which result in products with low heat resistance [50]. For instance, the low heat deflection of PLA, between 50 to 60°C, can cause packages to deform during storage [51]. So far PLA commercialization has been limited to applications that do not require high temperatures such as refrigerated food packaging and cold beverages cups. Researchers are looking for ways to increase the heat resistance of PLA. This could be achieved through increasing the crystallinity. Inducing crystallization can be accomplished by different methods including annealing, addition of nucleating agents or biaxial orientation [52]. It is known that PLLA and PDLA mixtures can form stereocomplex crystallites with increased crystallization rates [53].

Foaming of PLA can influence the material crystallinity. A significant increase in crystallinity has been reported when comparing foamed and unfoamed PLA samples [54], because of biaxial stretching during bubble growth. Additionally, dissolved CO_2 into PLA contributes to the development of crystallinity [55], because its plasticizing effect enhances chain mobility. Increase of cristallinity, induced by foaming, helps the stabilization of the cellular structure and increases the heat resistance of the foam.

Thermal properties can vary among different PLA types. PLA has a glass transition temperature between 40 and 70°C, and a melting temperature between 130 and 180°C [56]. Thermal properties are also affected by the L-lactic content; higher L-lactic content increases the T_m and T_g [57].

2.2.2.2 Rheological properties

Causing the melt to flow is the basis of converting plastics into useful articles. Consequently plastics rheology is intimately related to its processability, particularly the shear viscosity. Viscosity of PLA depends on the molecular weight (M_w). The zero shear viscosity (η_o) follows the relationship presented in equation 2.7.

$$\log(\eta_o) = -14.26 + 3.4\log(M_w) \qquad \text{(Equation 2.7)}$$

Equation 2.7 is representative of PLA with molecular weight in the 10-100 Kg/mol range at 180°C regardless of stereochemical composition [58]. PLA shows shear thinning behavior at common processing shear rates [59], between 10 to 1000 1/s, and the viscosity (η) versus shear rate ($\dot{\gamma}$) curve follows a power law as shown in equation 2.8.

$$\eta = K \cdot (\dot{\gamma})^{n-1} \qquad \text{(Equation 2.8)}$$

where K and n represent the melt viscosity coefficient and power law index, respectively. Capillary rheometry results showed a power law index (n) of 0.36 for PLA with M_W =100 Kg/mol at 180°C [59]. Branched PLA is known to have stronger shear thinning behavior and higher zero-shear viscosity. Control of the rheology is possible through blending on PLA with different molecular architectures without affecting thermal and mechanical properties [60].

One drawback when processing PLA is its susceptibility to thermal and hydrolytic degradation, which affect its viscosity measurements and processing. Special attention should be placed in drying the material prior to processing and in some cases the use of stabilizers may be necessary to prevent polymer degradation.

Another important rheological parameter is the melt strength, which is related to the ability of the melt to stretch. Melt strength is especially important in blown film, deep draw thermoforming, and foaming. Lower melt viscosity and melt strength is one of the deficiencies of PLA which limits its blow molding and foaming processability [19, 61]. In foam processing, lower melt strength will result in the shear thinning of the cell-wall during bubble growth which facilitates cell coalescence and the overall cell structure deterioration. Strategies to overcome this issue should be considered. Branching and crosslinking of PLA has been attempted to improve rheological properties [19, 61]. Some results will be discussed in the next section.

2.2.2.3 Mechanical properties

Polylactic acid possesses good mechanical properties in terms of tensile strength and modulus superior to many traditional plastics, e.g., polyethylene and polypropylene. It fractures through a crazing mechanism and has low impact resistance and low strain at break when compared to traditional petroleum-based plastics. Polylactic acid modulus of elasticity is between 3 to 4 GPa. It has a tensile strength of 50 to 70 MPa. It is a hard polymer with hardness measured in Rockwell H scale of 70 to 90 [62, 63].

Notched izod impact resistance of PLA can vary from 2 to 7 KJ/m^2 depending mostly on degree of crystallinity and is highly sensitive to notching. Unnotched PLA impact resistance is in the range of 13 to 35 KJ/m^2. Samples with higher degree of crystallinity possess higher impact resistance [62]. Impact modification is indispensable for PLA to compete in automotive and packaging markets. Increasing the impact resistance is important for both end-use and manufacturing. For instance, in a packaging production line the brittle polymer will break during thermoforming and hampers production speed [51]. Approaches to overcome brittleness and improve impact resistance are discussed in a separate section.

2.2.2.4 Barrier and sorption of CO_2 into PLA

The permeation of small molecules in a polymer, characterized by parameters such as permeability, diffusivity, and solubility, is important in many applications such as packaging. The ability of a molecule to easily permeate through a membrane or be obstructed by it is critical in designing a package system. PLA is a good barrier for CO_2 and aroma compounds similar to PET. However, it is a poor barrier to O_2 and water vapor [64]. Research efforts are being directed towards manipulation and control of PLA barrier properties to expand its applications.

In the context of foaming, sorption is the process by which gas molecules are absorbed by the polymer. The gas diffuses from a higher chemical potential to a lower chemical potential until equilibrium is reached. Solubility is the amount of gas absorbed at thermodynamic equilibrium and is important because it determines the amount of gas available for foaming.

The solubility of CO_2 in PLA at room temperature was examined by Matuana in the 1.38 to 5.52 MPa pressure range [36]. A maximum solubility of 16.4% [36] was observed and the Henry's law constant k_D was estimated to be 0.47 MPa. The data slightly differ from the Henry's law showing an upward curvature, attributed to the affinity between CO_2 and PLA. Using a magnetic suspension balance, Aionicesei and coworkers, measured solubility of poly(L-lactide) (PLLA) at supercritical conditions and room temperature. A solubility up to 43% was observed in the 10 to 30 MPa range. The shape of the sorption isotherm showed a downward curvature opposite to the observed in the subcritical region [22, 65].

Li et al., measured the solubility and diffusivity of CO_2 in PLA at high temperature (i.e., 180 and 200°C) and high pressure (i.e., up to 28MPa) [39], similar to the conditions experienced during extrusion foaming. The results were corrected to account for swelling, and a solubility up to 20% was measured in the PLA/CO_2 system (180°C and 27 MPa) [39]. In extrusion foaming, efficiently dissolving the gas into the polymer requires the pressure in the system to be well above the equilibrium pressure. According to their data, the equilibrium pressure to dissolve 10% of CO_2 in molten PLA at 180°C is 2000 psi (14 MPa). That means that if 10% CO_2 is injected in the extrusion barrel, the pressure in the system should be at least 2000 psi for the single phase solution to be created. Lower temperatures will make this pressure requirement lower since the solubility increases as temperature decreases, lowering the equilibrium pressure for the same amount of gas.

2.2.3 Property modification of PLA

Property modification of PLA can be accomplished by different means including copolymerization, plasticization, blending with other resins, fiber reinforcement, compounding with nanoparticles, foaming, etc. Modification is performed to obtain improved material properties compared to the neat PLA in order to make the material suitable for a specific application.

2.2.3.1 Copolymerization

Copolymerization allows two or more monomers to be combined into one polymeric chain to provide materials with a specific set of properties. A wide range of mechanical properties can be attained by this method. However, the process is not economically viable unless produced in a large industrial scale [66]. PLA has been synthesized into random copolymers, block copolymers, and graft copolymers to modify its properties [67]. Research in PLA copolymers has been mostly directed towards biomedical applications.

Poly(lactic-co-glycolic acid) is a random or block copolymer made by ring-opening polymerization of the cyclic dimers of lactic acid and glycolic acid. This material, as well as block copolymers comprising poly(ethylene glycol) (PEG) and PLA, are used in medical implants due to their biocompatibility and because the biodegradation rate of the copolymer can be modulated by adjusting the ratio of the constituents [68, 69]. Other co-monomers that have been combined with PLA include glycolide derivatives, lactones, cyclic amide esters, cyclic ether esters, cyclic carbonates, etc [67]. One restriction to form copolymers of PLA is that the other co-monomer must participate in ring-opening polymerization.

2.2.3.2 Plasticization

Plastic films, e.g. polyolefin films, are extensively used in multiple applications such as flexible packaging. However the non-biodegradability of the resins traditionally used is a drawback in view of sustainability. PLA has excellent characteristics in terms of transparency and barrier but low flexibility and brittleness, which prevent its processability. Packaging is one of the potential markets for PLA. However, brittleness causes tearing in the plastic film on a production line, which is not tolerable [36, 70]. Plasticization of PLA is then required in order to produce flexible films.

Flexibility and toughness of PLA can be improved with the use of plasticizers [66]. However, attention in choosing the right plasticizer is essential to maintain non-toxicity, miscibility, and ultimate biodegradability [70]. Migration of the plasticizer may cause contamination of products in contact with PLA. Oligomeric lactic acid, glycerol, and low-molecular weight esters are among the studied plasticizers for PLA [70].

Generally the introduction of a plasticizer is accompanied by a depression in the glass transition temperature (T_g) [71], which in turn results in lower tensile strength and modulus. Ljungber and Wesslèn studied triacetine, tributyl citrate, acetyl tributyl citrate, triethyl citrate, and acetyl triethyl citrate and their plasticizing effect on PLA through dynamic mechanical analysis (DMA) and differential scanning calorimetry (DSC). Significant reduction in T_g was observed when using triacetine or tributyl citrate in concentrations up to 30%. However, the plasticizer was only partially miscible with PLA and phase separation was observed [70]. Piorkowska and coworkers, plasticized semi-crystalline PLA with poly(propylene glycol), which decreased T_g and caused a sensitive drop in tensile strength and phase separation [72]. the major drawbacks of most of the available plasticizers seems to be the drop in tensile strength, large amount of plasticizer needed, and poor miscibility (evidenced by phase separation).

Increase in flexibility, accomplished by decreasing the T_g with the use of plasticizers, is linked to the decrease in tensile strength and modulus. Therefore, performance in terms of impact resistance and toughness is achieved at the expense of other important properties. Additionally, the cost of the final products increases due to the cost of additives. It is important to improve the flexibility and impact resistance of PLA while reducing the cost of manufactured parts.

2.2.3.3 Blending with other polymers

Polymer blending consists on the creation of a new material by mixing two or more polymers. It is a way to improve the properties of PLA and/or improve the cost effectiveness of the material. Studies on blending PLA with other polymers have focused on maintaining its biodegradability.

Due to its natural origin and abundant availability starch is the main candidate to blend with PLA. Incorporation of hydrophilic starch into hydrophobic PLA has been a subject of research with the goal of reducing cost while maintaining biodegradability. Starch usually adds rigidity to PLA and is miscible only at low concentrations, thus using compatibilizers and plasticizers is commonly observed in the blends [73]. Drawbacks of starch deal with its moisture sensitivity which limits its applications [74].

Blends of PLA with other biodegradable polymers such as polyhydroxyalkanoates (PHAs), poly(ε-caprolactone) (PCL) [75], and poly(butylenes succinate) (PBS) [76], have been reported. Also, to improve the toughness, PLA has been blended with polyethylene [77] and rubber [78].

In order to improve the brittle behavior of PLA, Semba and coworkers studied the effect of its blending with PCL and the addition of peroxide to induce crosslinking on the mechanical properties of the blends. Low concentrations of dicumyl peroxide, i.e., 0.3 phr, showed best results with a PLA/PLC blend ratio of 70/30. Ductile behavior was observed along with an increase in impact strength of 250% over neat PLA for the samples prepared with the optimum formulation. The values compared with those of acrylonitrile butadiene styrene (ABS) and high impact polystyrene (HIPS) [75].

Immiscibility of PLA blends is a common observation among different studies and the use of compatibilizers is a necessary condition to achieve property improvement. Chen and coworkers used funtionalized organoclay to compatibilize the immiscible blend of poly(l-lactide) (PLLA) and poly(butylene succinate) (PBS). The organocaly was treated with (glycidoxypropyl) trimethoxy silane to improve the dispersion and provide chemical interaction with both PLA and PBS. Improvement in both the elastic modulus (from 1.1 to 1.0 GPa) and elongation at break (from 4.4 to 118.1%) of the PLLA-PBS blends (75:25) with the addition the funtionalized organoclay in concentrations from 5 to 10 wt.% was observed[76]. Although the blending of PLA can render an increase in properties, the use of specialized polymers and compatibilizers may significantly increase the cost of the final products.

Blending of PLA with polyolefins to increase the toughness has been reported [77]. The study by Anderson and coworkers reported the production of super-tough PLA by blending a 80:20 mixture of PLA and linear low density polyethylene (LLDPE) with the addition of PLLA-PE block copolymer (5%) as compatibilizer. However, blends with non-biodegradable plastics may have a negative perception in view of sustainability.

2.2.3.4 Fiber reinforcing

Using wood-flour, or other natural fibers to reinforce polymer is a common practice that combines the properties of wood and plastics to form new materials with improved moisture sensitivity over wood and greater stiffness over neat plastics. Wood fiber content influences the processing and properties of Polymers. Generally, properties such as modulus of elasticity, are somewhere in between those of the polymer and the fiber depending on the relative amount of the constituents. In other words, they follow a rule of mixtures. Other properties such as tensile strength depend on the stress transfer from the matrix to the load bearing fiber [79]. Generally hydrophilic cellulosic fiber and hydrophobic polymer matrices result in poor interfacial interactions which reflect in lower mechanical properties such as tensile strength, which can be improved by adding coupling agents. Coupling agents are chemical compounds with functional groups capable of reacting with both the reinforcement and the matrix. A variety of coupling agents have been developed with over forty types available [80].

Most coupling agents are organic compounds with bi-functional groups in their molecular structure such as isocyanates, maleic anhydrides (MA), silanes, etc. They can modify the polymer matrix by grafting or even crosslinking at the interface. Modified polymer matrices with grafted MA are common types of coupling agents. For instance, the maleated polyolefin reacts with the hydroxyl groups of the wood component through esterification or hydrogen bonding [81].

With the aim of reducing the cost of final products while retaining biodegradability, blending of PLA with low cost cellulosic fibers has been investigated [82-84]. By applying different manufacturing techniques such as compression and injection molding, the effects of wood fiber content as well as fiber's pretreatment have been studied.

Huda and coworkers studied the thermo-mechanical properties of PLA composites reinforced with recycled newspaper cellulosic fibers. For the composites containing 30% fibers, tensile and flexural modulus were significantly higher than for neat PLA and the values compared with those of polypropylene/talc composites. On the other hand, tensile and flexural strength decreased. Thermal properties remained unaffected by the inclusion of fibers while notched Izod impact strength drastically decreased [83]. Pilla and coworkers used pine wood-flour as filler in PLA. Samples were produced by injection molding with wood loadings of up to 40%. Wood-flour content increased the modulus of elasticity but decreased toughness and elongation mainly due to decreased deformability of the matrix because of restriction imposed by the brittle cellulosic fibers. Additionally, the use of a silane coupling agent proved to be ineffective to improve the strength [84].

Oksman and coworkers produced PLA/flax composites with fiber contents of 30 and 40%. The components were mixed in a twin extruder and compression molded into testing samples. Tensile modulus increased but the impact strength decreased.

Recognizing the need to improve impact strength the study incorporated glycerol triacetate ester as a plasticizer; unfortunately, no significant improvement was observed [85]. In a different study from the same group, PLA composites with up to 25% microcrystalline cellulose were prepared [86]. Tensile modulus increased and tensile strength decreased with increased filler content. Wood-flour and wood pulp composites were used as reference materials and mechanically outperformed microcrystalline cellulose composites, mainly because of their higher aspect ratio which resulted in a better stress transfer across the interphase [86].

Based on the reviewed literature, filling PLA with cellulosic fibers can increase the tensile modulus and reduce the overall cost. However, while cost reduction can be achieved, toughness and impact resistance are deteriorated. Two major drawbacks of PLA include brittleness and low impact resistance; this approach worsens these two properties. Therefore, different approaches should be considered to increase the toughness while reducing the material cost.

2.2.3.5 Nanocomposites

The term nanocomposite is commonly referred to polymer matrices reinforced with nano-sized fillers (at least one dimension <100 nm) [87]. Some common fillers for this purpose include nanoclay (layered silicates), carbon nanotubes, cellulose nanocrystals, etc [88]. Nanocomposites have generated a lot of interest because remarkable improvement in properties (e.g., mechanical and thermal properties) can be obtained at low filler content, usually less than 5 wt.%, without affecting processability.

The high surface area inherent of the filler size allows for more filler-matrix interactions, thus the property enhancement.

Preparation of PLA nanocomposites with modified and unmodified montmorillonites (type of nanoclay) has been reported. The preparation methods include in-situ polymerization, melt-mixing, and solvent-casting. Significant mechanical and thermal properties improvement have been reported [89]. In their pure state, clays come as a stack of parallel silicate layers. Upon processing, the layers can be slightly separated (intercalated) or randomly dispersed in the matrix (exfoliated), depending on its affinity for the polymer. Increase in mechanical properties such as tensile strength and modulus, depends on the degree of exfoliation of the nanoclay. Agglomeration of the nanoclay is a common problem in nanocomposites preparation and lead to poor mechanical properties. A good dispersion of intercalated or exfoliated nanoclay is important to make use of their reinforcing potential. Krikorian and Pochan obtained Poly(L-lactic acid) nanocomposites with a spectrum from intercalated to fully exfoliated morphologies by altering the hydrophobicity of the organoclay. In this study, nano composites were prepared by dispersion of organoclay in solvent and subsequent mixing with PLLA [90]. Jiang and co-workers compared the performance of two nano-sized fillers, i.e., nano-sized precipitated calcium carbonate (NPCC) and organically modified montmorillonite clay, mixed with commercial PLA [91]. Clay nanocomposites showed best improvement in strain at break (3 fold increase) at low concentrations, i.e., 2.5 wt.%, and an overall higher modulus and tensile strain at similar concentrations compared to NPCC (in the 0 to 5 wt.% range) because of the larger aspect ratio and intercalation of the nanoclay.

Based on the above discussion, nanoclay modification is required in order to enhance the interaction of the filler with the matrix, and promote dispersion and intercalation. On the other hand, lack of toughness of the PLA nanocomposites is usually observed [92]. Platicization followed by nanocomposite preparation have been proposed to overcome some of this drawbacks [93].

In foam processing, solid particles have the potential to induce heterogeneous nucleation. Therefore, the nucleation potential of nanocomposites in foaming has been studied [24, 34, 94]. Okamoto and coworkers reported that the number of cells nucleated in a batch foamed polypropylene increased by 100 times by adding 7.5 wt.% of nanoclay [94]. Foamed PLA nanocompostites are discussed in the next section.

2.2.4 Microcellular foaming of PLA

2.2.4.1 Batch foaming of PLA

Recently, production of microcellular-foamed structures in PLA through batch foaming process has been used to address some limitations of the polymer [3, 24, 34, 36, 95]. Matuana reported significant improvements in the volume expansion ratio (a 2-fold expansion), impact resistance (up to a 4-fold increase), strain at break (up to a 2-fold increase), and toughness (up to a 4-fold increase) of foamed PLA over that of the unfoamed counterpart by creating microcells in the samples. This implies that foamed PLA exhibits enhanced ductility and impact resistance owing to the presence of microbubbles [36].

A wide range of morphologies can be produced in foamed PLA through batch microcellular foaming. Wang et al. 2007 produced low density PLA foams, down to 5% relative density compared to the unfoamed counterpart, using subcritical CO_2 as foaming agent. Unfortunately the morphology associated with the low density foams had large cell sizes of several hundreds of microns and low cell population density, i.e., $\sim 10^5$ cells/cm^3. Increasing the saturation pressure had a tremendous effect on the morphology lowering the cell size below 30 μm. The change in cell morphology with saturation pressure was attributed to changes in both degree of crystallinity and diffusivity parameter. An increase in the extent of crystallization, from 5 to 25%, was observed when increasing the saturation pressure from 2 to 3 MPa [95]. Similarly, higher saturation pressures induced a higher diffusivity of CO_2 in the PLA (10 times increase from 1 to 5 MPa). Similar results of crystallinity induced by CO_2 and the increased diffusivity with increased saturation pressure in PLA have been reported [55]. Foams with cell sizes in the 30 to 40 μm range and cell population densities, around 8 x 10^7 cells/cm^3, were produced at a 2.8 MPa saturation pressure showing a uniform cellular structure [55]. Higher saturation pressures, i.e., 4.1 MPa, resulted in smaller cells (1 to 10 μm) and high cell population densities ($>10^{10}$cells/cm^3). However, in the later case the cellular structure was less uniform. It was speculated that the higher diffusion coefficient may have deteriorated the uniformity of the cellular structure [55]. Matuana and Faruk manufactured microcellular foamed PLA and PLA/wood-flour composites using CO_2 in the batch process [96]. The effect of saturation pressure on the morphology and volume expansion ratio of neat PLA was investigated. The highest volume expansion (10 times) compared to unfoamed PLA was associated with lower saturation pressures up to 2.76 MPa, which corresponds to a critical gas concentration of 9.4%. Higher saturation pressures resulted in deteriorated morphologies due to the higher diffusion rates [96].

Since nanoparticles can act as heterogeneous nucleating agents, they have the potential to control the cellular structure. With the objective of understanding the correlation between cell morphology and the dispersed silicate particles, Fujimoto and coworkers studied the incorporation of nanoclay in PLA foamed with CO_2 in the batch process. The cellular structure showed closed cells sizing from several microns to fractions of a micron, i.e., 360 nm, . Achieving smaller cell sizes correlated with the degree of dispersion of the nanoclay [34]. Similar results were reported by Ema and coworkers focusing on the nucleating effect of the clay particles. Nanoclay induced heterogeneous nucleation lowering the activation energy barrier as compared to homogeneous nucleation, resulting in controlled cellular structures with cell sizes from microcellular to nanocellular [24].

A different approach to controlling the cellular structure of microcellular PLA is through modification of the rheology. Di and coworkers used chain extenders to increase the molecular weight of PLA and improve the viscoelastic properties. Lower cell sizes, from 227 to 24 μm, and an increase in cell-population density from 7.7×10^5 to 6.7×10^8 cells/cm^3 was achieved as a result of the increased viscosity and elasticity. In this case, a 20:80 mixture of CO_2 and N_2 was used as the physical foaming agent [19]. Zhu and coworkers investigated the effect of chain branching and the addition of lubricant on the morphology of PLA foamed with CO_2 [61]. Branched PLA showed superior viscoelastic properties and the occurrence of strain hardening, which produced better cell morphologies by preventing cell coalescence. Branched PLA produced smaller cell sizes compared to linear PLA (~250 μm vs. ~50 μm) because of the higher melt strength. Also, addition of lubricant resulted in an increase in cell-population density [61].

Microcellular foaming of wood fiber filled PLA has been investigated to reduce weight and improve performance of the material. Incorporation of wood-flour into the PLA matrix significantly affects the morphology and the expansion ratio of foamed composites [96]. In the study by Matuana and Faruk, cell size and expansion ratio decreased with increasing wood-flour content because the fibers make the matrix stiffer, which provided high resistance to the bubble growth. The wood fibers were pretreated with 1% silane coupling agent to enhance adhesion between fibers and the matrix. It is known that surface modification of wood fibers with coupling agent has strong effects on both the solubility of gas in the matrix and the cell morphology [30, 97]. Higher cell-population densities and void fractions due to fiber modification has been reported [97]. Microcellular foaming can also be used as means of overcoming the brittleness and low impact resistance of wood filled composites. Microcellular foamed PVC/wood composites produced in the batch process showed that the creation of a microcellular structure increased the impact resistance to values higher than the unfoamed and unfilled polymer [25].

The above mentioned studies give valuable insights in the production of microcellular PLA foams. However, the industrial implementation of microcellular foams remains unlikely in the batch foaming process because of its time-consuming nature and multiple steps involved in the production of foamed samples, i.e., manufacture of solid samples, saturation of solid samples with gas (sorption experiments), and nucleation of cells and cell growth [98-100]. It is important to develop the technology for the continuous production of microcellular foamed PLA and PLA wood fiber composites.

2.2.4.2 Continuous microcellular extrusion foaming of PLA

Commercial applications for microcellular foamed PLA and PLA composites necessitate the development of a continuous process. Research initiatives in extrusion foaming [41, 54, 101] and injection-molding processes [102] of PLA using supercritical CO_2 have already shown initial results.

Reignier and coworkers investigated the continuous-extrusion foaming of amorphous PLA, using CO_2 as a blowing agent [101]. They pointed out the importance of the plasticization effect of CO_2, which allows the process to be carried out at lower temperatures. The plasticization was measured in terms of T_g reduction and was established to be between 6 to 8°C/wt. % CO_2. They produced foams under various injection pressures (2.5-9.0 MPa), CO_2 contents (1.8-9.3 wt %), and processing temperatures (90-100°C). Neat PLA foamed samples achieved densities down to 21 kg/m^3 with cell sizes of 60-420 μm and the number of nucleated cells (or cell-population densities) in the range of 10^4-10^8 cells/cm^3. The processing window associated with the low density foams (21 kg/m^3) and high nucleation rate (10^7-10^8 cells/cm^3) involved an injection pressure (or an equivalent gas concentration of ~7 wt %) that corresponds to the critical pressure of CO_2 (7.38 MPa). Talc affected the cell morphology of PLA foams at lower CO_2 content (below ~5 wt %) because its addition into the matrix led to foams with much finer cells (~50 μm) and a higher cell-population density (10^8 cells/cm^3) compared to neat PLA foams (~400 μm and 10^4 cells/cm^3). This observation indicates that talc particles act as heterogeneous nucleating sites for cell nucleation. Nevertheless, the effect of talc on the cell morphology disappeared at higher CO_2 contents because the samples processed with or without talc had similar porous morphologies (~120 μm and 10^8 cells/cm^3).

Foaming of semicrystalline PLA has been demonstrated with results similar to those of amorphous PLA. Mihai and coworkers foamed semicrystalline PLA (2002D from NatureWorks) using a CO_2 concentration of 8 wt.% and also created low-density open-cell foams (25 kg/m^3) [54]. The foamed samples showed crystallinities of around 15% induced by CO_2 and the stretching during bubble growth. Unfoamed samples usually show little to no-crystallinity due to low crystallization rates of PLA. The use of 0.5 wt % talc did not modify the foam structure or change the degree of crystallinity.

Microcellular extrusion of an amorphous PLA resin (6300D from NatureWorks) intended for fiber melt spinning has also been produced with CO_2. The dependency of the expansion on the amount of blowing agent (2-9 wt %) has been study [41]. Densities in the 20-700 kg/m^3 range were produced with cell sizes of around 100 μm and a cell-population density of 10^5 cells/cm^3. Low density foams were associated with higher concentrations of CO_2, i.e., >6 wt.%.

Pilla and coworkers investigated the use of epoxy-functionalized chain extender on the foamability of semi-crystalline PLA (3001D, NatureWorks) to improve rheological properties of the melt. Increasing the molecular weight through chain extenders is known to increase the melt strength of the resin. When both talc and the chain extender were added in the formulation, foamed samples with densities down to 300 kg/m^3 and cell-population densities of approximately 10^7 cells/cm^3 were produced. An average cell size of around 30 μm was observed [103]. The use of talc as nucleating agent (i.e., 0.5 wt.%) was a necessary condition to achieve uniform morphologies with increased cell-population density. The addition of 1.0% chain extender doubled the volume expansion of the foams compared to the foamed neat PLA at the lowest die temperature, i.e., 130°C. Higher die temperatures led to lower expansion ratios, i.e., 140, 150, and 160°C.

Matuana and Diaz investigated the effect of wood-flour content on the cell morphology of extrusion foamed PLA with CO_2 [104]. Amorphous PLA with 20 wt.% wood-flour was foamed in a continuous extrusion process and compared with foamed neat PLA. Wood fibers were pretreated with a 1 wt.% silane coupling agent to enhance adhesion between the matrix and the filler [96] and 5 wt.% nanoclay was added as nucleating agent. Micrographs of the foamed samples showed a cell morphology with fine cells of 2 to 10 μm in size in PLA/wood-flour composite foams. Nevertheless, the samples also contained larger cells (>60 μm) and cracks making the morphology non-uniform. The high temperature profile used in the processing may have played an adverse role in the foaming process [104]. The processing temperature for the composite was 20°C above the processing temperature to foam the neat polymer. Since the addition of wood particles into a polymer significantly increases the viscosity of the melt [105], the higher processing temperature was required to make the composite more flowable in the microcellular extrusion system. Processing at lower temperature profiles led to overpressure in the system due to the increased viscosity of the composite melt. It has been shown that high processing temperatures in the extrusion barrel contribute to the wood component degradation by releasing water vapor and volatiles in the system during foaming [106], with damaging effects on the morphology. Guo and coworkers suggested a temperature of 170°C or less to suppress adverse effects from the volatiles generated by wood-flour during foaming. Above this temperature, these residues are detrimental to the foam morphology and should be kept to a minimum [106]. Additionally, high temperatures can also affect the consistency of the PLA which is sensitive to thermal degradation [63]. In a different study, the effect of wood-flour mesh size on the foamability of HDPE/wood-flour composites was investigated. The results showed that finer sizes of wood fibers lead to more uniform morphologies with smaller cell size because of their enhanced nucleating effect [107] .

These previous studies offered valuable insights, demonstrating the continuous-extrusion process of PLA foamed with supercritical CO_2. However, the morphology achieved in foamed PLA failed to satisfy the definition of microcellular foam because of a lower cell-population density (less than 10^9 cells/cm^3), with cells being larger than 60 μm in average size. Distinctions between these features and microcellular foam persist, where the cell-population density ranges from 10^9 cells/cm^3 and up, with fully grown cells being smaller than 10 μm in average size. Continuous extrusion of microcellular PLA with fine cell size (<10 μm) and high cell-population density (10^9 cells/cm^3 and up) will enable not only the production of foamed materials with superior mechanical properties (compared to their solid counterparts) but also the production of foamed structures in a thin film.

2.2.4.3 Injection molded microcellular PLA

Through a microcellular injection molding process, Pilla and coworkers manufactured foamed PLA and PLA/cellulose fiber composites [33]. The addition of cellulosic fibers increased the specific modulus of both foamed and unfoamed samples. By creating a cellular structure the storage modulus was increased but the specific strength and strain decreased. Adding cellulosic fibers reduces the cell size and increases the cell-population density because of the heterogeneous nucleation effect of the fibers. However, the morphology of neat PLA showed larger cells (>20 μm) and cell-population densities in the 10^7 cells/cm^3 range. In a subsequent study, the addition of hyperbranched polyester (HBP) was evaluated as a means to improve toughness and cell morphology in the microcellular PLA [108]. Hyperbrached polyester increased toughness and strain at break in both solid and microcellular foamed specimens while reducing the specific strength. The cell size decreased with the addition of HBP and the cell-population density increased. Addition of 2% nanoclay in the formulation further decreased the cell size and increased the cell-population density, i.e. ~12 μm and 1.6×10^7 cells/cm^3, respectively [108].

2.2.4.5 PLA foamed with chemical foaming agents

Although most research efforts to foam PLA have focused on inert gases as physical foaming agent, chemical foaming agents are a viable alternative to produce expanded PLA products. Utilization of existing machinery without adjustments (does not required a gas delivery system) is one of the advantages of this process. The main variables are type and amount of chemical foaming agent (endothermic or exothermic) along with the processing conditions, which influence the cellular structure of extruded foamed plastics.

A recent investigation showed that fine homogeneous cell morphologies (cell sizes ~100 μm) could be successfully achieved in extrusion foamed PLA using endothermic foaming agent. The effects of amount of CFA, the melt flow index (MFI) of the PLA and processing speed on the cellular structure were investigated. Results showed that the melt-flow index of PLA must lie within a range that provides a melt viscosity low enough to allow cell formation and growth but high enough to prevent cell coalescence [109]. The amount of CFA affected the cell-population density and the void fraction in the range studied (0-2%). Both cell-population density and void fraction increased as the CFA amount increased, given the more availability of gas for both nucleation and cell growth. However, at concentrations above 1.5% cell coalescence became dominant producing the opposite effect. The effect of processing speed (rotational screw speed) was analogous to the CFA content. Higher processing speeds result in lower residence times in the extruder and less gas for foaming because of incomplete decomposition of the CFA. Moderate speeds, i.e. ~40 rpm showed best results [109].

Lee and coworkers investigated the effect of exothermic foaming agent, azodicarbonamide (ADC), on the expansion of amorphous PLA [41]. The expansion increased with increased CFA content, reaching a maximum (2.5 times) at around 1% content of ADC. Higher CFA concentrations led to lower expansion because of the occurrence of premature foaming which reduce the efficiency of the foaming agent [41].

REFERENCES

REFERENCES

1 Lee, S. T. (2000) Foam extrusion : principles and practice. Technomic Pub. Co., Lancaster

2 Hutmacher, D. W. (2000) Scaffolds in tissue engineering bone and cartilage. Biomaterials. **21**, 2529-2543

3 Liao, X., Nawaby, A. V., Whitfield, P., Day, M., Champagne, M. and Denault, J. (2006) Layered open pore poly(L-lactic acid) nanomorphology. Biomacromolecules. **7**, 2937-2941

4 Lee, S.-T., Park, C. B. and S., R. N. (2007) Polymeric foams: science and technology. Taylor & Francis Group, Boca Raton

5 Rhodes, M. B. (1997) A perspective on cell morphology and foam properties. In Polymeric Foams. pp. 178-194, American Chemical Society

6 Elliott, J. A., Windle, A. H., Hobdell, J. R., Eeckhaut, G., Oldman, R. J., Ludwig, W., Boller, E., Cloetens, P. and Baruchel, J. (2002) In-situ deformation of an open-cell flexible polyurethane foam characterised by 3D computed microtomography. Journal of Materials Science. **37**, 1547-1555

7 Zeng, C. (2004) Synthesis, structure and properties of polymer nanocomposites. Ph.D. Thesis, Departent of Chemical Engineering. The Ohio State University

8 Heck, R. L. (1998) A review of commercially used chemical foaming agents for thermoplastic foams. Journal of Vinyl and Additive Technology. **4**, 113-116

9 Throne, J. L. (2004) Thermoplastic foam extrusion. Carl Hanser Verlag, Munich

10 Colton, J. S. and Suh, N. P. (1987) The nucleation of microcellular thermoplastic foam with additives .1. Theoretical considerations. Polymer Engineering and Science. **27**, 485-492

11 Colton, J. S. and Suh, N. P. (1987) The nucleation of microcellular thermoplastic foam with additives .2. Experimental results and discussion. Polymer Engineering and Science. **27**, 493-499

12 Colton, J. S. and Suh, N. P. (1987) Nucleation of microcellular foam - theory and practice. Polymer Engineering and Science. **27**, 500-503

13 Spitael, P., Macosko, C. W. and McClurg, R. B. (2004) Block copolymer micelles for nucleation of microcellular thermoplastic foams. Macromolecules. **37**, 6874-6882

14 Rabinovitch, E. B., Isner, J. D., Sidor, J. A. and Wiedl, D. J. (1997) Effect of extrusion conditions on rigid PVC foam. Journal of Vinyl & Additive Technology. **3**, 210-215

15 Decker, R. W. (1996) The role of lubricants in rigid PVC foam processing. Journal of Vinyl & Additive Technology. **2**, 121-124

16 Xanthos, M., Zhang, Q., Dey, S. K., Li, Y. and Yilmazer, U. (1998) Effects of resin rheology on the extrusion foaming characteristics of PET. Journal of Cellular Plastics. **34**, 498-+

17 Diaz, C. A. and Matuana, L. M. (2009) Continuous extrusion production of microcellular rigid PVC. Journal of Vinyl & Additive Technology. **15**, 211-218

18 Xanthos, M., Yilmazer, U., Dey, S. K. and Quintans, J. (2000) Melt viscoelasticity of polyethylene terephthalate resins for low density extrusion foaming. Polymer Engineering and Science. **40**, 554-566

19 Di, Y. W., Iannace, S., Di Maio, E. and Nicolais, L. (2005) Reactively modified poly(lactic acid): Properties and foam processing. Macromolecular Materials and Engineering. **290**, 1083-1090

20 Gong, K., Braden, M., Patel, M. P., Rehman, I. U., Zhang, Z. and Darr, J. A. (2007) Controlled release of chlorhexidine diacetate from a porous methacrylate system: Supercritical fluid assisted foaming and impregnation. Journal of Pharmaceutical Sciences. **96**, 2048-2056

21 Sun, X. H., Liu, H. J., Li, G., Liao, X. and He, J. S. (2004) Investigation on the cell nucleation and cell growth in microcellular foaming by means of temperature quenching. Journal of Applied Polymer Science. **93**, 163-171

22 Aionicesei, E., Skerget, M. and Knez, Z. (2008) Measurement of CO_2 solubility and diffusivity in poly(L-lactide) and poly(D,L-lactide-co-glycolide) by magnetic suspension balance. Journal of Supercritical Fluids. **47**, 296-301

23 Martini, J., Waldman, F. and Suh, N. P. (1982) Production and analysis of microcellular thermoplastic foams. SPE ANTEC Technical Papers. pp. 674-676, San Francisco, CA

24 Ema, Y., Ikeya, M. and Okamoto, M. (2006) Foam processing and cellular structure of polylactide-based nanocomposites. Polymer. **47**, 5350-5359

25 Matuana, L. M., Park, C. B. and Balatinecz, J. J. (1998) Cell morphology and property relationships of microcellular foamed PVC/wood-fiber composites. Polymer Engineering and Science. **38**, 1862-1872

26 Seeler, K. A. and Kumar, V. (1993) Tension-tension fatigue of microcellular polycarbonate - initial results. Journal of Reinforced Plastics and Composites. **12**, 359-376

27 Rachtanapun, P., Selke, S. E. M. and Matuana, L. M. (2003) Microcellular foam of polymer blends of HDPE/PP and their composites with wood fiber. Journal of Applied Polymer Science. **88**, 2842-2850

28 Park, C. B., Behravesh, A. H. and Venter, R. D. (1998) Low density microcellular foam processing in extrusion using CO_2. Polymer Engineering and Science. **38**, 1812-1823

29 Goel, S. K. and Beckman, E. J. (1994) Generation of microcellular polymeric foams using supercritical carbon-dioxide. I: Effect of pressure and temperature on nucleation. Polymer Engineering and Science. **34**, 1137-1147

30 Matuana, L. M., Park, C. B. and Balatinecz, J. J. (1997) Processing and cell morphology relationships for microcellular foamed PVC/wood-fiber composites. Polymer Engineering and Science. **37**, 1137-1147

31 Kumar, V. and Schimer, H. G. (1997) A semi-continuous process to produce microcellular foams. 5'684.055 U.S. Patent

32 Han, X. M., Koelling, K. W., Tomasko, D. L. and Lee, L. J. (2002) Continuous microcellular polystyrene foam extrusion with supercritical CO_2. Polymer Engineering and Science. **42**, 2094-2106

33 Kramschuster, A., Pilla, S., Gong, S., Chandra, A. and Turng, L.-S. (2007) Injection-molded solid and microcellular polylactide compounded with recycled paper shopping bag fibers. In 9th international conference on wood & biofiber composites. pp. 59-69, Forest Products Society, Madison, WI

34 Fujimoto, Y., Ray, S. S., Okamoto, M., Ogami, A., Yamada, K. and Ueda, K. (2003) Well-controlled biodegradable nanocomposite foams: From microcellular to nanocellular. Macromolecular Rapid Communications. **24**, 457-461

35 Chong, T. H., Ha, Y. W. and Jeong, D. J. (2003) Effect of dissolved gas on the viscosity of HIPS in the manufacture of microcellular plastics. Polymer Engineering and Science. **43**, 1337-1344

36 Matuana, L. M. (2008) Solid state microcellular foamed poly(lactic acid): Morphology and property characterization. Bioresource Technology. **99**, 3643-3650

37 Kikic, I., Lora, M., Cortesi, A. and Sist, P. (1999) Sorption of CO_2 in biocompatible polymers: experimental data and qualitative interpretation. Fluid Phase Equilibria. **158**, 913-921

38 Park, C. B. and Cheung, L. K. (1997) A study of cell nucleation in the extrusion of polypropylene foams. Polymer Engineering and Science. **37**, 1-10

39 Li, G., Li, H., Turng, L. S., Gong, S. and Zhang, C. (2006) Measurement of gas solubility and diffusivity in polylactide. Fluid Phase Equilibria. **246**, 158-166

40 Wong, A., Leung, S. N., Li, G. Y. G. and Park, C. B. (2007) Role of processing temperature in polystyrene and polycarbonate foaming with carbon dioxide. Industrial & Engineering Chemistry Research. **46**, 7107-7116

41 Lee, S. T., Kareko, L. and Jun, J. (2008) Study of thermoplastic PLA foam extrusion. Journal of Cellular Plastics. **44**, 293-305

42 Park, C. B., Baldwin, D. F. and Suh, N. P. (1995) Effect of the pressure drop rate on cell nucleation in continuous processing of microcellular polymers. Polymer Engineering and Science. **35**, 432-440

43 Tomasko, D. L., Li, H. B., Liu, D. H., Han, X. M., Wingert, M. J., Lee, L. J. and Koelling, K. W. (2003) A review of CO_2 applications in the processing of polymers. Industrial & Engineering Chemistry Research. **42**, 6431-6456

44 Matuana, L. M. and Diaz, C. A. (2010) Study of cell nucleation in microcellular poly(lactic acid) foamed with supercritical CO_2 through a continuous-extrusion process. Industrial & Engineering Chemistry Research. **49**, 2186-2193

45 Henton, D. E., Gruber, P., Lunt, J. and Jed, R. (2005) Polylactic acid technology. In Natural fibers, biopolymers, and biocomposites (Mohanty, A. K., Misra, M. and Drzal, L. T., eds.). pp. 527-577, Taylor & Francis/CRC Press, Boca Raton, FL

46 Dorgan, J. R., Williams, J. S. and Lewis, D. N. (1999) Melt rheology of poly(lactic acid): Entanglement and chain architecture effects. Journal of Rheology. **43**, 1141-1155

47 Evans, J. (2010) Bioplastics get growing. Plastics Engineering. **66**, 14

48 Gruber, P. and O'Brien, M. (2002) Polylactides "NatureWorks™ PLA". In Biopolymers (Steinbüchel, A. and Doi, Y., eds.). pp. 235-250, Wiley-VCH, Weinheim

49 Auras, R., Harte, B. and Selke, S. (2004) An overview of polylactides as packaging materials. Macromolecular Bioscience. **4**, 835-864

50 Xiao, H. W., Lu, W. and Yeh, J. T. (2009) Effect of plasticizer on the crystallization behavior of poly(lactic acid). Journal of Applied Polymer Science. **113**, 112-121

51 Stephen, M. (2010) Getting TOUGH on PLA. Canadian Plastics. **68**, 20-22

52 Tsai, C.-C., Wu, R.-J., Cheng, H.-Y., Li, S.-C., Siao, Y.-Y., Kong, D.-C. and Jang, G.-W. (2010) Crystallinity and dimensional stability of biaxial oriented poly(lactic acid) films. Polymer Degradation and Stability. **95**, 1292-1298

53 Schmidt, S. C. and Hillmyer, M. A. (2001) Polylactide stereocomplex crystallites as nucleating agents for isotactic polylactide. Journal of Polymer Science Part B-Polymer Physics. **39**, 300-313

54 Mihai, M., Huneault, M. A., Favis, B. D. and Li, H. B. (2007) Extrusion foaming of semi-crystalline PLA and PLA/thermoplastic starch blends. Macromolecular Bioscience. **7**, 907-920

55 Hu, X., Nawaby, A. V., Naguib, H. E., Day, M., Ueda, K. and Lia, X. (2005) Polylactic acid (PLA)-CO_2 foams at sub-critical conditions. SPE ANTEC Technical Papers. pp. 187-190, Boston, MA

56 Smith, R. (2005) Biodegradable polymers for industrial applications. Woodhead; CRC Press, Cambridge, Boca Raton, Fla.

57 Urayama, H., Moon, S. I. and Kimura, Y. (2003) Microstructure and thermal properties of polylactides with different L- and D-unit sequences: Importance of the helical nature of the L-sequenced segments. Macromolecular Materials and Engineering. **288**, 137-143

58 Dorgan, J. R., Janzen, J., Clayton, M. P., Hait, S. B. and Knauss, D. M. (2005) Melt rheology of variable L-content poly(lactic acid). Journal of Rheology. **49**, 607-619

59 Xu, Y., You, M. and Qu, J. (2009) Melt rheology of poly (lactic acid) plasticized by epoxidized soybean oil. Wuhan University Journal of Natural Sciences. **14**, 349-354

60 Lehermeier, H. J. and Dorgan, J. R. (2001) Melt rheology of poly(lactic acid): Consequences of blending chain architectures. Polymer Engineering and Science. **41**, 2172-2184

61 Zhu, W. L., Wang, J., Park, C. B., Pop-Iliev, R. and Randall, J. (2009) Effects of chain branching on the foamability of polylactide. SPE ANTEC Technical Papers. pp. 41-45, Chicago, IL

62 Perego, G., Cella, G. D. and Bastioli, C. (1996) Effect of molecular weight and crystallinity on poly(lactic acid) mechanical properties. Journal of Applied Polymer Science. **59**, 37-43

63 Garlotta, D. (2001) A literature review of poly(lactic acid). Journal of Polymers and the Environment. **9**, 63-84

64 Colomines, G., Ducruet, V., Courgneau, C., Guinault, A. and Domenek, S. (2010) Barrier properties of poly(lactic acid) and its morphological changes induced by aroma compound sorption. Polymer International. **59**, 818-826

65 Aionicesei, E., Skerget, M. and Knez, Z. (2009) Mathematical modelling of the solubility of supercritical CO_2 in poly(L-lactide) and poly(D,L-lactide-co-glycolide). Journal of Supercritical Fluids. **50**, 320-326

66 Jacobsen, S. and Fritz, H. G. (1999) Plasticizing polylactide - The effect of different plasticizers on the mechanical properties. Polymer Engineering and Science. **39**, 1303-1310

67 Dorgan, J. R., Braun, B., Wegner, J. R. and Knauss, D. M. (2006) Poly(lactic acids): A brief review. In Degradable Polymers and Materials. pp. 102-125, American Chemical Society

68 Kumar, N., Ravikumar, M. N. V. and Domb, A. J. (2001) Biodegradable block copolymers. Advanced Drug Delivery Reviews. **53**, 23-44

69 Cheng, Y., Deng, S., Chen, P. and Ruan, R. (2009) Polylactic acid (PLA) synthesis and modifications: a review. Frontiers of Chemistry in China. **4**, 259-264

70 Ljungberg, N. and Wesslen, B. (2002) The effects of plasticizers on the dynamic mechanical and thermal properties of poly(lactic acid). Journal of Applied Polymer Science. **86**, 1227-1234

71 Baiardo, M., Frisoni, G., Scandola, M., Rimelen, M., Lips, D., Ruffieux, K. and Wintermantel, E. (2003) Thermal and mechanical properties of plasticized poly(L-lactic acid). Journal of Applied Polymer Science. **90**, 1731-1738

72 Piorkowska, E., Kulinski, Z., Galeski, A. and Masirek, R. (2006) Plasticization of semicrystalline poly(L-lactide) with poly(propylene glycol). Polymer. **47**, 7178-7188

73 Zhang, J. F. and Sun, X. Z. (2004) Mechanical and thermal properties of poly(lactic acid)/starch blends with dioctyl maleate. Journal of Applied Polymer Science. **94**, 1697-1704

74 Yu, L. and Chen, L. (2009) Polymeric materials from renewable resources. In Biodegradable Polymer Blends and Composites from Renewable Resources (Yu, L., ed.). pp. 1-15, John Wiley & Sons, Inc

75 Semba, T., Kitagawa, K., Ishiaku, U. S. and Hamada, H. (2006) The effect of crosslinking on the mechanical properties of polylactic acid/polycaprolactone blends. Journal of Applied Polymer Science. **101**, 1816-1825

76 Chen, G. X., Kim, H. S., Kim, E. S. and Yoon, J. S. (2005) Compatibilization-like effect of reactive organoclay on the poly(L-lactide)/poly(butylene succinate) blends. Polymer. **46**, 11829-11836

77 Anderson, K. S., Lim, S. H. and Hillmyer, M. A. (2003) Toughening of polylactide by melt blending with linear low-density polyethylene. Journal of Applied Polymer Science. **89**, 3757-3768

78 Wang, Y. B. and Hillmyer, M. A. (2000) Synthesis of polybutadiene-polylactide diblock copolymers using aluminum alkoxide macroinitiators. Kinetics and mechanism. Macromolecules. **33**, 7395-7403

79 Keener, T. J., Stuart, R. K. and Brown, T. K. (2004) Maleated coupling agents for natural fibre composites. Composites Part a-Applied Science and Manufacturing. **35**, 357-362

80 Lu, J. Z., Wu, Q. L. and McNabb, H. S. (2000) Chemical coupling in wood fiber and polymer composites: A review of coupling agents and treatments. Wood and Fiber Science. **32**, 88-104

81 Chowdhury, J. and Wolcott, M. (2007) Compatibilizer selection to improve mechanical and moisture properties of extruded wood-HDPE composites. Forest Products Journal. **57**, 46

82 Suryanegara, L., Nakagaito, A. N. and Yano, H. (2010) Thermo-mechanical properties of microfibrillated cellulose-reinforced partially crystallized PLA composites. Cellulose. **17**, 771-778

83 Huda, M. S., Drzal, L. T., Misra, M., Mohanty, A. K., Williams, K. and Mielewski, D. F. (2005) A study on biocomposites from recycled newspaper fiber and poly(lactic acid). Industrial & Engineering Chemistry Research. **44**, 5593-5601

84 Pilla, S., Gong, S., O'Neill, E., Rowell, R. M. and Krzysik, A. M. (2008) Polylactide-pine wood flour composites. Polymer Engineering and Science. **48**, 578-587

85 Oksman, K., Skrifvars, M. and Selin, J. F. (2003) Natural fibres as reinforcement in polylactic acid (PLA) composites. Composites Science and Technology. **63**, 1317-1324

86 Mathew, A. P., Oksman, K. and Sain, M. (2005) Mechanical properties of biodegradable composites from poly lactic acid (PLA) and microcrystalline cellulose (MCC). Journal of Applied Polymer Science. **97**, 2014-2025

87 Jordan, J., Jacob, K. I., Tannenbaum, R., Sharaf, M. A. and Jasiuk, I. (2005) Experimental trends in polymer nanocomposites - a review. Materials Science and Engineering a-Structural Materials Properties Microstructure and Processing. **393**, 1-11

88 Podsiadlo, P., Choi, S. Y., Shim, B., Lee, J., Cuddihy, M. and Kotov, N. A. (2005) Molecularly engineered nanocomposites: Layer-by-layer assembly of cellulose nanocrystals. Biomacromolecules. **6**, 2914-2918

89 Bocchini, S., Fukushima, K., Di Blasio, A., Fina, A., Frache, A. and Geobaldo, F. (2010) Polylactic acid and polylactic acid-based nanocomposite photooxidation. Biomacromolecules. **11**, 2919-2926

90 Krikorian, V. and Pochan, D. J. (2003) Poly (L-lactic acid)/layered silicate nanocomposite: Fabrication, characterization, and properties. Chemistry of Materials. **15**, 4317-4324

91 Jiang, L., Zhang, J. W. and Wolcott, M. P. (2007) Comparison of polylactide/nano-sized calcium carbonate and polylactide/montmorillonite composites: Reinforcing effects and toughening mechanisms. Polymer. **48**, 7632-7644

92 Bhardwaj, R. and Mohanty, A. K. (2007) Advances in the properties of polylactides based materials: A review. Journal of Biobased Materials and Bioenergy. **1**, 191-209

93 Pluta, M. (2004) Morphology and properties of polylactide modified by thermal treatment, filling with layered silicates and plasticization. Polymer. **45**, 8239-8251

94 Okamoto, M., Nam, P. H., Maiti, P., Kotaka, T., Nakayama, T., Takada, M., Ohshima, M., Usuki, A., Hasegawa, N. and Okamoto, H. (2001) Biaxial flow-induced alignment of silicate layers in polypropylene/clay nanocomposite foam. Nano Letters. **1**, 503-505

95 Wang, X. X., Kumar, V. and Li, W. (2007) Low density sub-critical CO_2-blown solid-state PLA foams. Cellular Polymers. **26**, 11-35

96 Matuana, L. M. and Faruk, O. (2010) Effect of gas saturation conditions on the expansion ratio of microcellular poly(lactic acid)/wood-flour composites. Express Polymer Letters. **4**, 621-631

97 Matuana-Malanda, L., Park, C. B. and Balatinecz, J. J. (1996) Characterization of microcellular foamed PVC/cellulosic-fibre composites. Journal of Cellular Plastics. **32**, 449-469

98 Mengeloglu, F. and Matuana, L. M. (2001) Foaming of rigid PVC/wood-flour composites through a continuous extrusion process. Journal of Vinyl & Additive Technology. **7**, 142-148

99 Matuana, L. M. and Mengeloglu, F. (2002) Manufacture of rigid PVC/wood-flour composite foams using moisture contained in wood as foaming agent. Journal of Vinyl & Additive Technology. **8**, 264-270

100 Matuana, L. M. and Li, Q. X. (2004) Statistical modeling and response surface optimization of extruded HDPE/wood-flour composite foams. Journal of Thermoplastic Composite Materials. **17**, 185-199

101 Reignier, J., Gendron, R. and Champagne, M. F. (2007) Extrusion foaming of poly(lactic acid) blown with Co-2: Toward 100% green material. Cellular Polymers. **26**, 83-115

102 Kramschuster, A., Pilla, S., Gong, S., Chandra, A. and Turng, L. S. (2007) Injection molded solid and microcellular polylactide compounded with recycled paper shopping bag fibers. International Polymer Processing. **22**, 436-445

103 Pilla, S., Kim, S. G., Auer, G. K., Gong, S. Q. and Park, C. B. (2009) Microcellular extrusion-foaming of polylactide with chain-extender. Polymer Engineering and Science. **49**, 1653-1660

104 Matuana, L. M. and Diaz, C. A. (2009) Microcellular PLA/cellulosic-fiber composites foamed with supercritical CO_2 through a continuous-extrusion process. In 10th International Conference on Wood & Biofiber Plastic Composites. p. 36, Forest Products Society, Madison, WI

105 Shah, B. L. and Matuana, L. M. (2004) Online measurement of rheological properties of PVC/wood-flour composites. Journal of Vinyl & Additive Technology. **10**, 121-128

106 Guo, G., Rizvi, G. M., Park, C. B. and Lin, W. S. (2004) Critical processing temperature in the manufacture of fine-celled plastic/wood-fiber composite foams. Journal of Applied Polymer Science. **91**, 621-629

107 Guo, G., Lee, Y. H., Rizvi, G. M. and Park, C. B. (2008) Influence of wood fiber size on extrusion foaming of wood fiber/HDPE composites. Journal of Applied Polymer Science. **107**, 3505-3511

108 Pilla, S., Kramschuster, A., Lee, J., Clemons, C., Gong, S. Q. and Turng, L. S. (2010) Microcellular processing of polylactide-hyperbranched polyester-nanoclay composites. Journal of Materials Science. **45**, 2732-2746

109 Matuana, L. M., Faruk, O. and Diaz, C. A. (2009) Cell morphology of extrusion foamed poly(lactic acid) using endothermic chemical foaming agent. Bioresource Technology. **100**, 5947-5954

CHAPTER 3

Study of Cell Nucleation in Microcellular Poly(lactic acid) Foamed with Supercritical CO_2 through a Continuous-Extrusion Process

This chapter is slightly modified from a research paper that was published in Industrial & Engineering Chemistry Research, 49 (5): 2186–2193 (2010). It is co-authored by L.M. Matuana and C.A. Diaz.

3.1 Abstract

Using a continuous-extrusion foaming process, this study examined the effect of the processing temperature on the melt viscosity, pressure drop rate, and cell-population density of poly(lactic acid) (PLA) foams. The study was intended to understand the nucleation mechanisms in order to generate microcellular structures in neat PLA in a continuous-extrusion process using CO_2 as the blowing agent. Not only did the temperature affect the melt viscosity but also the cell nucleation rate owing to its effect on the pressure drop rate. When processed at high temperature, the melt viscosity decreased and PLA nucleated fewer bubbles, irrespective of the PLA type (amorphous vs semicrystalline), because of the lower pressure drop rate in the system. Conversely, processing at a lower temperature significantly increased the cell nucleation rate for both PLA types owing to the fact that a high melt viscosity induced a high pressure drop rate. The addition of nanoclay allowed both homogeneous and heterogeneous nucleation to occur during the foaming process. The results showed that the processing temperature is a sensible parameter to produce microcellular PLA with cell densities on the order of 10^9 cells/cm^3 and cell sizes of around 10 μm.

3.2 Introduction

Poly(lactic acid) or PLA, a plant-based biodegrable plastic, exhibits many properties equivalent or superior to those of many petroleum-based plastics. However, few commercial applications exist because of its low impact resistance and higher cost over synthetic plastics and also its narrow processing window because of its sensitivity to hydrolytic and thermal degradation [1, 2].

Blending PLA with various additives such as lubricants, impact modifiers, plasticizers, or a second polymer broadens its applications [3, 4]. Given the additional cost associated with additives, unfortunately, this approach could increase the manufacturing cost [5]. Additionally, plasticizers and impact modifiers reduce the glass transition temperature of the resin, making the material more flexible and tougher while simultaneously reducing properties such as tensile strength and modulus. Previous efforts to overcome the cost of PLA included its blending with fillers such as cellulosic fibers [6]. However, lowered cost comes at the expense of other properties such as ductility (lower elongation at break) and lower impact resistance because the incorporated brittle cellulosic fibers alter the ductile mode of failure of the matrix, making the composites more brittle than neat polymer [7-9]. Efforts are continuously made to further reduce the cost of PLA while enhancing its flexibility and toughness.

Foaming technology, such as microcellular foaming, enhances the ductility and impact resistance of polymer matrices while also providing a significant expansion ratio and weight reduction in plastic parts. The high expansion ratio induced by foaming generally reduces the material cost and consumption in mass-produced plastic parts without a major compromise to the required properties [10, 11].

The microcellular foaming process dissolves an inert gas into a plastic to create a swarm of bubbles. Microcellular plastics, produced first in a batch process, involve a solid sample placed into a chamber under high pressure in an inert gas atmosphere (e.g., CO_2, N_2, etc.), wherein gas molecules diffuse into the plastic, forming a single-phase solution. Subsequently, nucleated and grown cells form by creating a thermodynamic instability (i.e., sudden pressure drop and/or temperature increase). Characterization of the morphology of microcellular foams includes cell-population densities of 10^9 cells/cm^3 and up and cell sizes smaller than 10 μm.

Recently, production of microcellular-foamed structures in PLA through a batch foaming addressed some limitations of the polymer [5, 12-15]. A previous study showed significant improvements in the volume expansion ratio (a 2-fold expansion over that of unfoamed PLA), impact resistance (up to a 4-fold increase over that of unfoamed PLA), strain at break (up to a 2-fold increase over that of unfoamed PLA), and toughness (up to a 4-fold increase over that of unfoamed PLA) by creating microcells in PLA samples, implying that foamed PLA exhibits enhanced ductility and impact resistance owing to the presence of microbubbles [5]. Nevertheless, implementation in the industrial production of foams remains unlikely in the batch foaming process used to generate cellular foamed structures in PLA because of its time-consuming nature, with multiple steps involved in the production of foamed samples, i.e., manufacture of solid samples, saturation of solid samples with gas (sorption experiments), and nucleation of cells and cell growth [16-18].

Limitations of a batch-microcellular foaming process have recently redirected attention to the manufacturing PLA foams through continuous-extrusion [19-21] and injection-molding processes [22] using supercritical physical blowing agents. The continuous microcellular foaming implies that the polymer/gas mixing requires a shorter time frame, from hours/days in the batch process to seconds in the continuous process. Using gas in supercritical conditions and the polymer in the molten state enhances the diffusion. The creation of the single-phase solution takes place in the extrusion barrel with thermodynamic instability produced by a high pressure drop at the exit of the extruder with the use of a nozzle. Nucleation, cell growth, and bubble stabilization occur while the polymer exits the die [23, 24]. Compared with the batch foaming process, relatively few publications feature continuous microcellular foaming of PLA in extrusion.

Reignier and co-workers recently reported a thorough investigation of the continuous-extrusion foaming of amorphous PLA, using CO_2 as a blowing agent [20]. They produced low-density foams under various injection pressures (2.5−9.0 MPa), CO_2 contents (1.8−9.3 wt %), and processing temperatures (90−100 °C) and by the addition of 0.5 wt % talc in the resin as a nucleating agent. Neat PLA foamed samples achieved densities down to 21 kg/m^3 with cell sizes of 60−420 μm and the number of nucleated cells (or cell densities) in the range of 10^4−10^8 cells/cm^3. The processing window associated with the low-density foams (21 kg/m^3) and high nucleation rate (10^7−10^8 cells/cm^3) involved an injection pressure (or an equivalent gas concentration of ~7 wt %) that corresponds to the critical pressure of CO_2 (7.38 MPa). Talc affected the cell morphology of PLA foams at lower CO_2 content (below ~5 wt %) because its addition into the matrix led to foams with much finer cells (~50 μm) and a higher cell-population density (10^8 cells/cm^3) compared to neat PLA foams (~400 μm and 10^4 cells/cm^3). This observation indicates that talc particles act as heterogeneous nucleating sites for cell nucleation. Nevertheless, the effect of talc on the cell morphology disappeared at higher CO_2 contents because the samples processed with or without talc had similar porous morphologies (~120 μm and 10^8 cells/cm^3).

Microcellular extrusion of semicrystalline PLA (2002D from NatureWorks) and starch (75% amylopectin and 25% amylose) blends using a CO_2 concentration of 8 wt % also created low-density open-cell foams (25 kg/m^3) [19]. Obtaining fine cell structure and low-density foam required interfacial modification of the PLA/starch blends using maleated PLA. The use of 0.5 wt % talc did not modify the foam structure, and the paper neglected to include the number of cells nucleated in PLA.

Microcellular extrusion of an amorphous PLA resin (6300D from NatureWorks) intended for fiber melt spinning has also been produced with CO_2 to study the expansion and cell-population density dependency on the amount of blowing agent (2−9 wt %) [21]. Densities in the 20−700 kg/m^3 range were produced with cell sizes of around 100 μm and a cell-population density of 10^5 cells/cm^3.

While these previous studies offered valuable insights, demonstrating the continuous-extrusion process of PLA foamed with supercritical CO_2, the morphology achieved in foamed PLA failed to satisfy the definition of microcellular foam because of a lower cell-population density (less than 10^9 cells/cm^3), with cells being larger than 60 μm in average size. Distinctions between these features and microcellular foam persist, where the cell-population density ranges from 10^9 cells/cm^3 and up, with fully grown cells being smaller than 10 μm in average size. Continuous extrusion of microcellular PLA with fine cell size (<10 μm) and high cell density (10^9 cells/cm^3 and up) will enable not only the production of foamed materials with superior mechanical properties compared to their solid counterparts but also the production of foamed structures in a thin film.

Because the nucleation process, which governs the cell morphology of materials, is one of the critical steps in producing microcellular plastics, the aim of the present study was to understand the nucleation mechanisms in neat PLA in order to generate microcellular structures in a continuous-extrusion process.

3.2.1 Background on Cell Nucleation

The basis for the continuous microcellular process lies in the concept of thermodynamic instability to promote high cell nucleation rates in a flowing polymer matrix. As pointed out by Park and co-workers [25], achieving these high nucleation rates involves first forming a polymer/gas solution under high pressure, followed by rapidly decreasing the solubility of gas in the polymer by a rapid pressure drop and/or a rapid temperature increase, which induces a greater thermodynamic instability in the system. Moreover, the classical nucleation theory (equation 3.1) predicts this phenomenon [26]:

$$N_{nucl} = C_o \cdot f_o \exp\left(\frac{-\Delta G}{kT}\right) \quad \text{(Equation 3.1)}$$

with N_{nucl} as the cell nucleation rate, C_o the concentration of gas molecules, f_o the frequency factor for gas molecules joining the nucleus, k Boltzmann's constant, T the system temperature, and ΔG the free energy barrier to initiate homogeneous (ΔG_{hom}) or heterogeneous (ΔG_{het}) cell nucleation, given by the equations

$$\Delta G_{\mathrm{hom}} = \frac{16 \cdot \pi \cdot \gamma_{bp}^{3}}{3 \Delta p^{2}} \quad \text{(Equation 3.2)}$$

$$\Delta G_{het} = \frac{16 \cdot \pi \cdot \gamma_{bp}^{3}}{3 \Delta p^{2}} f(\theta) \quad \text{(Equation 3.3)}$$

with γ_{bp} as the surface energy of the polymer-bubble interface, Δp the pressure drop of the gas/polymer solution [25], and $f(\theta)$ depending on the contact angle at the polymer-nucleating agent interface. Heterogeneous nucleation occurs at the interface between the polymer and another phase.

The classical nucleation theory (equation 3.1) predicts that minimization of the free energy barrier for nucleation (ΔG) will promote high cell nucleation rates. Although many relevant factors can affect the cell nucleation rate (equation 3.1), a higher pressure drop of the gas/polymer solution lowers the free energy barrier to initiate nucleation (eqs 1.2 and 1.3), resulting in a higher nucleation rate. Park and co-workers demonstrated that the pressure drop rate in the die (*-dp/dt*) given by equation 3.4 correlates with the thermodynamic instability necessary to nucleate high numbers of cells; i.e., the higher the pressure drop rates, the higher the cell-population densities [25, 27-29]:

$$\frac{-dp}{dt} \approx \frac{-\Delta p}{\Delta t} \approx \frac{-\Delta p \cdot q}{\pi \cdot r_o^2 \cdot L} \qquad \text{(Equation 3.4)}$$

with Δt as the average residence time of the flowing polymer/gas solution in the nozzle, L the length of the nozzle, q the volumetric flow rate of the polymer through the nozzle, and r_o the radius of the nozzle.

Because the pressure drop rate depends on the nozzle geometry (r_o and L) and polymer flow properties (Δp and q), the potential in using these parameters as effective process and material variables for controlling the cell nucleation in continuous microcellular processing exists.

Selection in this study designated control of the melt rheology through processing temperatures as a strategy to alter the rate of pressure drop during foaming. The processing temperature has a great influence on the density and porous morphology of foams because of its effect on the melt viscosity, as described by the Arrhenius relation

$$\eta = A_o \exp\left(\frac{E_a}{RT}\right) \qquad \text{(Equation 3.5)}$$

with η as the melt viscosity, A_o a constant, R the universal gas constant, T the absolute temperature, and E_a the activation energy of melt flow [30].

Generally, as the processing temperature is varied, the melt viscosity changes inversely; i.e., the higher the processing temperature, the lower the melt viscosity, and vice versa, subsequently leading to a change in the pressure generated during the extrusion process. The melt viscosity, an important parameter in foaming, affects the pressure built into the system, thus affecting the cell nucleation rate. Additionally, the melt viscosity plays an important role during the growth and stabilization of nucleated cells. Consequently, the effect of the processing temperature on the melt viscosity, pressure drop rate, and cell-population density must be examined to understand the nucleation mechanisms in neat and filled PLA foams.

3.3 Experimental

3.3.1 Materials

Two different grades of PLA from NatureWorks were used as matrices. The semicrystalline (PLA 2002D) and amorphous (PLA 8302D) grades had d-lactic contents of approximately 4% and 10%, respectively. Table 3.1 lists the properties of these resins measured by the authors [31]. Montmorillonite clay modified with methyl, tallow (~65% C18, ~30% C16, and ~5% C14), and quaternary bis(2-hydroxyethyl)ammonium salt (Cloisite 30B) purchased from Southern Clay Products (Gonzales, TX) was used as the nucleating agent, and CO_2 with a purity of 99.5% supplied by Airgas was the physical foaming agent.

Table 3.1. Characteristics of different PLA resins used in this study [31].

		Melt properties		Thermal properties	
PLA grade	Density of the solid (g/cm^3)	MFR (g/10 min)	ρ_m (g/cm^3)[a]	χ_c (%)	T_m (°C)
2002D semicrystalline	1.25	3.4	1.142	15	149
8302D amorphous	1.25	6.5	1.149	1.2	

[a] Value used in the calculation of the volumetric flow rate of the polymer melt (*q*) in equation 3.4.

3.3.2 Rheological Measurements

The alterations in the melt viscosity induced by the processing temperature remain vitally important for cell nucleation as well as during cell growth and stabilization. While facilitating bubble growth requires melts with relatively low viscosity, the viscosity must increase by cooling or strain hardening to a level adequate for bubble stabilization. Consequently, understanding the conditions for a proper cell nucleation as well as expansion and stabilization of the cellular structure entails examination of the dependence of the melt viscosity on the temperature.

The viscosities of semicrystalline PLA (PLA 2002D) were measured as a function of the temperature, in the range of 160−205 °C, with 15 °C increments. Measurements were performed online on an Intelli-Torque Plasticorder Torque rheometer (C. W. Brabender Instruments Inc., South Hackensack, NJ) equipped with a 19.1 mm single-screw extruder (*L*/*D* ratio 30:1; C. W. Brabender Instruments Inc., South Hackensack, NJ). The polymer was fed into the extruder and pushed through a capillary die with different *L*/*D* ratios (10:1, 15:1, and 20:1) of capillary inserts. The extruder's barrel temperature profile and die temperature were kept constant to maintain a constant melt temperature for accurate viscosity measurements. However, the rotational screw speeds varied from 10 to 50 rpm to generate different shear rates during experiments [32]. Experiments followed ASTM standard D5422 without injection of CO_2 into the system.

The apparent shear stress (τ_a), which measures the resistance to flow through a capillary die, is given by

$$\tau_a = \frac{\Delta P}{4(L/D)} \qquad \text{(Equation 3.6)}$$

with ΔP as the pressure drop across the capillary and L/D the length-to-diameter ratio of the capillary insert. The apparent shear rate at the wall of the capillary for a Newtonian fluid uses the following formula:

$$\dot{\gamma}_a = \frac{32 \cdot Q}{\pi \cdot D^3} \qquad \text{(Equation 3.7)}$$

with Q as the volumetric flow rate of the polymer melt and D the diameter of the capillary.

Obtaining the true melt viscosity calls for correction of the data to account for an excess of pressure drop at the capillary entry (Bagley correction) and the shear-thinning effect (Rabinowitsch correction) [32, 33].

First, the Bagley correction was applied to the shear-stress values as an additional length of the capillary “end effect” (e). Measurements of the viscosity at the same shear rate with at least two different capillaries were performed to apply the Bagley correction, calculated as follows:

$$\tau_w = \frac{\Delta P}{4(L/D + e)} \qquad \text{(Equation 3.8)}$$

Second, the apparent shear rate, which gives only Newtonian behavior (constant viscosity), required a correction for shear-thinning fluids (pseudoplastic fluids). The Rabinowitsch correction was done to calculate the true shear rate at the wall ($\dot{\gamma}_w$) of the capillary by using the following equation:

$$\dot{\gamma}_w = \frac{3n+1}{4n}\dot{\gamma}_a \qquad \text{(Equation 3.9)}$$

with *n* as the flow behavior index obtained as the slope of the linear plot of log τ_w versus log $\dot{\gamma}_a$. The true melt viscosity (η) was then calculated, from the corrected shear stress and shear rate, as follows:

$$\eta = \frac{\tau_w}{\dot{\gamma}_w} \qquad \text{(Equation 3.10)}$$

3.3.3 Compounding of Materials

PLA in pellet or powder form used in the formulations was oven-dried at 55 °C for 8 h prior use. Two different foamed formulations were made including (i) neat PLA and (ii) PLA filled with nanoclay.

Neat PLA (formulation i) was foamed by feeding dried pellets directly into the extruder. In the case of PLA/nanoclay (formulation ii), the resin was first ground to enhance the dispersion of nanoclay. Powdered PLA was then mixed with 5 wt % nanoclay (based on the amount of PLA) in a kitchen mixer (Blender MX1050XTS from Waring Commercial Xtreme, Torrington, CT) at 22 000 rpm for 30 s. The blended material was oven-dried at 55 °C for 8 h prior to foaming experiments.

3.3.4 Extrusion Foaming

Figure 3.1 shows a schematic of the foaming system used in this study, similar to the one developed by Park and associates [23, 24]. The process used a 19.1 mm single-screw extruder (*L*/*D* ratio 30:1; C. W. Brabender Instruments Inc., South Hackensack, NJ) with a mixing screw powered by a 5 hp driver with a speed-control gearbox (Brabender Prep Center). A positive-displacement syringe pump (model 260D; Teledyne Isco, Lincoln, NE) delivered the gas into the extrusion barrel. A diffusion-enhancing device (static mixer Omega FMX8441S) attached to the extruder ensured the creation of a polymer/gas solution with a rapid pressure drop induced by a nozzle die with 0.5 mm diameter. All foaming experiments were performed with a fixed amount of gas injected (5 wt %) and a screw rotational speed of 80 rpm. Table 3.2 summarizes the processing temperatures used for each PLA grade. Samples were collected after the process reached steady-state conditions and were cooled by air.

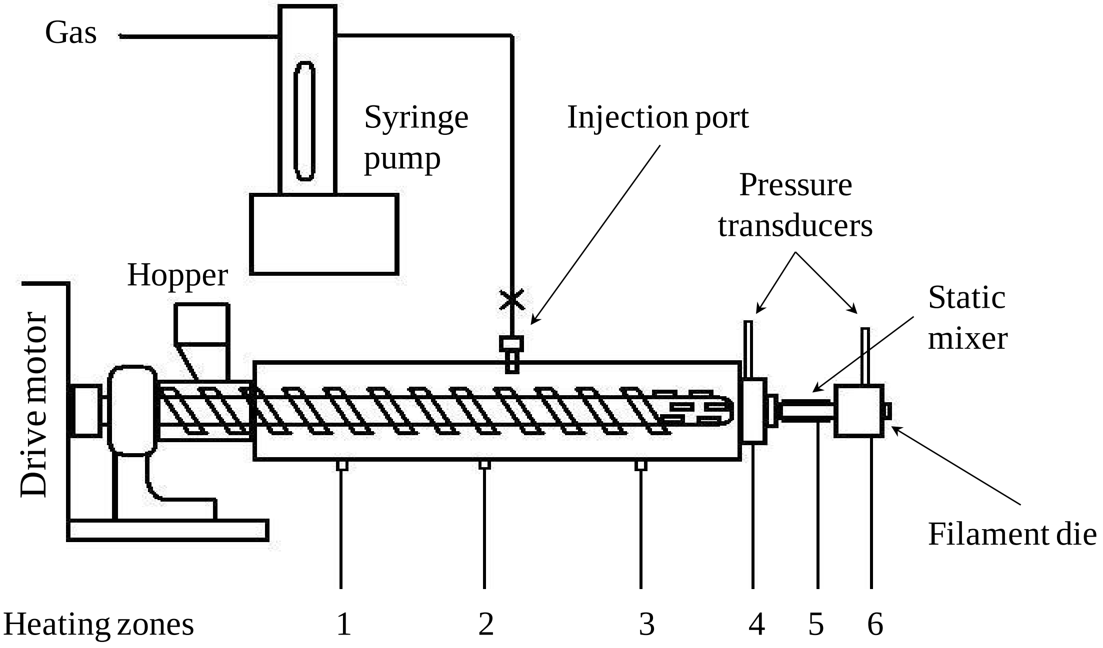

Figure 3.1. Schematic of the single-screw extrusion foaming system.

Table 3.2. Definition of temperature profiles according to the set temperature on each heating zone shown in Figure 3.1.

PLA grade	Temperature profile level	Set temperature for each heating zone (°C)					
		1	2	3	4	Static mixer	Nozzle
amorphous(8302D)	high	180	180	175	165	165	160
	intermediate	170	170	165	155	155	150
	low	160	160	155	145	145	140
semicrystalline(2002D)	high	210	210	205	195	195	190
	intermediate	190	190	185	185	175	170
	low	170	170	165	155	155	150

Foamed extrudates were collected to measure the mass output (or the volumetric flow rate of the polymer through the nozzle *q*) needed in the calculation of the average residence time of the flowing polymer/gas solution in the nozzle (equation 3.4), while a pressure transducer installed in the filamentary die (Figure 3.1) measured the pressure drop of the polymer/gas solution at the steady state of each processing temperature. These two parameters are needed to estimate the pressure drop rate according to equation 3.4.

3.3.4 Scanning Electron Microscopy (SEM)

The morphology of the foamed samples was analyzed by SEM. SEM images were taken using either a JEOL JSM-6400 or a JEOL JSM 7500F (field emission) scanning electron microscope with accompanying *analiSYS* software. The accelerating voltage was set to either 12 kV for JSM-6400 or 5 kV for JSM-7500F. Samples were fractured in liquid nitrogen and coated with gold prior to the test.

Images obtained by the SEM micrographs allowed for characterization of the number of cells nucleated per unit volume of the original unfoamed polymer or cell-population density (N_0) [17]:

$$N_o = \left(\frac{nM^2}{A}\right)^{3/2}\left[\frac{1}{1-V_f}\right] \qquad \text{(Equation 3.11)}$$

with *n* as the number of cells in the micrographs and *A* and *M* the area and magnification factor of the micrograph, respectively. V_f, the void fraction, was measured following the approach described in our previous work [5]. The densities of both unfoamed and foamed PLA samples were measured according to ASTM standard D792 (Buoyancy method) to calculate the void fraction.

SEM images made possible the measurement of the cell size by averaging the diameters of at least 100 randomly selected cells using well-established procedures [7, 16, 17, 34-36].

3.4 Results and Discussion

3.4.1 Rheological Characteristics of PLA

The melt viscosity of PLA, an important parameter in foaming, affects the pressure built into the system (the cell nucleation rate) and plays a key role during the growth of the newly formed nuclei and the subsequent stabilization of the foamed cellular structure.

Figure 3.2 illustrates a double-logarithmic plot of the true viscosity versus the true shear rate of semicrystalline PLA at a temperature range of 160−205 °C. Irrespective of the test temperature, PLA melts showed shear-thinning (i.e., pseudoplastic) behavior because their viscosities decreased linearly with increasing shear rate and with *n* values of less than 1 (Table 3.3). The results indicate that the melts obeyed the power law

$$\eta = K \cdot \left(\dot{\gamma}_w\right)^{n-1} \qquad \text{(Equation 3.12)}$$

where *K* and *n*, listed in Table 3.3 and obtained from a linear regression of the curves in Figure 3.2, represent the melt viscosity coefficient and flow index, respectively.

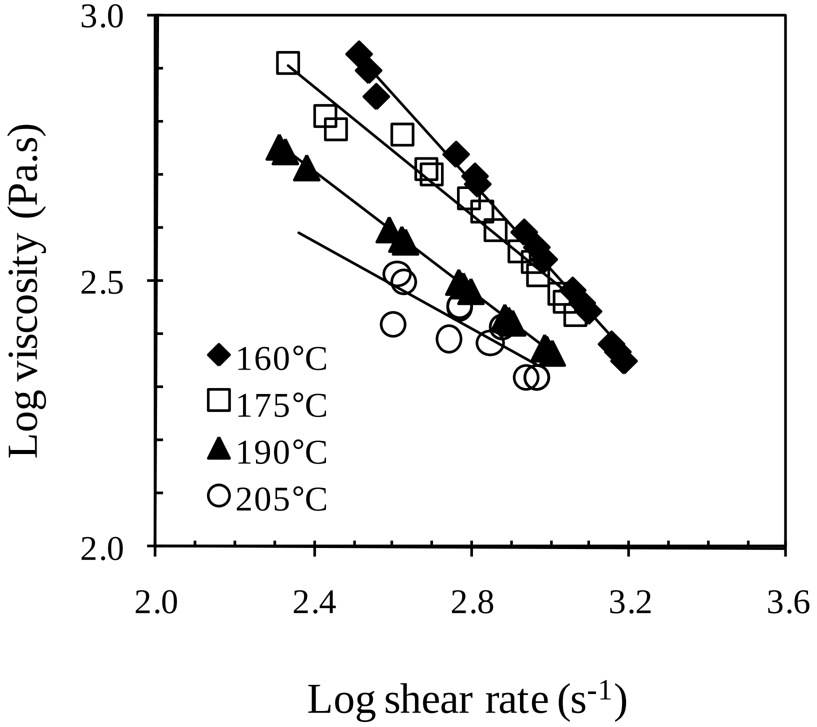

Figure 3.2. True viscosity of semicrystalline PLA (2002D) as a function of the true shear rate at various temperatures (160, 175, 190, and 205 °C).

Table 3.3. Melt viscosity coefficient (*K*) and power law flow index (*n*) for semicrystalline PLA (2002D) measured at various temperatures.

	regression parameters $\eta = K^{n-1}$		
temperature (°C)	K (kPa·s^{n})	n	R^{2}
160	104.11	0.169	0.9932
175	20.26	0.399	0.9674
190	11.38	0.438	0.9999
205	3.71	0.586	0.6966

This decreased viscosity of the melts with increasing shear rate was expected because shearing better orients the molecular chains of the polymer and reduces the number of entanglements, which results in decreased interactions between chain segments [30].

Increasing the test temperature decreased the melt viscosity of PLA (Figure 3.2) because of the greater free space available for molecular chain motion at higher temperature. In other terms, the ability of macromolecular chain motion is enhanced and the resistance between the melt layers decreases by increasing the processing temperature, leading to a reduction in the melt viscosity. With a rise in the test temperature, the melt viscosity coefficient (K) decreased, whereas the flow index (n) increased significantly (Table 3.3), suggesting that the melts became less viscous (lower K values) and less pseudoplastic (higher n values). However, it is worth mentioning that the obtained viscosity data at a higher processing temperature of 205 °C (Figure 3.2) had a significant scatter ($R^2 = 0.6966$ in Table 3.3) probably because of the sensitivity of PLA to hydrolytic and thermal degradation when processed at higher temperature, particularly at lower shear rate or equivalently longer residence time [1, 2]. Moreover, the reduction in the melt viscosity of PLA as a function of the test temperature followed the Arrhenius-type relationship given in equation 3.5 because the logarithmic viscosity of PLA varied linearly with the reciprocal temperature (Figure 3.3). The activation energy of viscous flow (E_a) obtained from the slopes of the curves shown in Figure 3.3 decreased significantly with increasing shear rate (Table 3.4), implying that the effect of the test temperature on the melt viscosity became less pronounced at higher shear rate. Nevertheless, it should be pointed out that, because the shear rate encountered in the extruder during processing is in the range of 10^2–10^3 s^{-1} [37], the temperature profile used during the extrusion foaming process will significantly affect the melt viscosity (Figure 3.2).

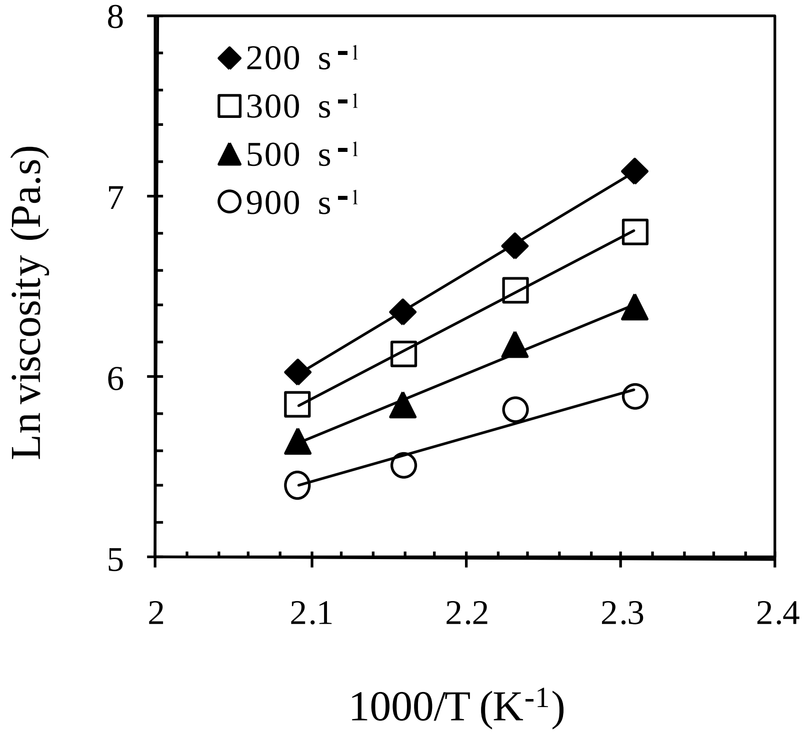

Figure 3.3. True viscosity of semicrystalline PLA (2002D) as a function of the reciprocal temperatures (1/*T*) at various shear rates (200, 300, 500, and 900 s^{-1}).

Table 3.4. Activation energy (E_a) and the A_0 constant for viscous flow of semicrystalline PLA (2002D) at various shear rates.

	shear rate			
	$200\ s^{-1}$	$300\ s^{-1}$	$500\ s^{-1}$	$900\ s^{-1}$
E_a (kJ/mol)	43.02	36.99	29.4	20.66
A_0 (Pa·s)	0.0082	0.0316	0.173	1.2229
R^2	0.999	0.999	0.989	0.938

Not only did the temperature affect the melt viscosity but also the pressure developed in the system (or pressure drop Δp) during the extrusion of microcellular PLA. Table 3.5 summarizes the effect of the different processing temperatures on the pressure drop, average residence time of the flowing PLA/CO_2 solution, and calculated pressure drop rate. Processing at lower temperature developed higher pressure in the system, regardless of the PLA grade. With insensitivity of the average residence time of flow through the nozzle to the processing temperatures, increasing the pressure in the system resulted in higher pressure drop rates.

Table 3.5. Effect of the processing temperature on the pressure drop rate for different grades of PLA.

PLA grade	temperature profile level	Δp (MPa)	flow rate (cm^3/s)	residence time (10^{-4} s)	pressure drop rate (GPa/s)
amorphous(8302D)	high	12.4	0.772	3.814	32.8
	intermediate	14.1	0.798	3.692	38.3
	low	16.6	0.81	3.634	45.5
semicrystalline(2002D)	high	12.1	0.832	3.542	34.1
	intermediate	14.5	0.809	3.639	39.8
	low	17.9	0.836	3.524	50.9

It should be pointed out that the viscosity of PLA illustrated in Figures 3.2 and 3.3 was measured without injection of CO_2 into the extrusion system. The dissolution of supercritical fluids in the polymer significantly reduces the viscosity of the polymer because of the plasticizing effect of the dissolved gas and the increased free volume [28, 29, 36, 38, 39]. Similarly, the viscosity of the gas/polymer solutions (e.g., polystyrene/CO_2 and polycarbonate/CO_2) decreases with increasing temperature [29]. In the same manner, it is expected that the viscosity of the PLA/CO_2 solution will also decrease with increasing temperature. Although the viscosity of PLA reported in this study was measured without the addition of any CO_2 in the system, it is believed that the PLA/CO_2 solution processed at a lower temperature profile would have higher melt viscosity than the PLA/CO_2 solution processed at a higher temperature profile. Moreover, because the pressure drop (Δp) is related to the shear stress (equation 3.6), i.e., viscosity, the data summarized in Table 3.5 clearly support this assertion; processing at lower temperature developed a higher pressure drop of the PLA/CO_2 solution in the system as a result of the viscosity increase.

3.4.2 Effect of the Temperature Profile on the Morphology

Figure 3.4 shows the effects of the processing temperature and PLA grade on the cell morphology of microcellular foamed samples. Table 3.6 lists the cell-population density and average cell size of foamed PLA.

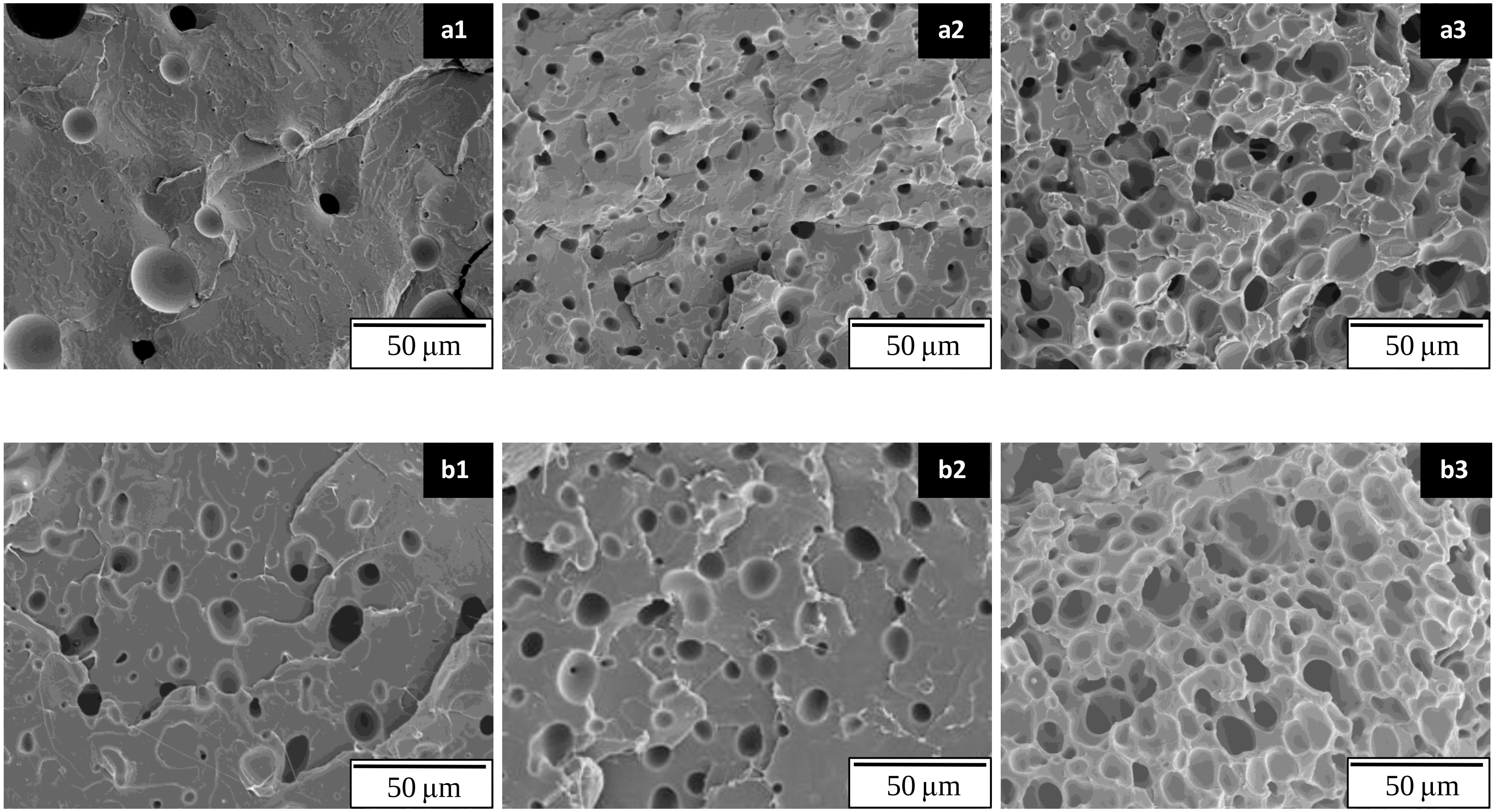

Figure 3.4. SEM micrographs showing the effects of the processing temperature profile levels and PLA grade on the cell morphology for amorphous PLA processed at high (a1), intermediate (a2), and low (a3) temperatures as well as for semicrystalline PLA processed at high (b1), intermediate (b2), and low (b3) temperatures. All pictures were taken at the same magnification (750X).

Table 3.6. Pressure drop rate, cell-population density, and average cell size of foamed PLA samples.

	PLA grade			
	cell-population density (10^9 cells/cm^3)		average cell size (μm)	
temperature profile level	amorphous	semicrystalline	amorphous	semicrystalline
high	0.01	0.04	18.3	16.3
intermediate	0.2	0.1	12.1	15.2
low	1	1.5	7.9	6.9

When processed at high temperature, PLA nucleated fewer bubbles, irrespective of the PLA type (parts a1 and b1 of Figure 3.4). Processing at high temperature lowered the melt viscosity, thus preventing sufficient pressure from building in the system to form a one-phase PLA/CO_2 solution and, consequently, resulting in a lower pressure drop rate. The diffusivity (D) of CO_2 could also account for the lower nucleation rate observed at high processing temperature because the diffusivity of CO_2 is a function of the temperature, as given by the following Arrhenius-type relation [29]:

$$D = D_o \exp\left(-\frac{\Delta E_D}{RT}\right) \qquad \text{(Equation 3.13)}$$

with D_0 as the preexponential factor (diffusion coefficient constant), ΔE_D the activation energy for diffusion of gas in a polymer, R the universal gas constant, and T the processing temperature in the absolute scale.

As the processing temperature was increased, the viscosity of the PLA/CO_2 solution decreased (according to equation 3.5) and the gas diffusion rate into the polymer increased (according to equation 3.13) because of the mobility of gas molecules at high temperature. Therefore, it is believed that the increased gas diffusivity (higher gas-depletion rate), which promoted gas loss to the environment, also accounted for a smaller amount of CO_2 available for cell nucleation. When the processing temperature was too high, the surface of the extrudate was not effective in blocking gas escape. Very similar results were obtained by Park et al. in a study on low-density microcellular foam processing of high-impact polystyrene in extrusion using CO_2 as a blowing agent [24].

Conversely, processing at a lower temperature significantly increased the cell nucleation rate (Figures 3.4a3 and 3.4b3) for both PLA types because of the fact that a high melt viscosity induced a high pressure drop rate. This trend was expected because the higher pressure drop rate of the polymer/gas solution lowers the free energy barrier to initiate nucleation, resulting in a higher nucleation rate. These results agree with those reported by other investigators showing that increasing the pressure drop rate significantly increased the number of nucleated cells [25, 27-29]. Additionally, the nucleation of bubbles appropriately used most of the gas injected into the system due to the lower gas diffusion (lower gas-depletion rate) at low processing temperature (equation 3.13). Higher melt viscosity also prevented gas depletion in the PLA/CO_2 solution when the processing temperature was lower.

The data presented in Table 3.6 also indicate the importance of a larger pressure drop rate occurring at low processing temperature on the number of nucleated cells. The cell-population density, by reduction of the processing temperature from a high to low profile, marked a 2 orders of magnitude increase. Microcellular morphology was successfully produced in PLA through a continuous-extrusion process. Irrespective of the PLA type, the number of nucleated bubbles, with an order of 10^9 cells/cm^3 and an average cell size of less than 10 μm, satisfies the definition of microcellular plastics. As the melt viscosity increased with a decrease in the temperature, the cell coalescence decreased, and, consequently, most nucleated cells survived during the cell growth step.

3.4.3 Effect of the Nucleating Agent

As was previously mentioned, heterogeneous nucleation occurs at the interface between the polymer and another phase. Generally, the addition of external nucleating agents (e.g., solid particles such as talc, nanoclay, etc.) provides sites for heterogeneous nucleation of cells because of their nature in reducing the surface energy at the polymer−particle interface [40]. The free energy barrier for nucleation (ΔG_{het}), reduced by lowering the surface energy of the polymer−particle interface (equation 3.3), promotes high cell nucleation rates (equation 3.1).

The effect of nanoclay addition on the cell morphology of semicrystalline PLA foams was assessed by filling semicrystalline PLA with 5 wt % nanoclay. This formulation was microcellular foamed using the low-temperature profile for semicrystalline PLA (Table 3.2), which provided the best conditions for microcellular PLA foamed in a continuous-extrusion process. Figure 3.5 presents SEM micrographs illustrating this effect.

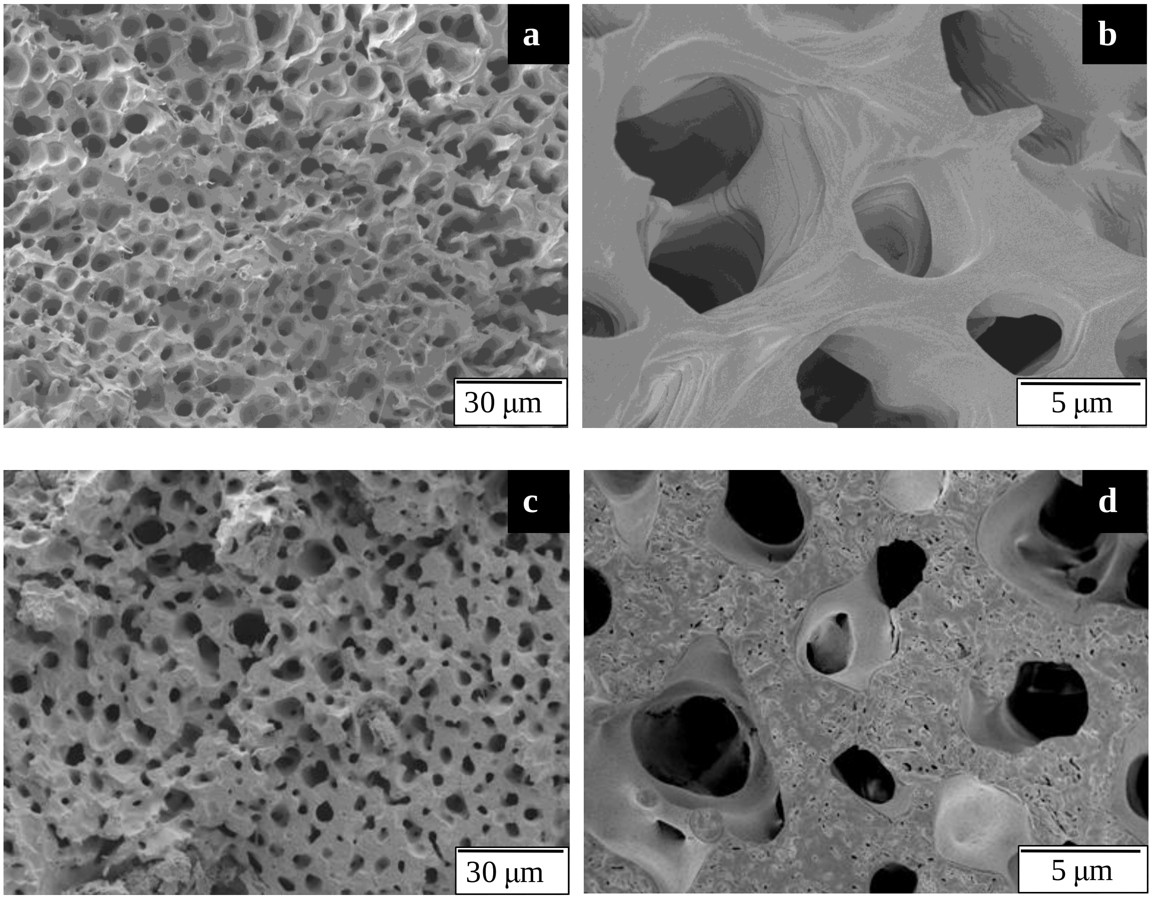

Figure 3.5. Field-emission SEM micrographs (JEOL JSM 7500F) illustrating the effect of nanoclay addition on the cell morphology of semicrystalline PLA foams: (a and b) without nanoclay; (c and d) with nanoclay. Micrographs a and c were taken at low magnification (750X), whereas micrographs b and d were taken at high magnification (5000X).

The SEM images taken at low magnification revealed no apparent differences in morphology between the neat PLA (Figure 3.5a) and PLA filled with nanoclay (Figure 3.5c), suggesting that the addition of a nucleating agent had no effect on the homogeneous nucleation. By contrast, SEM images taken at high magnification revealed noticeable differences between the neat and filled PLA. For the neat PLA, observations indicate a solid membrane between grown bubbles (Figure 3.5b), whereas this membrane contained a large number of fine cells in PLA filled with nanoclay (Figure 3.5d), with the fine cells measured in nanometers. Increased cell nucleation accounts for this behavior because of the presence of the heterogeneous nucleation sites. This bicellular structure was also observed in our previous work on microcellular foaming of rigid PVC using CO_2 as the foaming agent in both batch and continuous-extrusion processes [7, 41] and may be indicative of two nucleation stages (homogeneous and heterogeneous) occurring during foaming.

It is believed that larger cells were nucleated earlier from the rapid pressure drop in the nozzle (homogeneous nucleation), while the finer cells resulted later from the presence of solid particles (nanoclay) in PLA, which provided sites for heterogeneous nucleation because of their nature in reducing the surface energy at the polymer–particle interface. Cell nucleation and cell growth are competing processes for gas consumption during foaming [36]. The final cell size is determined by the amount of gas used for the cell growth in the end [7]. Because the available amount of gas was shared by both homogeneously and heterogeneously nucleated cells growing simultaneously, cells nucleated earlier (homogeneous) had a longer time for growth, resulting in cells of larger size compared to cells nucleated later (heterogeneous), which had a shorter time for growth, leading to cells of smaller size.

3.5 Conclusions

The aim of the present study was to understand the nucleation mechanisms in PLA in order to generate microcellular structures in a continuous-extrusion process using CO_2 as the blowing agent. Particular emphasis also focused on assessing the effect of nanoclay as a nucleating agent. Examination of the effect of the processing temperature on the melt viscosity, pressure drop rate, and cell-population density aided in understanding the nucleation mechanisms in PLA foams.

The processing temperature had a strong effect of the rheology of the melt. Increasing the test temperature significantly decreased the melt viscosity of PLA, and this reduction in the melt viscosity of PLA as a function of the test temperature followed the Arrhenius-type relationship.

Not only did the temperature affect the melt viscosity but also the cell nucleation rate because of its effect on the pressure developed in the system during the extrusion of microcellular PLA. Microcellular morphology was successfully produced in PLA through a continuous-extrusion process. Irrespective of the PLA type, the number of nucleated bubbles, with an order of 10^9 cells/cm^3 and an average cell size of less than 10 μm, satisfies the definition of microcellular plastics.

When processed at high temperature, PLA nucleated fewer bubbles, irrespective of the PLA type. Processing at high temperature lowered the melt viscosity, thus preventing sufficient pressure from building into the system and, consequently, resulting in a lower pressure drop rate. The increased gas diffusivity, which promoted gas loss to the environment, also accounted for a smaller amount of injected CO_2 available for cell nucleation. Conversely, processing at a lower temperature significantly increased the cell nucleation rate for both PLA types because of the fact that a high melt viscosity induced a high pressure drop rate.

The presence of the nanoclay did not affect the homogeneous nucleation but increased the heterogeneous nucleation, with the fine cells measured in nanometers. The addition of nanoclay allowed both homogeneous and heterogeneous nucleation stages to occur during the foaming process.

3.6 Acknowledgment

This project was supported by the National Research Initiative of the USDA Cooperative State Research, Education and Extension Service (Grant 2006-35504-17414). The authors gratefully acknowledge Valerie Edge, an undergraduate student at Michigan State University, for her thoughtful and constructive comments on the paper.

REFERENCES

REFERENCES

1 Garlotta, D. (2001) A literature review of poly(lactic acid). Journal of Polymers and the Environment. **9**, 63-84

2 Auras, R., Harte, B. and Selke, S. (2004) An overview of polylactides as packaging materials. Macromolecular Bioscience. **4**, 835-864

3 Jacobsen, S. and Fritz, H. G. (1999) Plasticizing polylactide - The effect of different plasticizers on the mechanical properties. Polymer Engineering and Science. **39**, 1303-1310

4 Baiardo, M., Frisoni, G., Scandola, M., Rimelen, M., Lips, D., Ruffieux, K. and Wintermantel, E. (2003) Thermal and mechanical properties of plasticized poly(L-lactic acid). Journal of Applied Polymer Science. **90**, 1731-1738

5 Matuana, L. M. (2008) Solid state microcellular foamed poly(lactic acid): Morphology and property characterization. Bioresource Technology. **99**, 3643-3650

6 Pilla, S., Gong, S., O'Neill, E., Rowell, R. M. and Krzysik, A. M. (2008) Polylactide-pine wood flour composites. Polymer Engineering and Science. **48**, 578-587

7 Matuana, L. M., Park, C. B. and Balatinecz, J. J. (1997) Processing and cell morphology relationships for microcellular foamed PVC/wood-fiber composites. Polymer Engineering and Science. **37**, 1137-1147

8 Matuana, L. M., Park, C. B. and Balatinecz, J. J. (1997) The effect of low levels of plasticizer on the rheological and mechanical properties of polyvinyl chloride newsprint-fiber composites. Journal of Vinyl & Additive Technology. **3**, 265-273

9 Matuana, L. M., Woodhams, R. T., Balatinecz, J. J. and Park, C. B. (1998) Influence of interfacial interactions on the properties of PVC/cellulosic fiber composites. Polymer Composites. **19**, 446-455

10 Waldman, F. A. (1982) The processing of microcellular foam. S.M. Thesis, Department of Mechanical Engineering, Massachusetts Institute of Technology, Cambridge, MA

11 Martini, J. E., Suh, N. P. and Waldman, F. A. (1984) Microcellular closed cell foams and their method of manufacture U. S. 4,473,665 Patent

12 Fujimoto, Y., Ray, S. S., Okamoto, M., Ogami, A., Yamada, K. and Ueda, K. (2003) Well-controlled biodegradable nanocomposite foams: From microcellular to nanocellular. Macromolecular Rapid Communications. **24**, 457-461

13 Ema, Y., Ikeya, M. and Okamoto, M. (2006) Foam processing and cellular structure of polylactide-based nanocomposites. Polymer. **47**, 5350-5359

14 Liao, X., Nawaby, A. V., Whitfield, P., Day, M., Champagne, M. and Denault, J. (2006) Layered open pore poly(L-lactic acid) nanomorphology. Biomacromolecules. **7**, 2937-2941

15 Wang, X. X., Kumar, V. and Li, W. (2007) Low density sub-critical CO_2-blown solid-state PLA foams. Cellular Polymers. **26**, 11-35

16 Mengeloglu, F. and Matuana, L. M. (2001) Foaming of rigid PVC/wood-flour composites through a continuous extrusion process. Journal of Vinyl & Additive Technology. **7**, 142-148

17 Matuana, L. M. and Mengeloglu, F. (2002) Manufacture of rigid PVC/wood-flour composite foams using moisture contained in wood as foaming agent. Journal of Vinyl & Additive Technology. **8**, 264-270

18 Matuana, L. M. and Li, Q. X. (2004) Statistical modeling and response surface optimization of extruded HDPE/wood-flour composite foams. Journal of Thermoplastic Composite Materials. **17**, 185-199

19 Mihai, M., Huneault, M. A., Favis, B. D. and Li, H. B. (2007) Extrusion foaming of semi-crystalline PLA and PLA/thermoplastic starch blends. Macromolecular Bioscience. **7**, 907-920

20 Reignier, J., Gendron, R. and Champagne, M. F. (2007) Extrusion foaming of poly(lactic acid) blown with Co-2: Toward 100% green material. Cellular Polymers. **26**, 83-115

21 Lee, S. T., Kareko, L. and Jun, J. (2008) Study of thermoplastic PLA foam extrusion. Journal of Cellular Plastics. **44**, 293-305

22 Kramschuster, A., Pilla, S., Gong, S., Chandra, A. and Turng, L. S. (2007) Injection molded solid and microcellular polylactide compounded with recycled paper shopping bag fibers. International Polymer Processing. **22**, 436-445

23 Park, C. B. and Cheung, L. K. (1997) A study of cell nucleation in the extrusion of polypropylene foams. Polymer Engineering and Science. **37**, 1-10

24 Park, C. B., Behravesh, A. H. and Venter, R. D. (1998) Low density microcellular foam processing in extrusion using CO_2. Polymer Engineering and Science. **38**, 1812-1823

25 Park, C. B., Baldwin, D. F. and Suh, N. P. (1995) Effect of the pressure drop rate on cell nucleation in continuous processing of microcellular polymers. Polymer Engineering and Science. **35**, 432-440

26 Colton, J. S. and Suh, N. P. (1987) The nucleation of microcellular thermoplastic foam with additives .1. Theoretical considerations. Polymer Engineering and Science. **27**, 485-492

27 Xu, X., Park, C. B., Xu, D. L. and Pop-Iliev, R. (2003) Effects of die geometry on cell nucleation of PS foams blown with CO_2. Polymer Engineering and Science. **43**, 1378-1390

28 Lee, J. W. S., Wang, K. Y. and Park, C. B. (2005) Challenge to extrusion of low-density microcellular polycarbonate foams using supercritical carbon dioxide. Industrial & Engineering Chemistry Research. **44**, 92-99

29 Wong, A., Leung, S. N., Li, G. Y. G. and Park, C. B. (2007) Role of processing temperature in polystyrene and polycarbonate foaming with carbon dioxide. Industrial & Engineering Chemistry Research. **46**, 7107-7116

30 Muksing, N., Nithitanakul, M., Grady, B. P. and Magaraphan, R. (2008) Melt rheology and extrudate swell of organobentonite-filled polypropylene nanocomposites. Polymer Testing. **27**, 470-479

31 Matuana, L. M., Faruk, O. and Diaz, C. A. (2009) Cell morphology of extrusion foamed poly(lactic acid) using endothermic chemical foaming agent. Bioresource Technology. **100**, 5947-5954

32 Shah, B. L. and Matuana, L. M. (2004) Online measurement of rheological properties of PVC/wood-flour composites. Journal of Vinyl & Additive Technology. **10**, 121-128

33 Willett, J. L., Jasberg, B. K. and Swanson, C. L. (1995) Rheology of thermoplastic starch - effects of temperature, moisture-content, and additives on melt viscosity. Polymer Engineering and Science. **35**, 202-210

34 Matuana, L. M., Park, C. B. and Balatinecz, J. J. (1998) Cell morphology and property relationships of microcellular foamed PVC/wood-fiber composites. Polymer Engineering and Science. **38**, 1862-1872

35 Li, Q. X. and Matuana, L. M. (2003) Foam extrusion of high density polyethylene/wood-flour composites using chemical foaming agents. Journal of Applied Polymer Science. **88**, 3139-3150

36 Han, X. M., Koelling, K. W., Tomasko, D. L. and Lee, L. J. (2003) Effect of die temperature on the morphology of microcellular foams. Polymer Engineering and Science. **43**, 1206-1220

37 Dealy, J. M. and Wissbrun, K. F. (1990) Melt rheology and its role in plastics processing: theory and applications. Van Nostrand Reinhold, New York

38 Lee, M., Park, C. B. and Tzoganakis, C. (1999) Measurements and modeling of PS/supercritical CO_2 solution viscosities. Polymer Engineering and Science. **39**, 99-109

39 Leung, S. N., Wong, A., Park, C. B. and Guo, Q. P. (2009) Strategies to estimate the pressure drop threshold of nucleation for polystyrene foam with carbon dioxide. Industrial & Engineering Chemistry Research. **48**, 1921-1927

40 Lee, S.-T., Park, C. B. and S., R. N. (2007) Polymeric Foams: Science and Technology. Taylor & Francis Group, Boca Raton

41 Diaz, C. A. and Matuana, L. M. (2009) Continuous extrusion production of microcellular rigid PVC. Journal of Vinyl & Additive Technology. **15**, 211-218

CHAPTER 4

Rheology Modification Approach to Continuous Microcellular Foaming of Polylactic Acid/Wood-Flour Composites

4.1 Abstract

This study investigated the effects of wood-flour and rheology modifier contents on the melt viscosity and cell morphology of microcellular foamed polylactic acid (PLA)/wood-flour composites produced through a continuous extrusion process. The melt viscosity of PLA increased as the relative amount of wood-flour increased in the composites. In contrast, increasing the rheology modifier content produced the opposite effect reducing the viscosity of the composites. A linear relationship was identified for the effect of rheology modifier on melt flow index (MFI) for the PLA/wood-flour composites and was used to formulate composites with lower, similar, and higher viscosities than the neat PLA. Matching the viscosity of the composites with that of neat PLA resulted in the best cell morphologies. Lower concentrations of rheology modifier resulted in unprossesable conditions because of the increased viscosity which generated elevated pressures in the system above operational limits. Higher concentrations of rheology modifier resulted in foams with poor cell morphologies. By matching the viscosity of the composites with that of the neat PLA, foamed composites with wood-flour contents up to 30 wt.% were manufactured. The results confirmed that microcellular structures, with cell sizes of around 10 μm and cell-population densities in the order of 10^9 cells/cm^3, were successfully produced in the PLA/wood-flour composites.

4.2 Introduction

Polylactic acid (PLA) is a thermoplastic made from lactic acid derived from renewable resources such as corn and sugar beets. Recently, large scale production and commercialization of PLA have prompted this material to lead the market of biodegradable plastics as an environmentally sustainable substitute to petroleum-based plastics. Despite the good publicity and environmental benefits of green materials, the shift to bio-plastics is still limited by the higher cost of the resins and the better performance of traditional plastics. PLA is more brittle and has a lower impact resistance than traditional plastics such as polystyrene and polyethylene. Also, it has narrow processing windows due to its sensitivity to thermal and hydrolytic degradation [1].

With the aim of reducing the cost of final products while retaining biodegradability, blending of PLA with low cost cellulosic fibers has been investigated [2-4]. Filling PLA with cellulosic fibers can increase the tensile modulus and reduce the overall cost. However, while cost reduction can be achieved, toughness and impact resistance are deteriorated [3]. To overcome these shortcomings, one alternative is to create microcellular structures in PLA/wood-flour composites because the presence of micro-bubbles can inhibit crack propagation by blunting the crack tip increasing the energy for crack propagation [5]. Microcellular foamed PVC/wood-flour composites produced in the batch process showed that the creation of a microcellular structure increased the impact resistance to values higher than the unfoamed and unfilled polymer [6]. The basic approach is to saturate the solid samples with large amounts of an inert gas under high pressure and induce a thermodynamic instability by a sudden drop in solubility. Unfortunately, the batch process is not appealing for industrialization because of its long cycle times. Continuous processes, such as extrusion foaming, have been developed based on the concept of thermodynamic instability created by a rapid pressure drop at extruders exit with the use of a nozzle die [7]. This process has been demonstrated on neat PLA. However, there are no studies on microcellular extrusion foaming of PLA/wood-flour composites.

Diaz and Matuana studied the effect of processing temperature on the cell morphology of microcellular PLA foams in a continuous extrusion process using CO_2 as foaming agent [9]. The viscosity of the melt proved to be of paramount importance to successfully produce microcellular foams in PLA because it controlled the pressure built in the system and the pressure drop rate, necessary to nucleate a swarm of bubbles [9, 10]. Nevertheless, the addition wood-flour affects the microcellular extrusion process because of their effect on the rheology of the melt [11, 12], heterogeneous cell nucleation [13], and foamability [14]. In the molten state, wood-flour increases the viscosity of the resin [11, 15] affecting the operating conditions in a foam extrusion system because of its effect on melt viscosity, thus affecting the cell nucleation rate [9].

Reported studies on extrusion foaming of wood fiber composites have focused on assessing the effects of extrusion parameters, wood (content, size and moisture), blowing agent (type and concentration), etc., on the cell morphology [5, 11, 14, 17, 18]. However, there are no studies considering the melt viscosity as a key parameter in the foaming process. It is important to develop approaches to control the melt viscosity to produce microcellular structures in the composites.

One way to alter the viscosity of the composites is through changes in the processing temperature. Increasing the melt temperature is known to reduce the viscosity of the melt, as described by an Arrhenius relationship [9, 19]. Unfortunately, since increasing the temperature can accelerate the degradation of the fibers releasing water vapor and volatiles detrimental for the foaming process [17] and initiate the degradation of PLA [1], a different approach should be considered.

An alternative means to alter the viscosity of the composites is through changes in the material formulation. Li and co-workers studied the effects of wood-flour and internal lubricant contents on the rheological properties of wood-flour filled polypropylene. The results showed that increasing the wood-flour content increased the apparent viscosity of the melt because the solid wood particles in the molten polymer increased the resistance against the flow. By contrast, the addition of internal lubricant significantly decreased the melt viscosity of the composites by reducing the friction between polymer chains and wood particles [20]. Nearly a 50% reduction in apparent viscosity was observed by adding 5 wt.% of an ester based internal lubricant [20]. Low molecular weight additives are known for their low viscosity and plasticizing effects, a desirable characteristic to control the viscosity of a blend. By controlling the viscosity of the melt through changes in the formulation, the foaming process can be carried out at same conditions as for the neat PLA without raising the processing temperature. Also, processing at lower temperatures would favor the foamability of the composites [17].

In this study the effects of wood-flour and rheology modifier contents on the melt viscosity and cell morphology of foamed samples were investigated to identify melt properties suitable for microcellular foam processing of PLA/wood-flour composites.

4.3 Experimental

4.3.1 Materials

A semi-crystalline grade of polylactic acid (PLA 2002D) from NatureWorks^{TM} was used as matrix with an approximately D-lactic content of 4% and a melt flow index between 6.9 g/10min (210°C/2.16 kg). The wood-flour used was softwood-flour (pine) grade 12020, supplied by American Wood-flour Fibers (Schofield, WI). To promote heterogeneous nucleation, talc (Mistron Vapor-R) from Luzenac Corporation, with a median particle size of 2 μm and a specific surface area of 13.4 m^2/g, was used. The rheology modifier used in the study was Epolene E-43, low molecular weight maleic anhydride-modified polypropylene (MAPP), supplied by Eastman Chemicals (Rochester, NY). CO_2 with a purity of 99.5%, supplied by Airgas, was used as physical foaming agent.

4.3.2 Rheological Measurements

Since wood-flour and additives concentrations change the rheology of PLA composites [12], the effect of wood-flour and rheology modifier contents on the viscosity of the melt was measured via melt flow index (MFI), on-line capillary rheometry, and rotational rheometry with extensional viscosity fixture.

MFI was measured according to the procedure outlined in ASTM D1238 (Procedure A) using a Melt Indexer (model LMI 4000) by Dynisco Polymer Testing Inc. The melt temperature was set at 210°C and an applied dead load of 2.16 kg (including the piston) was employed. A melt time of 2 min was set in order to avoid PLA thermal degradation.

On-line capillary rheometry measurements were performed on an Intelli-Torque Plasticorder® Torque Rheometer (C.W. Brabender Instruments Inc.) equipped with a 19.1 mm single-screw extruder (L/D ratio 30:1). A capillary die with three different inserts (L/D ratios: 10:1, 15:1, 20:1) were use for the experiment. The temperature profile in the extruder and die was kept constant to maintain a constant melt temperature for accurate viscosity measurements. All of the heating zones were set to 170°C. The rotational screw speeds varied from 10 to 80 rpm to generate different shear rates during experiments [12]. Experiments followed ASTM standard D5422 without injecting CO_2 in the system as described in our previous study [9]. The melt density used in the viscosity calculations was measured as described in a previous work [21].

Both Bagley and Rabinowitsch corrections were performed account for the excess of pressure drop due to entrance flow and the shear thinning effect of pseudoplastic fluids respectively. A detailed description of the calculations can be found elsewhere [9, 22].

4.3.2.1 Extensional viscosity

Two methods were used to characterize the effect of wood-flour and rheology modifier contents on the extensional viscosity of PLA: on-line capillary rheometry and dynamic rotational rheometer. From the entrance pressure drop in the on-line capillary measurements, apparent extensional viscosity was calculated using the Cogswell’s equations [22-24].

The extensional viscosity is the ratio of the extensional strain rate ($\dot{\varepsilon}_A$) and the extensional shear stress (σ_E) calculated as follows:

$$\dot{\varepsilon}_A = \frac{4\dot{\gamma}_a^2 \eta_a}{3(n+1)\Delta P_e} \qquad \text{(Equation 4.1)}$$

$$\sigma_E = \frac{3}{8}(n+1)\Delta P_e \qquad \text{(Equation 4.2)}$$

where ($\dot{\gamma}_a$) is the apparent shear rate, (η_a) the apparent shear viscosity and (ΔP_e) the pressure drop at the capillary entrance, calculated from the end effect as:

$$\Delta P_e = 4 \cdot e \cdot \sigma_w \qquad \text{(Equation 4.3)}$$

Finally, the apparent extensional viscosity can be calculated as:

$$\eta_{EC} = \frac{\sigma_E}{\dot{\varepsilon}_A} = \frac{9(n+1)^2(\Delta P_e)^2}{32\eta_a \dot{\gamma}_a^2} \qquad \text{(Equation 4.4)}$$

Direct measurement of the extensional viscosity was done using the extensional viscosity fixture (EVF) on the ARES extensional rheometer from TA instruments (New Castle, DE). Rectangular samples with 18 ×10 ×0.78 mm dimensions were molded at 180°C. Extensional viscosity was measured at a fixed Henky strain rate (0.1 s^{-1}) as a function of time at 160°C. Further discussion of the method can be found elsewhere [25, 26].

4.3.3 Compounding of Materials

PLA in powder form (ground from pellets) and wood-flour used in the formulations were oven dried at 55 ^{o}C for 8 hrs and 105°C for 48 hrs prior to use, respectively. PLA, wood-flour, rheology modifier and 0.5 wt. % of talc were mixed in a kitchen mixer (Blender MX1050XTS from Warning Commercial Xtreme) at 22,000 rpm for approximately 45 sec.

4.3.4 Extrusion Foaming

Figure 4.1 shows a schematic of the foaming system used in this study. The process used a 19.1 mm single screw extruder (*L/D* ratio 30:1, C.W. Brabender Instruments Inc.) with a mixing screw powered by a 5 hp driver with speed-control gearbox (Brabender Prep Center). A positive displacement syringe-pump (Teledyne Isco., Model 260D) delivered the gas into the extrusion barrel. A diffusion enhancing device (static mixer Omega FMX8441S) attached to the extruder ensured the creation of a polymer/gas solution with a rapid-pressure drop induced by a nozzle die with a 0.5 mm diameter. All foaming experiments were performed with gas injected at a constant volume of 5 mL/min (approximately 5 wt. %) and screw rotational speed of 80 rpm. The processing temperatures was set in the extruder barrel 170-170-165°C from hopper to extruder's exit, 165°C in the static mixer and 150°C in the nozzle die. Samples were collected after the process reached steady state conditions and cooled by air.

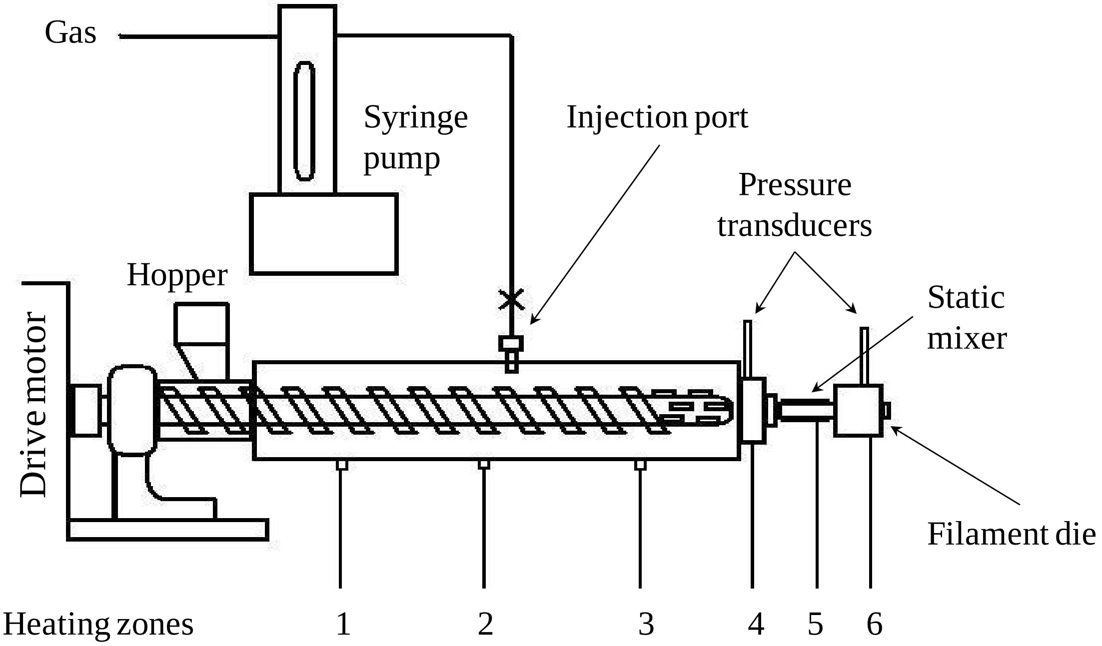

Figure 4.1. Schematic of the single-screw extrusion foaming system.

4.3.5 Density measurements

Densities measurements were carried out according to ASTM standard D792 (buoyancy method), for unfoamed (ρ_u) and foamed (ρ_f) samples. By measuring the weights of at least five samples in the air (m_1) and in an immersion liquid (m_2), i.e., n-hexane, the density was calculated as:

$$\rho = \frac{m_1 \cdot \rho_{FL}}{(m_1 - m_2)} \qquad \text{(Equation 4.5)}$$

where ρ_{FL} is the density of *n*-hexane (0.6594 g/cm^3). The void fraction (V_f) was then determined using the following equation:

$$V_f = \frac{(\rho_u - \rho_f)}{\rho_u} \cdot 100 \qquad \text{(Equation 4.6)}$$

4.3.6 Scanning Electron Microscopy

Morphology of foamed samples was analyzed via scanning electron microscopy (SEM JEOL JSM-6400, 10 kV). Samples were fractured in liquid nitrogen and coated with gold prior to the test. The images obtained aided the characterization of cell population density using Eq. 7 [27]:

$$N_o = \left(\frac{nM^2}{A} \right)^{3/2} \left[\frac{1}{1 - V_f} \right] \qquad \text{(Equation 4.7)}$$

with n as the number of cells in the micrographs, and A and M as the area and the magnification factor of the micrograph, respectively. V_f is the void fraction described in Eq. 6.

Cell sizes were measured using image analysis software, UTHSCSA Image Tool. After a proper spatial calibration of the micrograph, the diameter of at least 100 randomly selected cells was manually measured and the average cell size calculated. Breaking the cell size values into classes allowed the making of histograms and cumulative percentage plots.

4.4 Results and Discussion

4.4.1 Rheological Characterization

The effects of wood-flour and rheology modifier contents on melt viscosity were characterized via melt flow index (MFI). MFI denotes the rate of extrusion of molten resin through a die under specific temperature and load in g/10 min and is an indirect measurement of the viscosity. Higher MFI values correspond to lower viscosity. Figure 4.2 is the plot of MFI as a function of rheology modifier contents for varying amounts of wood-flour, i.e., 10, 20 and 30 wt.%. Without rheology modifier (0% E-43), increasing the amount of wood-flour reduced the MFI, making the melt more viscous. This is attributed to the interaction between wood-flour particles and the matrix [11]. Solid wood-flour particles embedded in the polymer matrix increase the friction towards the flow of the melt resulting in higher viscosity [28].

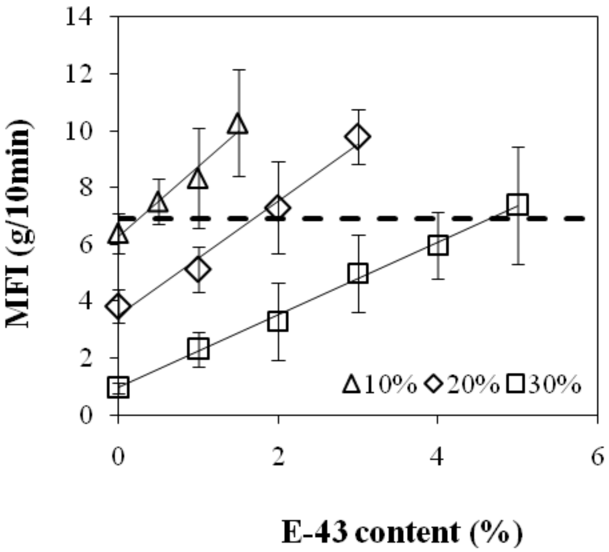

Figure 4.2. Effect of wood-flour and rheology modifier contents on the MFI of PLA 2002D at 210°C. The dashed line represents the MFI of neat PLA 2002D.

The addition of rheology modifier increased the MFI as its relative amount increased irrespective of the wood-flour concentration, easing the flowability of the composite. Low molecular weight additives can produce a plasticizing effect. Generally, the additive separates the polymer chains, increasing their flexibility [29]. Also, the additive can produce a lubricating effect reducing the friction between the polymer and the wood-flour [20].

In the range studied, the effect of adding rheology modifier on MFI was linear for all three wood-flour contents (Figure 4.2). Drawing a line parallel to the X-axis at a MFI value of 6.9 g/10 min (MIF of neat PLA, dashed line in Figure 4.2), intercepts with the MFI versus rheology modifier lines at rheology modifier concentrations of 0.3, 1.7, and 4.7 wt. %, for the composites containing 10, 20, and 30 wt. % wood respectively (see Table 4.1). Above these concentrations, the formulations have a viscosity lower than that of neat PLA (higher MFI) while below the formulations showed higher viscosities (lower MFI) than neat PLA. It is hypothesized that formulations with viscosities similar to that of neat PLA will yield the best morphologies. Table 4.1 shows the linear regression equation for the effect of rheology modifier content on MFI for each wood-flour content and the interception with the MFI of neat PLA, matching point.

Table 4.1. Linear relationships of the effect of rheology modifier content on MFI for each wood-flour content.

Wood-flour content (%)	Linear equation	R^2	Predicted E-43 concentration (%)
10	2.495x + 6.256	0.966	0.253
20	2.006x + 3.504	0.982	1.688
30	1.279x + 0.959	0.996	4.637

To corroborate the results from MFI, and to gain a deeper understanding on the role of wood-flour and rheology modifier on the melt rheology, shear viscosity as a function of shear rate was measured in selected formulations (i.e., neat PLA, PLA with 20 wt. % wood-flour, and PLA with 20 wt. % wood-flour and 2 wt. % rheology modifier). Although MFI is related to the viscosity of the melt it does not provide the actual flow properties during processing operations. Viscosity characterization at typical extrusion shear rates (100 to 1000 s^{-1}) [30] is important to understand the flow of the material during foaming. Figure 4.3 shows the double-logarithmic plots of the true viscosity versus the true shear rate of the three formulations. Irrespective of the formulation the melts showed shear thinning behavior and obeyed the power law as described by Eq. 8:

$$\eta = K \cdot \left(\dot{\gamma}_w\right)^{n-1} \qquad \text{(Equation 4.8)}$$

where K and n are constants representing the melt viscosity coefficient and power law flow index, respectively [9]. The values for K and n, obtained from the curve fitting of the power law equation, are listed in Table 4.2.

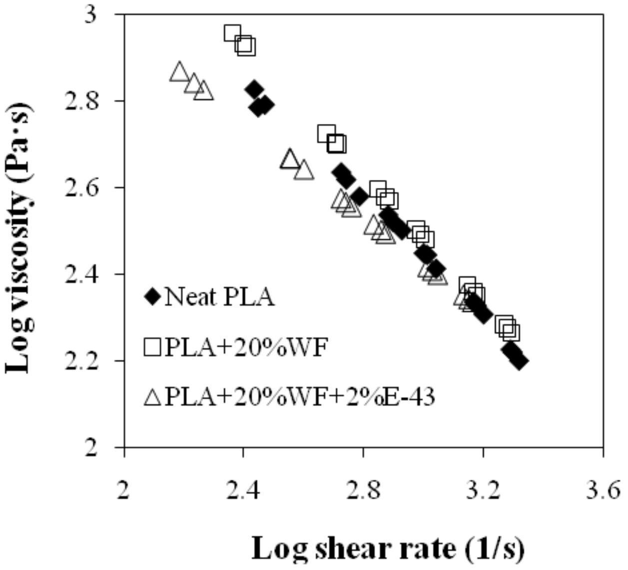

Figure 4.3. True viscosity vs. true shear rate of PLA, PLA with 20 wt. % wood-flour, and PLA with 20 wt. % wood-flour and 2 wt. % rheology modifier.

Table 4.2. Melt viscosity coefficient (*K*) and power law flow index (*n*) for neat PLA, PLA with 20 wt. % wood-flour, and PLA with 20 wt. % wood-flour and 2 wt. % rheology modifier.

Material composition	Regression parameters $\eta = K\dot{\gamma}^{n-1}$		R^2
	K (kPa·s^n)	n	
Neat PLA	30.6	0.318	0.9951
PLA+20%WF	51.7	0.257	0.9999
PLA+20%WF+2%E-43	11.4	0.456	0.9999

When comparing the neat PLA with the composite with 20 wt. % wood-flour, a shift of the curve upwards was observed as well as a higher viscosity coefficient (Table 4.2), indicating that the composite melt was more viscous. A change in the flow index, from 0.32 to 0.26, indicates a stronger shear thinning effect when the wood-flour fibers are present. Shear thinning responds to the alignment and disentanglement of the polymeric chains when subjected to shear; adding of wood-flour fibers is known to accentuate this behavior because the fibers also align and induce higher local shear rates in the thin polymeric layer between wood-flour particles, thus the observed reduction in *n* [31]. Adding the rheology modifier (E-43 in table 4.2) lowered the viscosity of the melt to similar or lower values than neat PLA and also changed the flow index, from 0.26 to 0.46, making the melt less pseudoplastic (n=1 means the flow is Newtonian). This behavior is attributed to the plasticizing effect of the additive, which increases the mobility of the polymer chains and the flow of wood-flour particles. Similar results have been observed in polypropylene/wood-flour composites [20].

Beside shear viscosity, elastic properties of the melt such as extensional viscosity also play an important role in foam processing. Extensional viscosity is responsible for entrance pressures when the polymer flows though contracting channels or tubes [32], affecting the pressures drop during on-line capillary rheometry measurements and the pressures built in the extrusion system when foaming. Also, as bubbles grow during foam processing, the polymer is stretched making the elastic properties of the melt a decisive factor in controlling the cell morphology [16]. The polymer resistance to stretching is proportional to the stretching rate, namely extensional viscosity [33]. Figure 4.4a shows the double logarithmic plot of apparent extensional viscosity versus apparent strain rate calculated from the end effects using the Cogswell's equations, Eqs. 1 to 4. Irrespective of the formulation, as the extensional strain rate increased the extensional viscosity decreased in a linear manner, thus a power law relation persists, similar to that of the shear viscosity (Figure 4.3). Neat PLA showed the lowest extensional viscosity. When wood-flour is added in the formulation the extensional viscosity increases, confirming the toughening effect of wood-flour. Strong dependence of extensional viscosity on wood-flour content has been shown in HDPE/Maple wood-flour flour composites with extensional viscosity increasing with increasing wood-flour loading [15]. Adding 2 wt. % rheology modifier to the PLA/wood-flour composite did not produce a significant change in the extensional viscosity and the curve overlapped the one without the additive.

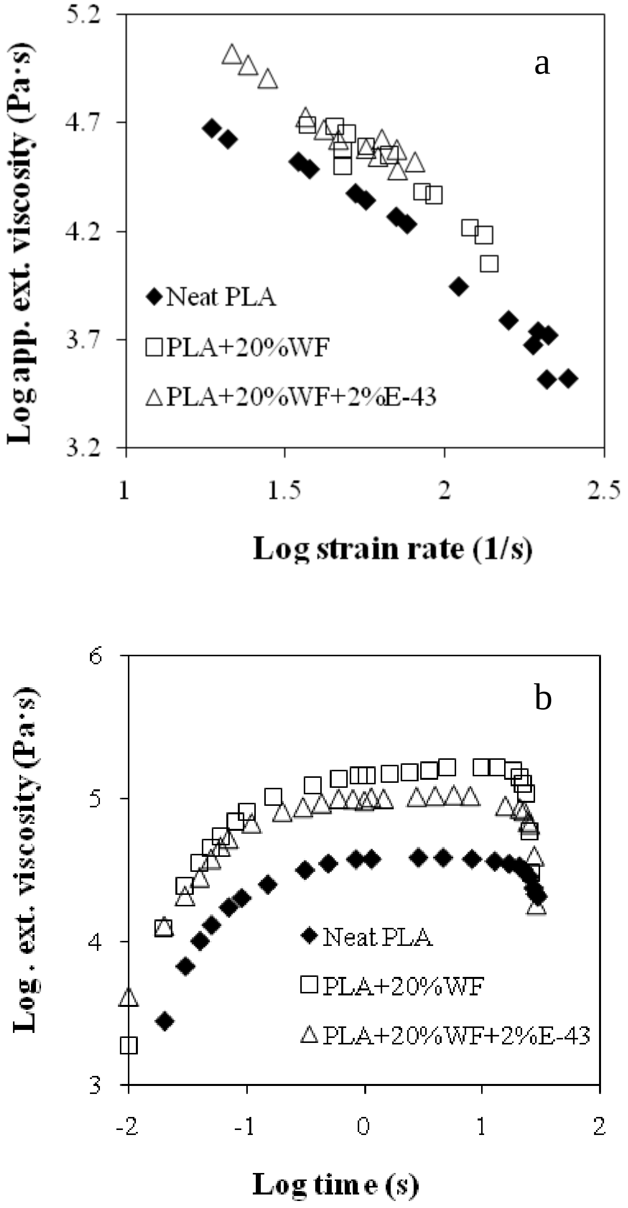

Figure 4.4. Extensional viscosity measured by (a) on-line capillary rheometry, and (b) ARES-EVF rheometer for PLA, PLA with 20 wt. % wood-flour, and PLA with 20 wt. % wood-flour and 2 wt. % rheology modifier.

Extensional viscosity measurements in a rotational rheometer were performed to corroborate the results from capillary rheometry (Figure 4.4b). Neat PLA showed the lowest extensional viscosity whereas PLA/20%wood-flour showed the highest. The addition of rheology modifier (E-43) slightly reduced the extensional viscosity of the composite. As expected from the chain architecture of PLA, none of the formulation showed strain hardening. Similar results were reported by other investigators [26].

4.4.2 Effect of rheology modifier content on cell morphology

Foaming was perform on PLA/20 wt. % wood-flour composites with different amounts of rheology modifier (below the matching point, close to the matching point, and above the matching point) to understand the effect of rheology modifier on the foamability of the composites. Below the matching point (i.e., 1.3 wt. %, MFI=6) the foaming process was unstable and the pressure increased to a point the system had to be shut down. During the foaming process, the melt experience contraction flow through the static mixer and the nozzle (Figure 4.1), generating entrance pressures which led to a rise in pressure above the operational limits in the extrusion system when the melt was too stiff. Also, the nozzle used for these experiments was particularly small, i.e., 0.5 mm of diameter, and without the proper lubrication, provided by the rheology modifier, the wood-flour particles may agglomerate leading to the nozzle being blocked. Foaming was successful in formulations with rheology modifier amounts close and higher to the matching point (i.e., 2, 4, and 6 wt. %, MFI=7.5, 11.5, and 15.5 respectively). However, the cell morphology significantly varied.

Figure 4.5 shows the effect of rheology modifier content on the cell morphology. For a concentration close to the matching point, i.e., 2 wt. % (Figure 4.5a), the morphology was uniform with cell sizes in the order of 10 μm (see Table 4.3). As the amount of E-43 increased from 2 to 6 wt. %, the morphology was deteriorated showing big cracks and cell coalescence (Figures 4.5b and c) also reflected in the measured cell-population density and average cell size (Table 4.3). It is believed that the softer melt at higher rheology modifier concentrations did not provide sufficient melt strength to trap the growing bubbles leading to cell coalescence [16]. The void fraction decreased as the amount of E-43 (see Figure 4.6) increased because the melt became too soft favoring cell coalescence which may have led to channels for the gas to escape to the environment during foaming. The results clearly showed that the composite with rheology modifier amount close to the matching point produced the best morphology and confirmed the adequacy of the strategy proposed to set the amount of E-43 based on the MFI.

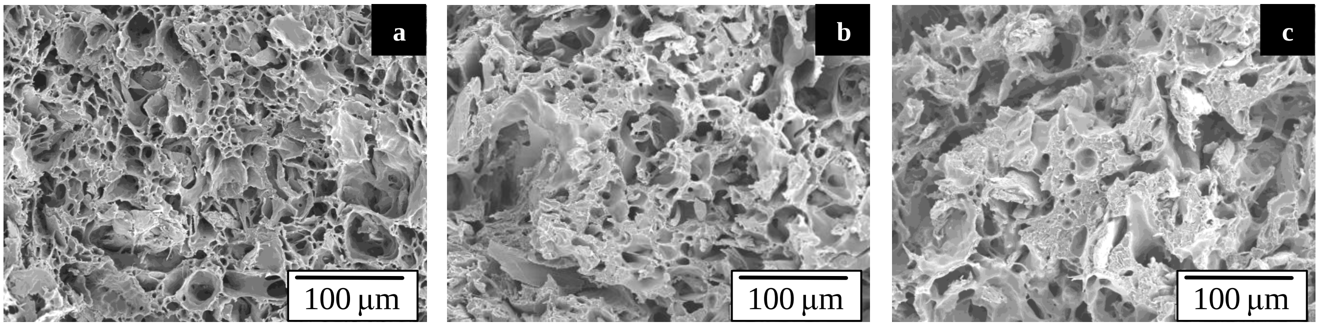

Figure 4.5. Effect of rheology modifier content on cell morphology of foamed PLA samples containing 20 wt.% wood-flour. (a) 2 wt.%, (b) 4 wt.%, (c) 6 wt.%. Pictures originally taken at 350X.

Table 4.3. Effect of rheology modifier content on cell-population density and cell size.

E-43 content (%)	Cell-population density[a] (10^9 cells/cm^3)	Average cell size (μm)
2	0.67 ± 0.106^A	9.2
4	0.28 ± 0.094^B	15.5
6	0.08 ± 0.043^C	18.3

[a] The superscript letters represent the ANOVA results. The means with different letters are significantly different.

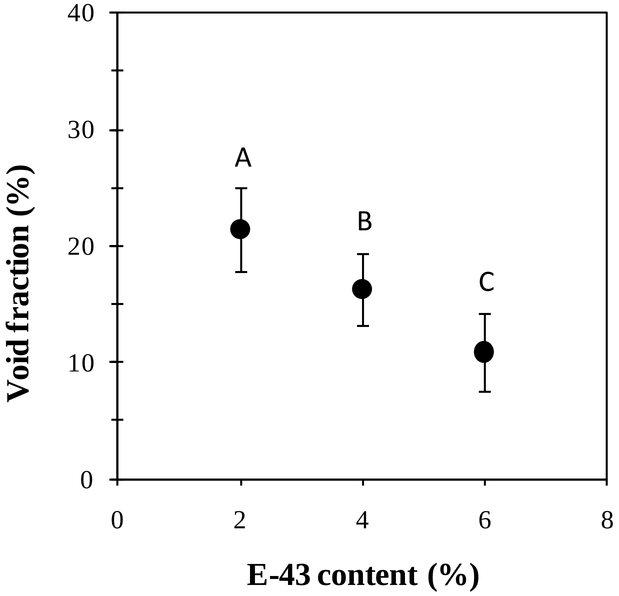

Figure 4.6. Effect of rheology modifier content on void fraction of foamed PLA samples containing 20 wt.% wood-flour and varying amounts of rheology modifier. The letters in the graph represent the ANOVA results. The means with different letters are significantly different ($p<0.05$).

4.4.3 Effect of wood-flour content on cell morphology

Foaming of PLA composites with wood-flour contents varying from 0 to 30 wt. % was performed and the morphology is shown in Figure 4.7. Rheology modifier contents of 0.3, 2 and 5 wt. % E-43 were used for the composites containing 10, 20 and 30 wt. % wood-flour respectively, matching the MFI of PLA as previously discuss. The amounts of rheology modifier used were slightly higher than those predicted in Table 4.1 to ensure processability of the composites. The micrographs clearly show a foamed matrix with embedded wood-flour particles, corroborating the idea that the gas solubilize only in the wood component [8]. Foamed composites with 10 and 20 wt. % wood-flour rendered fine celled uniform morphologies as seen in Figure 4.7b and c. At the highest wood-flour content (i.e., 30 wt.%), the cellular structure showed large cells with irregular shape.

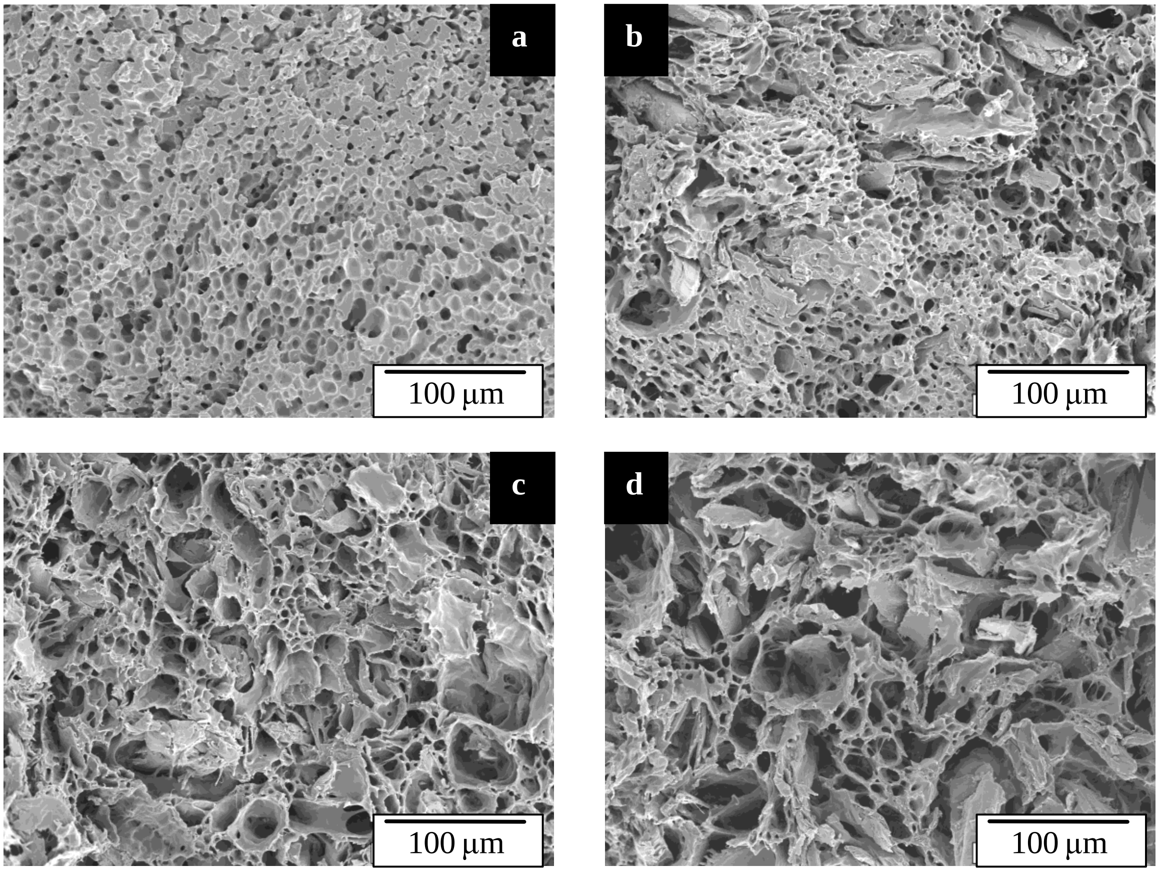

Figure 4.7. Effect of wood-flour content on cell morphology of foamed PLA samples. (a) 0% wood-flour, (b) 10% wood-flour, (c) 20% wood-flour, (d) 30% wood-flour. Pictures originally taken at 350X.

The effects of wood-flour content on cell-population density and average cell size of foamed composite are presented in Table 4.4. The cell-population density decreased gradually with increasing amounts of wood-flour. Several factors affected the cell-population density. Since the plastic component available to dissolve the gas and form bubbles is reduced as the amount of wood-flour increased, the number of cells nucleated per unit volume was reduced at higher wood-flour contents. Without wood-flour (Figure 4.7a) the bubble nucleation is mainly homogeneous [9]. For small amount of wood-flour, i.e., 10 wt.% (Figure 4.7b), this nucleation mechanism remained the dominant one. However, at higher wood-flour concentrations, i.e., 30 wt. %, bubbles may have nucleated at the interface of the wood-flour and the plastic reducing the overall nucleation rate, thus the lower cell-population density.

Table 4.4. Effect of wood-flour content on cell-population density and cell size of foamed samples.

Wood-flour content (%)	Cell-population density[a] (10^9 cells/cm^3)	Average cell size (μm)
0	1.46 ± 0.54^{A}	7.4
10	1.13 ± 0.33^{AB}	8.9
20	0.83 ± 0.13^{B}	9.3
30	0.36 ± 0.12^{C}	11.3

[a] The superscript letters represent the ANOVA results. The means with different letters are significantly different (log transformation applied).

The void fraction of the foamed composites is plotted in Figure 4.8. The addition of wood-flour did not significantly affect the void fraction which remained around 20% irrespective of wood content. Figure 4.9 shows the effect of wood-flour content on the cell size distribution of the foamed samples. For Neat PLA more than 90% of the cells have cell sizes below 10 μm, with high cell uniformity given by the steeper curve. At 10 and 20 wt.% wood-flour contents, samples showed similar cell size distributions with about 60% of the cells being smaller than 10 μm and 90% smaller than 15 μm. At 30 wt.% wood, the cell size distribution becomes broader and less uniform, less steeper curve, showing that big cells are present in the samples. High wood-flour concentration may have provided sites for undissolved gas pockets during processing leading to uncontrolled cell growth and overall deterioration of the morphology [34]. Additionally, wood-flour can release vapor and volatiles which may have play a deleterious effect on the cell structure, especially at the highest wood-flour content [17].

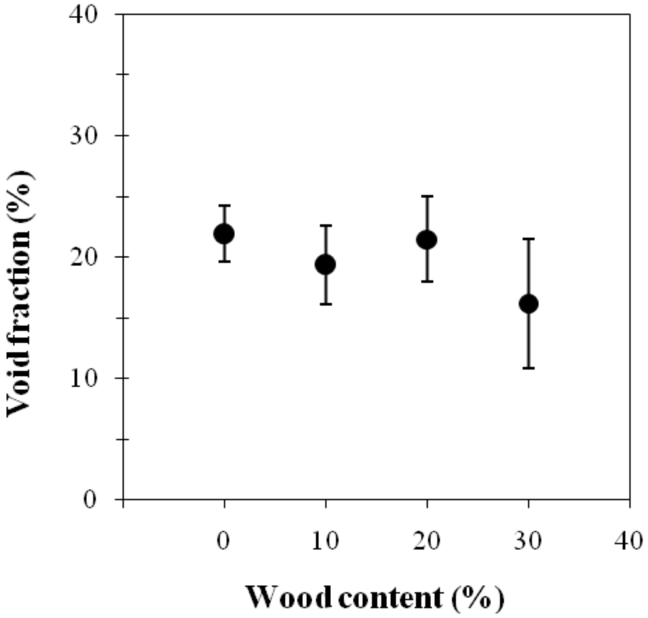

Figure 4.8. Effect of wood-flour content on void fraction fraction of foamed PLA/wood-flour composites samples. The differences in means were not statistically significant.

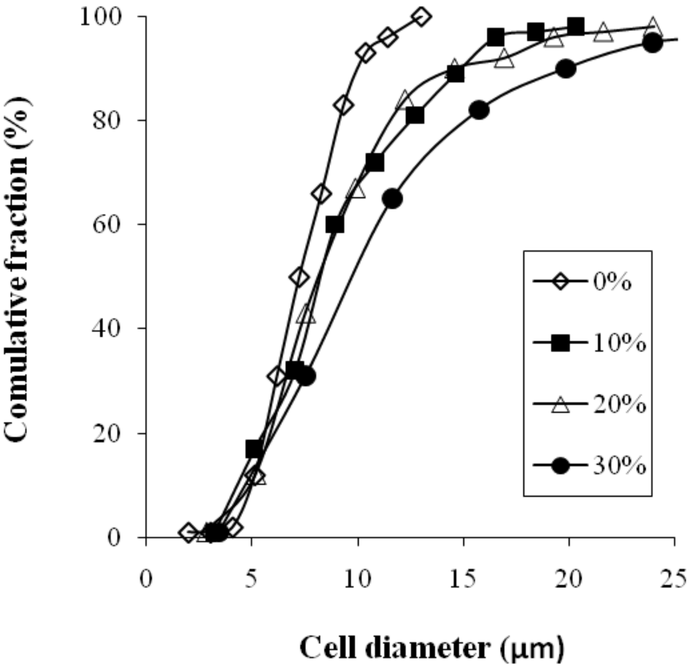

Figure 4.9. Effect of wood-flour content on cell size distribution of foamed samples.

Microcellular structures with cell sizes in the order of 10 μm and cell-population densities of 10^9 cell/cm^3 were produced in PLA containing up to 20 wt. % wood. The method proposed for matching the viscosity of the composites to that of the neat PLA by means of low molecular weight rheology modifier proved to be a suitable approach to facilitate the microcellular foaming of PLA/wood-flour composites.

4.5 Conclusions

This study investigated the effect of wood-flour and rheology modifier contents on the melt viscosity and cell morphology of microcellular foamed polylactic acid/wood-flour composites produced through a continuous extrusion process with supercritical carbon dioxide as foaming agent. The viscosity of the melt was of key importance in the production of microcellular foams as they affected the processability and foamability of the composites.

The melt viscosity of PLA increased as the relative amount of wood-flour increased in the composites. In contrast, increasing amounts of rheology modifier produced the opposite effect reducing the viscosity of the composites. A linear relationship was identified for the effect of rheology modifier on melt flow index (MFI) for the PLA/wood-flour composites and was used to formulate composites with lower, similar, and higher viscosities than the neat PLA. Matching the viscosity of the composites with that of neat PLA resulted in the best cell morphologies. Lower concentrations of rheology modifier resulted in unprossesable conditions because of the increased viscosity which generated elevated pressures in the system above operational limits. Higher concentrations of rheology modifier resulted in foams with poor cell morphologies. The low viscosity of composites with high amounts of rheology modifier facilitated the gas escape and cell coalescence resulting in lower void fractions.

By matching the viscosity of the composites with that of the neat PLA, foamed composites with wood-flour contents up to 30 wt.% were manufactured. The results confirmed that microcellular structures, with cell sizes of around 10 μm and cell densities in the order of 10^9 cells/cm^3, were successfully produced in the PLA/wood-flour composites. The results show the feasibility of using low molecular weight additives to control the viscosity of the composites in order to tailor the melt viscosity of PLA/wood-flour composites.

4.6 Acknowledgements

This project was supported by the National Research Initiative of the USDA Cooperative State Research, Education and Extension Service, grant number 2006-35504-17414.

REFERENCES

REFERENCES

1 Garlotta, D. (2001) A literature review of poly(lactic acid). Journal of Polymers and the Environment. **9**, 63-84

2 Suryanegara, L., Nakagaito, A. N. and Yano, H. (2010) Thermo-mechanical properties of microfibrillated cellulose-reinforced partially crystallized PLA composites. Cellulose. **17**, 771-778

3 Huda, M. S., Drzal, L. T., Misra, M., Mohanty, A. K., Williams, K. and Mielewski, D. F. (2005) A study on biocomposites from recycled newspaper fiber and poly(lactic acid). Industrial & Engineering Chemistry Research. **44**, 5593-5601

4 Pilla, S., Gong, S., O'Neill, E., Rowell, R. M. and Krzysik, A. M. (2008) Polylactide-pine wood flour composites. Polymer Engineering and Science. **48**, 578-587

5 Faruk, O., Bledzki, A. K. and Matuana, L. M. (2007) Microcellular foamed wood-plastic composites by different processes: a review. Macromolecular Materials and Engineering. **292**, 113-127

6 Matuana, L. M., Park, C. B. and Balatinecz, J. J. (1998) Cell morphology and property relationships of microcellular foamed PVC/wood-fiber composites. Polymer Engineering and Science. **38**, 1862-1872

7 Park, C. B. and Suh, N. P. (1996) Filamentary extrusion of microcellular polymers using a rapid decompressive element. Polymer Engineering and Science. **36**, 34-48

8 Matuana-Malanda, L., Park, C. B. and Balatinecz, J. J. (1996) Characterization of microcellular foamed PVC/cellulosic-fibre composites. Journal of Cellular Plastics. **32**, 449-469

9 Matuana, L. M. and Diaz, C. A. (2010) Study of cell nucleation in microcellular poly(lactic acid) foamed with supercritical CO_2 through a continuous-extrusion process. Industrial & Engineering Chemistry Research. **49**, 2186-2193

10 Park, C. B., Baldwin, D. F. and Suh, N. P. (1995) Effect of the pressure drop rate on cell nucleation in continuous processing of microcellular polymers. Polymer Engineering and Science. **35**, 432-440

11 Guo, G., Lee, Y. H., Rizvi, G. M. and Park, C. B. (2008) Influence of wood fiber size on extrusion foaming of wood fiber/HDPE composites. Journal of Applied Polymer Science. **107**, 3505-3511

12 Shah, B. L. and Matuana, L. M. (2004) Online measurement of rheological properties of PVC/wood-flour composites. Journal of Vinyl & Additive Technology. **10**, 121-128

13 Rodrigue, D., Souici, S. and Twite-Kabamba, E. (2006) Effect of wood powder on polymer foam nucleation. Journal of Vinyl & Additive Technology. **12**, 19-24

14 Mengeloglu, F. and Matuana, L. M. (2001) Foaming of rigid PVC/wood-flour composites through a continuous extrusion process. Journal of Vinyl & Additive Technology. **7**, 142-148

15 Li, T. Q. and Wolcott, M. P. (2005) Rheology of wood plastics melt. Part 1. Capillary rheometry of HDPE filled with maple. Polymer Engineering and Science. **45**, 549-559

16 Diaz, C. A. and Matuana, L. M. (2009) Continuous extrusion production of microcellular rigid PVC. Journal of Vinyl & Additive Technology. **15**, 211-218

17 Guo, G., Rizvi, G. M., Park, C. B. and Lin, W. S. (2004) Critical processing temperature in the manufacture of fine-celled plastic/wood-fiber composite foams. Journal of Applied Polymer Science. **91**, 621-629

18 Zhang, S. W., Rodrigue, D. and Riedl, B. (2005) Preparation and morphology of polypropylene/wood flour composite foams via extrusion. Polymer Composites. **26**, 731-738

19 Muksing, N., Nithitanakul, M., Grady, B. P. and Magaraphan, R. (2008) Melt rheology and extrudate swell of organobentonite-filled polypropylene nanocomposites. Polymer Testing. **27**, 470-479

20 Li, H. J., Law, S. and Sain, M. (2004) Process rheology and mechanical property correlationship of wood flour-polypropylene composites. Journal of Reinforced Plastics and Composites. **23**, 1153-1158

21 Matuana, L. M., Faruk, O. and Diaz, C. A. (2009) Cell morphology of extrusion foamed poly(lactic acid) using endothermic chemical foaming agent. Bioresource Technology. **100**, 5947-5954

22 Dealy, J. M. and Wissbrun, K. F. (1990) Melt rheology and its role in plastics processing: theory and applications. Van Nostrand Reinhold, New York

23 Huang, J. C. and Leong, K. S. (2002) Shear viscosity, extensional viscosity, and die swell of polypropylene in capillary flow with pressure dependency. Journal of Applied Polymer Science. **84**, 1269-1276

24 Tzoganakis, C., Vlachopoulos, J., Hamielec, A. E. and Shinozaki, D. M. (1989) Effect of molecular-weight distribution on the rheological and mechanical-properties of polypropylene. Polymer Engineering and Science. **29**, 390-396

25 Hadinata, C., Boos, D., Gabriel, C., Wassner, E., Rullmann, M., Kao, N. and Laun, M. (2007) Elongation-induced crystallization of a high molecular weight isotactic polybutene-1 melt compared to shear-induced crystallization. Journal of Rheology. **51**, 195-215

26 Zhu, W. L., Wang, J., Park, C. B., Pop-Iliev, R. and Randall, J. (2009) Effects of chain branching on the foamability of polylactide. SPE ANTEC Technical papers. pp. 41-45, Chicago, IL

27 Matuana, L. M. and Mengeloglu, F. (2002) Manufacture of rigid PVC/wood-flour composite foams using moisture contained in wood as foaming agent. Journal of Vinyl & Additive Technology. **8**, 264-270

28 Azizi, H. and Ghasemi, I. (2009) Investigation on the dynamic melt rheological properties of polypropylene/wood flour composites. Polymer Composites. **30**, 429-435

29 Harper, C. A. (2002) Handbook of Plastics, Elastomers & Composites. McGraw-Hill

30 Giles, H. F., Wagner, J. R. and Mount, E. M. (2005) Extrusion : the definitive processing guide and handbook. William Andrew Pub., Norwich, NY

31 Klyosov, A. A. (2007) Rheology and a Selection of Incoming Plastics for Composite Materials. John Wiley & Sons, Inc.

32 Pandey, A. and Lele, A. (2007) Exploring the utility of an axisymmetric semi-hyperbolic die for determining the transient uniaxial elongation viscosity of polymer melts. Journal of Non-Newtonian Fluid Mechanics. **144**, 170-177

33 Throne, J. L. (2004) Thermoplastic Foam Extrusion. Carl Hanser Verlag, Munich

34 Lee, J. W. S., Wang, K. Y. and Park, C. B. (2005) Challenge to extrusion of low-density microcellular polycarbonate foams using supercritical carbon dioxide. Industrial & Engineering Chemistry Research. **44**, 92-99

CHAPTER 5

Process-morphology-property relationships of microcellular poly(lactic-acid) produced through a continuous extrusion process

5.1 Abstract

High density microcellular polylactic acid foams were produced by a continuous microcellular extrusion process using the Mucell technology with supercritical carbon dioxide as foaming agent. In this study, characterization of the physico-mechanical properties of foamed samples as a function of cell morphology was done to establish process-morphology-property relationships. Tensile and Taber stiffness tests were performed on microcellular polylactic acid filaments prepared under different processing conditions. Processing variables such as amount of gas injected, extruders speed, gear pump speed, and processing temperature affected the development of the cellular structure. The results show the dependence of tensile strength and modulus on foam relative density.

5.2 Introduction

Microcellular plastics refer to any polymeric materials with small bubbles of 10 μm or less in diameter and cell densities (number of bubbles per unit volume) of 10^9 cells/cm^3 or more [1]. It is made by subjecting the plastic with a large amount of dissolved gas to a thermodynamic instability to nucleate a large number of cells [2]. Microcellular foams have the potential of improving material properties such as impact strength, toughness, and fatigue life while reducing plastic consumption [2, 3], thus reducing cost. These unique characteristics of microcellular plastics make the technology ideal for brittle polymers such as polylactic acid (PLA), since the presence of small bubbles can blunt the crack-tips and act as crazing initiation sites making the material tougher [2, 4].

Polylactic acid (PLA), a plastic derived from starch of corn, sugar beets, etc., has attracted much attention as replacement for traditional petroleum-based thermoplastics because it exhibits physical and mechanical properties close to those of many synthetic plastics in addition to being biodegradable [5, 6]. However, it is more brittle and more expensive than traditional oil-based plastics [7, 8], which have limited its large-scale applications. Consequently, improving the flexibility and impact resistance of PLA while reducing the cost of manufactured parts is an important factor for its market expansion.

Production of microcellular foamed structures in polylactic acid has addressed some of the limitations of the material such as low impact resistance and brittleness. Using a batch microcellular process, improvements in impact resistance (up to a 4-fold increase over that of unfoamed PLA), strain at break (up to a 2-fold increase over that of unfoamed PLA), and toughness (up to a 4-fold increase over that of unfoamed PLA) have been reported [5]. However, the industrial implementation of the batch process remains unlikely because of the multiple steps involved in the production of foamed samples and long saturation times [9]. Interest in industrialization of this technology calls for continuous processes, such as extrusion to produce the foams. The potential for industrialization has prompted researchers in exploring avenues for the continuous production of microcellular foams.

Different studies have been reported on continuous foaming of PLA in extrusion systems [9-12]. Matuana and Diaz studied the nucleation mechanisms to produce microcellular PLA using supercritical CO_2. Observations made included the critical role of the processing temperature on the cell morphology since lower temperatures increased the viscosity of the melt generating adequate pressure drop and pressure drop rates to induce high nucleation rates, i.e. higher than 10^9 cells/cm^3 [9]. Pilla et al., investigated the effects of adding epoxy-functionalized chain extender on the foaming ability of PLA processed via the microcellular extrusion process [11]. Wang and coworkers compared the expansion ratio and cell-population density of linear versus branched PLA. The expansion was more than doubled (from 17.6 to 41) when foaming the branched resin because of its higher melt strength [12]. Most of the studies found focused on the cell morphology of the foamed material without consideration of its mechanical properties. One of the reasons to avoid testing of mechanical properties may be the shape of the extrudate. When produced through a nozzle die, in many cases the extrudate is a filament with irregular cross section [9, 12], making the testing a cumbersome task. Although the mechanical properties have been evaluated in the batch process it remains important to test them in samples made by the continuous process.

Reignier and coworkers investigated the foam behavior of linear PLA in a twin extrusion system using carbon dioxide. They produced low density foams (>30 times expansion ratio) and evaluated compression modulus and strength. The foams were of similar density from 20.8 to 24.2 kg/m^3 and a correlation between density and mechanical properties could not be established. Interestingly, both the modulus and strength correlated with the gas content which varied from 7.3 to 9.4 wt. %. Higher CO_2 contents yielded lower modulus and strength. This behavior was attributed to a higher level of plasticization induced by residual CO_2. Mechanical property evaluation is scarce in continuous microcellular foaming of PLA. There is the need for a systematic study of mechanical properties in a wide range of morphologies in order to allow the determination of morphology-property relationships.

The aim of this study is to characterize the physico-mechanical properties of foamed PLA samples as a function of cell morphology to establish process-morphology-property relationships and develop predictive models for the foamed materials in the continuous extrusion process.

5.3 Experimental

5.3.1 Materials

A semi-crystalline grade of polylactic acid (PLA 2002D) from NatureWorks^{TM} was used as matrix with an approximately D-lactic content of 4% and a melt flow index between 5 to 7 g/10min (210°C/2.16 kg). CO_2 with a purity of 99.5%, supplied by Airgas, was used as physical foaming agent.

5.3.2 Extrusion Foaming

Figure 5.1 shows a schematic of the foaming system used in this study. The process used a 19.1 mm single screw extruder (*L/D* ratio 30:1, C.W. Brabender Instruments Inc.) with a mixing screw powered by a 5 hp driver with speed-control gearbox (Brabender Prep Center). Supercritical carbon dioxide was injected to the extruder at approximately 2/3 of the distance down the barrel length using a MuCell® supercritical fluid system (Trexel Inc.). A diffusion enhancing device (static mixer Omega FMX8441S) attached to the extruder ensured the creation of a polymer/gas solution. The resulting single phase PLA/gas solution went through the gear pump (Zenith, PEP-II 1.2 cc/rev), where the volumetric flow was controlled by the motor. The gear pump controls the polymer melt volumetric flow rate, independent of temperature and pressure changes [13]. Subsequently the PLA/gas solution entered the die where a rapid-pressure drop was induced by a nozzle with a 0.5 mm diameter. Cell nucleation and growth occurred at the die exit. The processing temperature profile in the extruder was kept constant at 170-170-165-155 °C from hoper to extruder’s exit and varied for the static mixer, gear pump and die. Samples were collected after the process reached steady state conditions and cooled by air.

This study has two main experiments. The first set of experiments consisted of producing an array of foamed samples at different processing conditions with the purpose of generating different morphologies. Table 5.1 list the processing conditions used to produce foamed samples with different void fractions. Cell morphology and mechanical characterization were performed to establish morphology-property relationships. The second set of experiments was aimed at elucidating process-morphology relationships through a design of experiments.

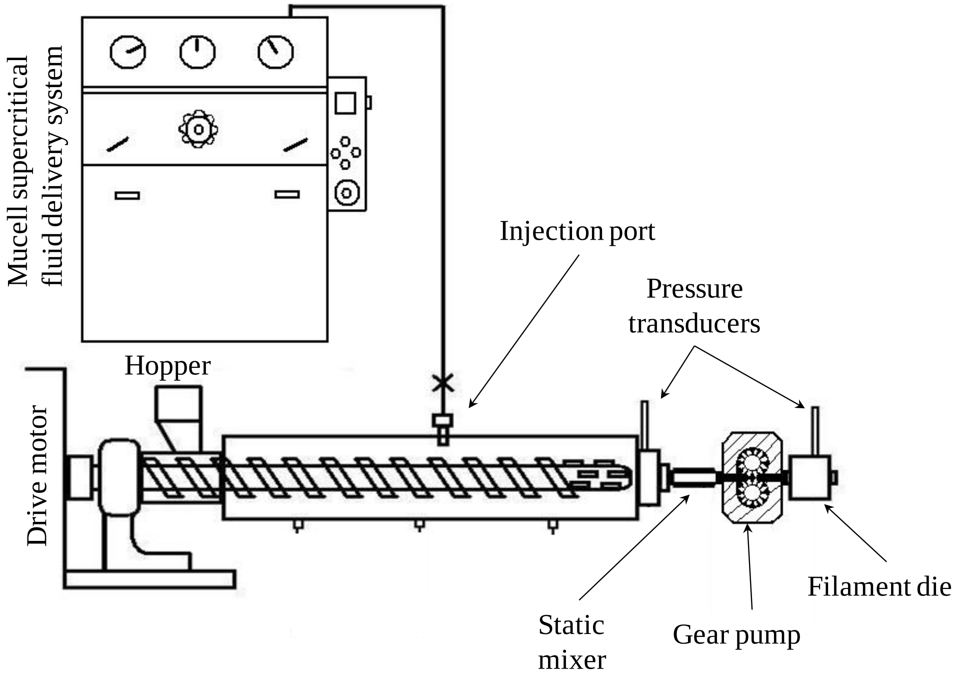

Figure 5.1. Schematic of the single-screw extrusion foaming system.

Table 5.1. List of the processing conditions used to produce foamed PLA samples.

Sample	Static mixer (°C)	Gear pump temp. (°C)	Die temperature (°C)	Screw speed (rpm)	Gear pump speed (cc/min)	Gas flow rate (Kg/hr)	Void fraction (%)
a	155	160	150	60	63	0.16	9 ± 1.5
b	155	150	150	40	64	0.15	16.8 ± 2.4
c	155	145	140	60	59	0.18	18.9 ± 3.1
d	150	140	135	40	64	0.15	39.7 ± 3.7

5.3.3 Tensile test

Tensile properties were measured with an Instron 5585H testing machine using the Instron Bluehill 2.14 software and a 5 kN load cell. There is no standardized procedure to test the obtained specimens which are foamed PLA filaments of around 0.5 mm in diameter with irregular cross section. For this reason a method was developed based on the ASTM standards C1557 and D3822 intended for tensile testing of ceramic fibers (glass, carbon, etc.) and man-made single textile fibers, respectively. The samples were mounted on cardboard tabs and glued with Loctite Super Glue at a gage length of 1.0 in. To improve the gripping, two tabs were used to hold the foamed specimen in a sandwich like manner. Drying of the glue for at least 24 hours was allowed before the test. Each specimen was centrally placed in the clamps of the tensile tester and the cardboard was carefully cut at both sides of the foamed filament. Tensile test was carried out using a crosshead speed of 3.81 mm/min. The diameter of the filaments was measured using optical microscopy prior to the test.

5.3.4 Taber stiffness test

Flexural modulus of elasticity was measured by means of Taber stiffness. The Taber units can be converted to modulus of elasticity by taking into account the shape, allowing the comparison between samples. Diaz et al., demonstrated the feasibility of using the Taber unit to calculate flexural modulus of elasticity [14]. The stiffness measurements on the Taber unit followed the procedures outlined in the ASTM standard D5342. The study used a Taber V-5 stiffness tester model 150-D. Foamed filaments were directly mounted in the unit.

5.3.5 Density measurements

Density measurements were carried out according to ASTM standard D792 (buoyancy method), for unfoamed (ρ_u) and foamed (ρ_f) samples. By measuring the weights of at least five samples in the air (m_1) and in an immersion liquid (m_2), i.e., n-hexane, the density was calculated as:

$$\rho = \frac{m_1 \cdot \rho_{FL}}{(m_1 - m_2)} \qquad \text{(Equation 5.1)}$$

where ρ_{FL} is the density of *n*-hexane (0.6594 g/cm^3). The void fraction (V_f) was then determined using the following equation:

$$V_f = \frac{(\rho_u - \rho_f)}{\rho_u} \qquad \text{(Equation 5.2)}$$

5.3.6 Scanning Electron Microscopy

Morphology of foamed samples was analyzed via scanning electron microscopy (SEM JEOL JSM-6400, 10 kV). Samples were fractured in liquid nitrogen and coated with gold prior to the test. The images obtained aided the characterization of cell-population density using Equation 5.3 [15]:

$$N_o = \left(\frac{nM^2}{A} \right)^{3/2} \left[\frac{1}{1 - V_f} \right] \qquad \text{(Equation 5.3)}$$

with n as the number of cells in the micrographs, and A and M as the area and the magnification factor of the micrograph, respectively. V_f is the void fraction described in Equation 5.2.

Cell sizes were measured using image analysis software, UTHSCSA Image Tool. After a proper spatial calibration of the micrograph, the diameter of at least 100 randomly selected cells was manually measured and the average cell size calculated.

5.4 Results and Discussion

5.4.1 Cell morphology analysis

Varying the processing parameters allowed for the production of foamed samples with different cell morphologies. Figure 5.2 shows the morphologies obtained ranging from lower (a) to higher (d) void fractions. Noticeably, irrespective of the void fraction the cells have similar sizes while the number of bubbles increased with void fraction. To confirm this observation a quantitative analysis of the cell size and cell-population density as a function of void fraction was performed and plotted in Figure 5.3. The average cell size did not significantly change with void fraction whereas the cell-population density increased with increasing void fractions. The void fraction depends on both the number of bubbles (cell-population density) and the size of the bubbles. Since there is no significant difference in the cell size among samples, the cell-population density is the main parameter determining the density reduction (void fraction). The results suggest that nucleation is the dominant phenomena in the development of the cellular structure because the number of cells correlated with the void fraction. The invariant cell size may be explained by the viscoselastic properties of the material, i.e., the melt strength. The melt strength plays a key role during foam expansion controlling the cell growth [16]. It is known that linear PLA, such as the one used in this study, have poor melt strength [12], thus the cell growth may have been limited to a certain extent resulting in the invariant cell size.

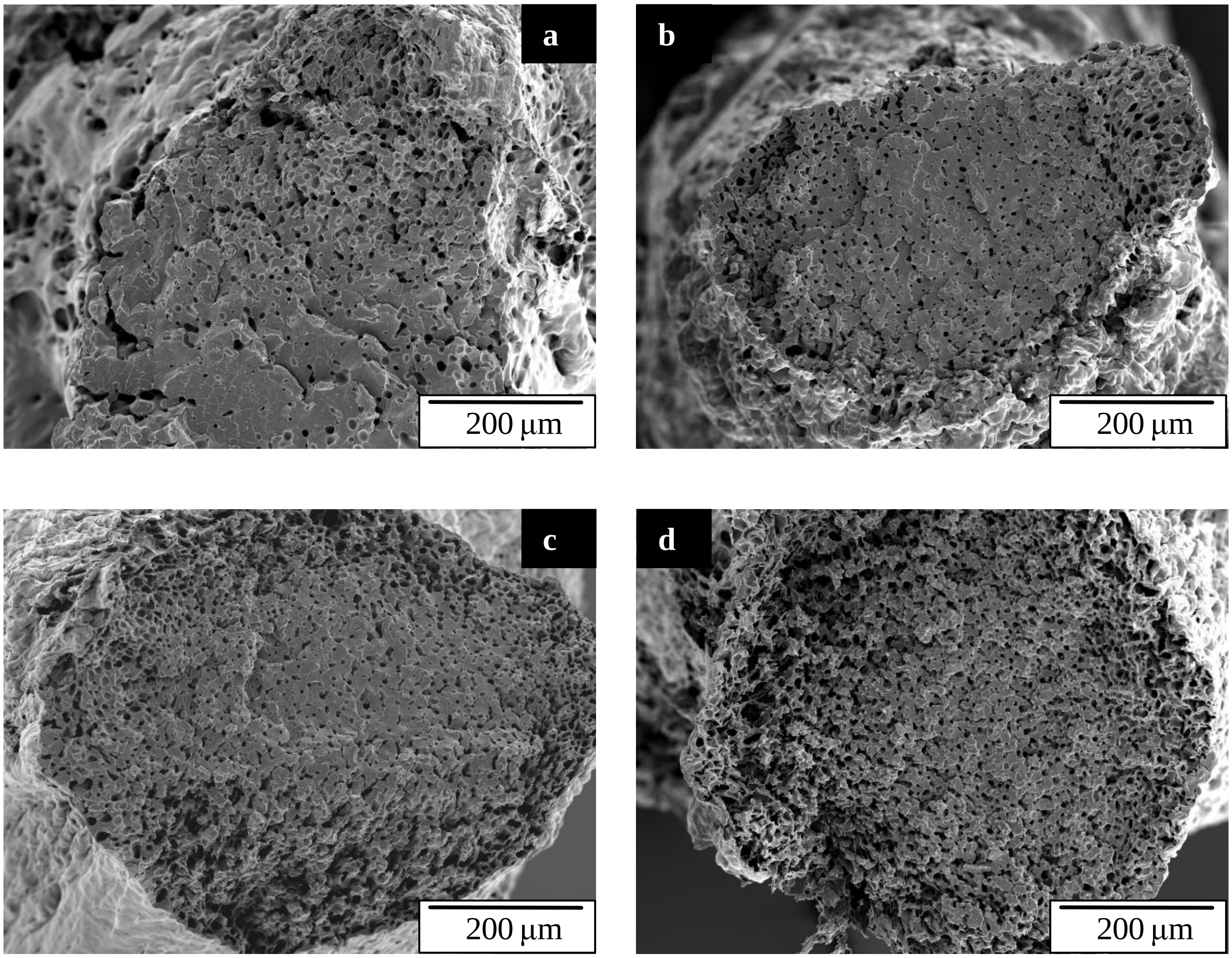

Figure 5.2. Morphology of foamed samples corresponding to the different foaming conditions in Table 5.2.

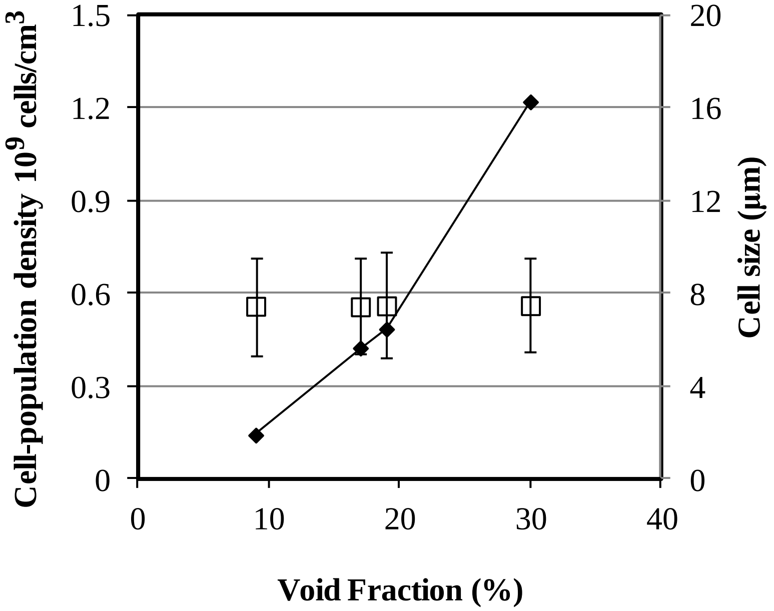

Figure 5.3. Cell-population density and cell size as a function of void fraction for foamed PLA samples. Solid diamonds represent the cell-population density and the clear squares represent the cell size.

5.4.2 Modulus of elasticity vs. relative density

Normalized tensile modulus of elasticity (From Instron) and normalized flexural modulus of elasticity (from Taber) were plotted against relative density (Figures 5.4 and 5.5a). The normalization consisted of dividing the modulus of the sample by the modulus of the matrix (unfoamed material) [17, 18]. Models in the literature to predict properties of cellular materials are usually expressed in terms of the normalized property as a function of relative density [19, 20], where the relative density is defined as:

$$\text{Relative Density} = \frac{\rho_f}{\rho} = 1 - V_f \qquad \text{(Equation 5.4)}$$

where ρ_f is the density of the foam, ρ is the density of the matrix or unfoamed material and V_f if the void fraction.

The lines in Figure 5.4 represent available models for the relationship between relative density and modulus. Different models have been proposed in the literature comprising theoretical and empirical approaches [17]. The empirical square power-law has been widely used [17, 18, 21] and is valid for most high density foams [17]. The square power-law is defined in Equation 5.5 and plotted in Figure 5.4.

$$E_f / E_m = \left(\rho_f / \rho_m\right)^2 \qquad \text{(Equation 5.5)}$$

The other two models plotted in Figure 5.4 are the constant macro-stress model and the Gibson-Ashby model. Constant macro-stress assumes spherical micro-inclusions embedded in an unbounded matrix without considering interactions between the inclusions and the matrix [17]. The Gibson-Ashby model assumes a cubic array of cells on which the cell struts, cell walls, and the internal gas pressure contribute to the modulus [17].

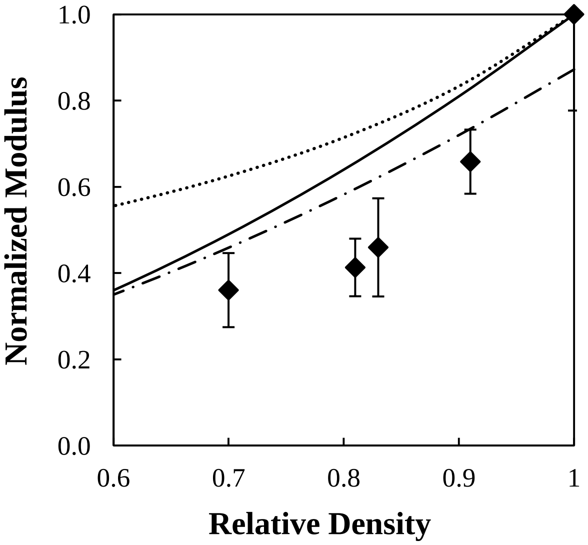

Figure 5.4. Normalized modulus versus relative density of foamed PLA samples. Solid lines show the prediction from different models: (········): constant macro-stress, (———): square power-law, (—·—·—·—): Gibson-Ashby.

The three models plotted in Figure 5.4 overestimate the modulus of elasticity of the foamed samples. The Gibson-Ashby model showed the lowest deviations from the experimental data. Noticeably, the normalized modulus does not reach unity when the relative density is 1 because the model was developed for low density foams. Similar observations were reported by Xiao and coworkers who observed normalized modulus evidently smaller than the square power-law model in polycarbonate foams prepared by compression molding, in a similar range of void fractions [22]. The dependency of the modulus of elasticity on void fraction is also due to the fact that the cell-population density varies as shown in Figure 5.3.

Normalized flexural modulus of elasticity measured by means of Taber stiffness was plotted against relative density in Figure 5.5a; the solid line represents the square power-law model. Similar to the tensile modulus, the experimental values are lower than the predicted ones by the square power-law relationship. The comparison between normalized flexural and tensile modulus is shown in Figure 5.5b. A linear relationship is observed between the two variables where the normalized flexural modulus was slightly higher than the normalized tensile modulus since the values fell above the solid line (the solid line represents a 1:1 relationship).

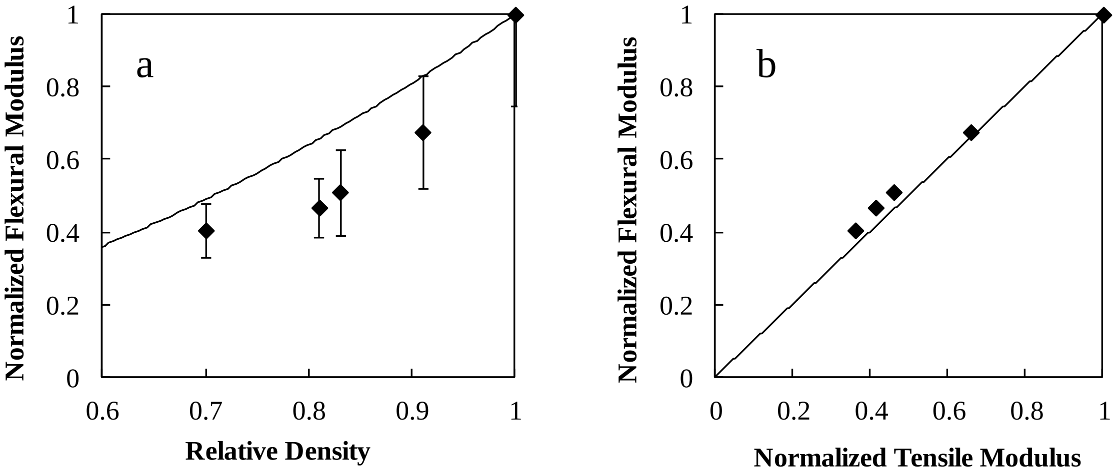

Figure 5.5. Normalized flexural modulus versus (a) relative density and (b) normalized tensile modulus of foamed PLA samples.

5.4.3 Tensile strength vs. relative density

In Figure 5.6 the normalized tensile strength is plotted against relative density. Again, the lines represent available models. The tensile stress decreases with decreasing relative density. However this trend is due to the fact that the cell-population density also varies.

The Gibson-Ashby model and the Nicolais-Narkis model were used to compare with the experimental results due to their reported good representation of experimental data [19]. In this case the Nicolais-Narkis model showed the lowest deviations from the experimental points. However, high variability was observed in the experimental data. The high standard deviation showed by the error bars may be due to the irregularity of the foamed rods. The irregular cross section area of the foamed rods may have induced stress concentrators decreasing the overall strength of the material.

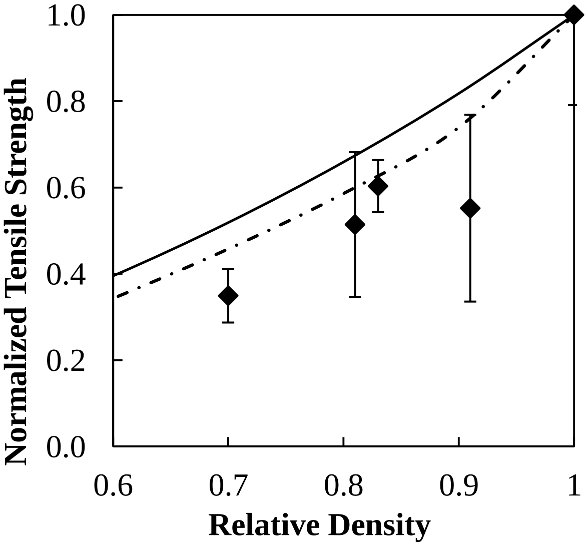

Figure 5.6. Normalized tensile strength versus relative density of foamed PLA samples. Solid lines show the prediction from different models: (−−−−): Nicolais-Narkis, (−·−·−·−): Gibson-Ashby.

The foamed filaments have irregular shape, and are not uniform along the length. The calculation of the cross-section area was done assuming that the filament is perfectly round. However, the foamed filaments differ from the ideal uniform shape (see Figure 5.2). Figure 5.7 presents an optical microscope image of a characteristic shape of the foamed PLA filaments and show the irregularity of the shape along the length making the determination of the cross sectional area a complex task. The inaccuracy in determining the cross-section diameters may be one of the reasons for the observed high standard deviations in strength and modulus as they are inversely proportional to the square of the diameter. For a cylindrical geometry the tensile stress (σ) is defined as:

$$\sigma = 4F \Big/ \pi D^2 \qquad \text{(Equation 5.6)}$$

where F is the tensile load and D is the cross-section diameter. A foamed filament is expected to fail at the smallest cross section. However, significant defects can make the sample fail at a different location having a high stress concentration, affecting the calculation of tensile strength and modulus. A similar scenario on which the irregularity of the samples affects the determination of mechanical properties is the single fiber tensile test of natural fibers where standard deviations over 30% are common [23]. It is important to develop strategies to improve the uniformity of the samples and the consistency of the cellular structure for an accurate measurement of mechanical properties.

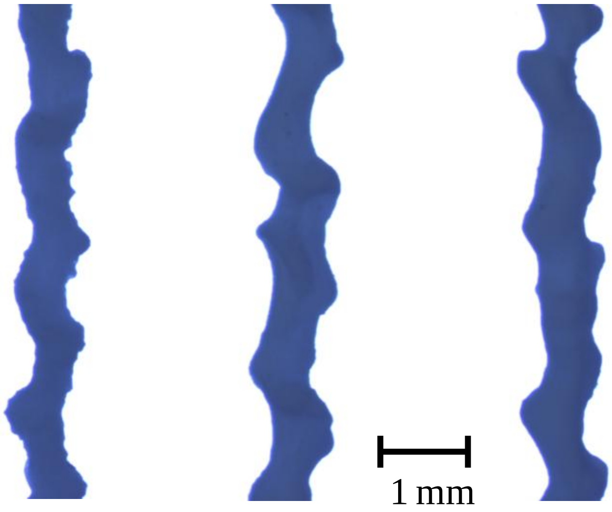

Figure 5.7. Optical microscope image of the foamed filaments shape along the length. For interpretation of the references to color in this and all other figures, the reader is referred to the electronic version of this dissertation

Figure 5.8 shows the data points for energy at break and strain at break for unfoamed (relative density=1) and foamed PLA plotted against the relative density. The data is scattered and a trend cannot be identified. Correlating the energy at break and strain at break with the relative density showed low R^2 values of 0.32 and 0.13 respectively. An increase in toughness was expected for the foamed samples because the inclusion of micro-bubbles can inhibit the crack propagation by blunting the crack tip increasing the energy needed to propagate the crack [4]. However, this claim cannot be corroborated with the experimental data. Noticeably, the highest value of energy at break was from a foamed sample. Inconsistent cellular structures and the irregularity of the filaments may have caused the high variation observed.

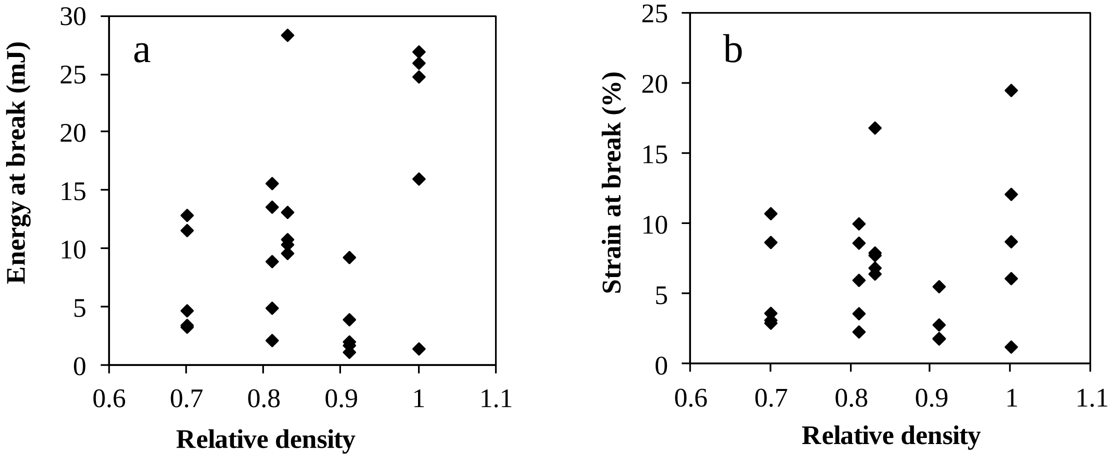

Figure 5.8. Energy and strain at break plotted against relative density for solid and foamed PLA samples.

5.5 Conclusions

This study examined the physico-mechanical properties of microcellular foamed polylactic acid (PLA) as a function of cell morphology to establish process-morphology-property relationships. Tensile and Taber stiffness tests were performed on microcellular PLA filaments prepared under different processing conditions. The processing variables evaluated, i.e., amount of gas injected, extruders speed, gear pump speed, and processing temperature affected the development of the cellular structure. The results show the dependency of tensile strength and modulus on foam relative density. However, this trend is due to the fact that the cell-population density also varies. Inconsistent cellular structures and the irregularity of the filaments may have caused the high variation in mechanical properties. The irregular shape along the length makes the calculation of the cross-section area difficult and induces stress concentrators which affected the failure mode of the foamed filaments.

REFERENCES

REFERENCES

1 Park, C. B., Behravesh, A. H. and Venter, R. D. (1998) Low density microcellular foam processing in extrusion using CO_2. Polymer Engineering and Science. **38**, 1812-1823

2 Suh, N. P. (2003) Impact of microcellular plastics on industrial practice and academic research. Macromolecular Symposia. **201**, 187-201

3 Park, C. B. and Suh, N. P. (1996) Rapid polymer/gas solution formation for continuous production of microcellular plastics. Journal of Manufacturing Science and Engineering-Transactions of the Asme. **118**, 639-645

4 Matuana, L. M. and Mengeloglu, F. (2001) Microcellular foaming of impact-modified rigid PVC/wood-flour composites. Journal of Vinyl & Additive Technology. **7**, 67-75

5 Matuana, L. M. (2008) Solid state microcellular foamed poly(lactic acid): Morphology and property characterization. Bioresource Technology. **99**, 3643-3650

6 Garlotta, D. (2001) A literature review of poly(lactic acid). Journal of Polymers and the Environment. **9**, 63-84

7 Bhardwaj, R. and Mohanty, A. K. (2007) Modification of brittle polylactide by novel hyperbranched polymer-based nanostructures. Biomacromolecules. **8**, 2476-2484

8 Martin, O. and Averous, L. (2001) Poly(lactic acid): plasticization and properties of biodegradable multiphase systems. Polymer. **42**, 6209-6219

9 Matuana, L. M. and Diaz, C. A. (2010) Study of cell nucleation in microcellular poly(lactic acid) foamed with supercritical CO_2 through a continuous-extrusion process. Industrial & Engineering Chemistry Research. **49**, 2186-2193

10 Lee, S. T., Kareko, L. and Jun, J. (2008) Study of thermoplastic PLA foam extrusion. Journal of Cellular Plastics. **44**, 293-305

11 Pilla, S., Kim, S. G., Auer, G. K., Gong, S. Q. and Park, C. B. (2009) Microcellular Extrusion-Foaming of Polylactide with Chain-Extender. Polymer Engineering and Science. **49**, 1653-1660

12 Wang, J., Zhu, W., Park, C. B. and Randall, J. (2009) Impact of molecular branching on microcellular foaming of polylactic acid in extrusion. SEP ANTEC Technical Papers. pp. 36-40

13 Naguib, H. E. and Park, C. B. (2002) Strategies for achieving ultra low-density polypropylene foams. Polymer Engineering and Science. **42**, 1481-1492

14 Diaz, C. A., Afrifah, K. A., Jin, S. and Matuana, L. M. (2011) Estimation of modulus of elasticity of plastics and wood plastic composites using a Taber stiffness tester. Composites Science and Technology. **71**, 67-70

15 Matuana, L. M. and Mengeloglu, F. (2002) Manufacture of rigid PVC/wood-flour composite foams using moisture contained in wood as foaming agent. Journal of Vinyl & Additive Technology. **8**, 264-270

16 Naguib, H. E., Park, C. B. and Reichelt, N. (2004) Fundamental foaming mechanisms governing the volume expansion of extruded polypropylene foams. Journal of Applied Polymer Science. **91**, 2661-2668

17 Zhang, Y. L., Rodrigue, D. and Ait-Kadi, A. (2003) High-density polyethylene foams. II. Elastic modulus. Journal of Applied Polymer Science. **90**, 2120-2129

18 Matuana, L. M., Park, C. B. and Balatinecz, J. J. (1998) Cell morphology and property relationships of microcellular foamed PVC/wood-fiber composites. Polymer Engineering and Science. **38**, 1862-1872

19 Zhang, Y. L., Rodrigue, D. and Ait-Kadi, A. (2003) High-density polyethylene foams. III. Tensile properties. Journal of Applied Polymer Science. **90**, 2130-2138

20 Gibson, L. J. and Ashby, M. F. (1988) Cellular solids : structure & properties. Pergamon Press, Oxford

21 Reignier, J., Gendron, R. and Champagne, M. F. (2007) Extrusion foaming of poly(lactic acid) blown with Co-2: Toward 100% green material. Cellular Polymers. **26**, 83-115

22 Xiao, Z., Guan, R., Jiang, Y. and Li, Y. (2007) Tensile property of thin microcellular PC sheets prepared by compression molding. Express Polymer Letters. **1**, 217-225

23 Hu, W., Ton-That, M. T., Perrin-Sarazin, F. and Denault, J. (2010) An Improved Method for Single Fiber Tensile Test of Natural Fibers. Polymer Engineering and Science. **50**, 819-825

24 Colton, J. S. and Suh, N. P. (1987) The nucleation of microcellular thermoplastic foam with additives .1. Theoretical considerations. Polymer Engineering and Science. **27**, 485-492

CHAPTER 6

Conclusions and Future Work

6.1 Conclusions

Poly(lactic acid) (PLA), a biodegradable thermoplastic derived from renewable resources, stands out as a substitute to petroleum-based plastics. In spite of its excellent properties, commercial application is limited because PLA is more expensive and more brittle than petroleum-based resins. PLA can be blended with cellulosic fibers to reduce material cost. However, the lowered cost comes at the expense of flexibility and impact strength, which can be enhanced through the production of microcellular structures in the composite. Characterization of the morphology of microcellular foams includes cell-population densities of 10^9 cells/cm^3 and up and cell sizes smaller than 10 μm. Continuous microcellular foaming has been developed based on the concept of thermodynamic instability created by a rapid pressure drop of a polymer/gas single phase solution. Understanding of the nucleation dynamics is the key to achieving high nucleation rates. Consequently, the effects of the processing temperature and material compositions on the melt viscosity, pressure drop rate, and cell-population density were examined to understand the nucleation mechanisms in neat and filled PLA foams. The following conclusions were drawn from the experimental results.

1) The processing temperature had a strong effect of the rheology of the melt. Increasing the test temperature significantly decreased the melt viscosity of PLA affecting the cell nucleation rate because of its effect on the pressure generated in the system during the extrusion of microcellular PLA. Processing at a lower temperature significantly increased the cell nucleation rate of PLA (Anorphous and semi-crystalline) because of the fact that a high melt viscosity induced a high pressure drop rate.

2) The presence of the nanoclay did not affect the homogeneous nucleation but

increased the heterogeneous nucleation, with the fine cells nucleated at the membrane of homogeneously nucleated bubbles. The addition of nanoclay allowed both homogeneous and heterogeneous nucleation stages to occur during the foaming process.

3) The melt viscosity of PLA increased as the relative amount of wood-flour increased in the composites because of the interaction between wood-flour and the matrix increasing the friction towards the flow. In contrast, increasing amounts of rheology modifier produced the opposite effect reducing the viscosity of the composites because of the lubrication effect of the low molecular weight additive.

4) Matching the viscosity of the PLA/wood-flour composites with that of neat PLA resulted in adequate processing conditions for microcellular foaming and resulted in the best cell morphologies. Lower concentrations of rheology modifier resulted in unprossesable conditions because of the increased viscosity which generated elevated pressures in the system above operational limits. Higher concentrations of rheology modifier resulted in foams with poor cell morphologies because of the low viscosity which facilitated the gas escape and cell coalescence.

5) The physico-mechanical properties of microcellular foamed polylactic acid (PLA) as a function of cell morphology were studied to establish process-morphology-property relationships. The processing variables, i.e., amount of gas injected, extruders speed, gear pump speed, and processing temperature affected the development of the cellular structure. Tensile strength and modulus modulus of elasticity of foamed samples correlated with the relative density.

6.2 Future work

Production of microcellular structures in polylactic acid (PLA) and PLA/wood-flour composites was demonstrated in the continuous extrusion process injecting carbon dioxide as foaming agent. The filamentary extrusion was used as means to produce microcellular foams by a rapid pressure drop at the nozzle die. Control over the rheology of the melt proved to be of key importance to effectively nucleate a swarm of bubbles. However, it is important to extrapolate the results achieved in the filament to other shapes such as films. For this purpose the use of annular dies and cast film dies should be investigated. Successful production of microcellular foamed films and other shapes will not only contribute to the scale-up of the technology to an industrial level but also allow for a more precise characterization and modeling of process-morphology-property relationships.

This study investigated the effects of the processing temperature and material compositions on the melt viscosity, pressure drop rate, and cell-population density of microcellular PLA and PLA/wood-flour composites. However, other approaches such as nozzle design (nozzle geometry) have the potential to modify the processing conditions (i.e., pressure drop and pressure drop rate) and expand the processing windows to produce microcellular PLA and PLA/wood-flour composites.

This study investigated the effect of extensional viscosity on the foamability of PLA to a limited extend. However, it is known of the importance of extensional properties, such as melt strength, in the foaming process. PLA grades intended for foaming applications are now commercially available as well as branching agents specially designed for PLA. Assessment of the performance of such materials should be investigated in view of expanding the range of properties and density reduction in foamed PLA.